AD-A117 851 NAVAL OCEAN SYSTEMS CENTER SAN DIEGO CA F/G 4/1
DEVELOPMENT OF A MINICOMPUTER ATMOSPHERIC NOISE MODEL.(U)
MAY 82 D B SAILORS, R P BROWN
UNCLASSIFIED NOSC/TR-778 NL

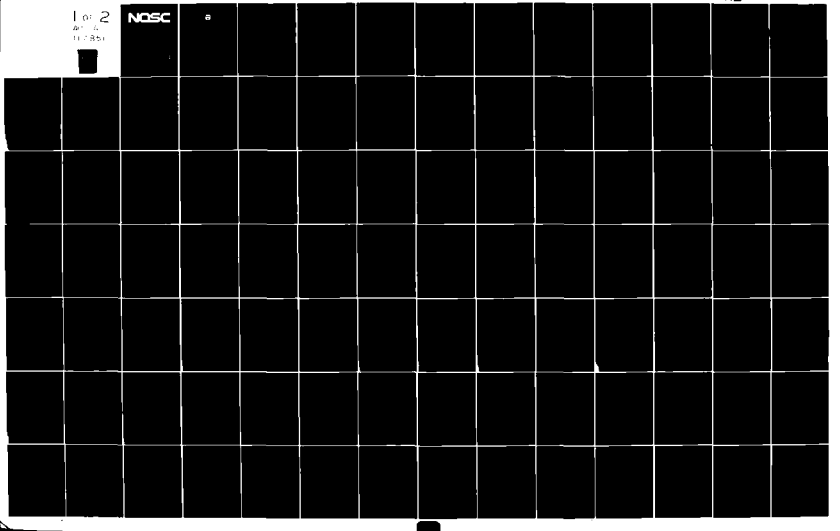

(12)

NOSC

NOSC TR 778

NOSC TR 778

Technical Report 778

DEVELOPMENT OF A MINICOMPUTER ATMOSPHERIC NOISE MODEL

DB Sailors
RP Brown

1 May 1982

Approved for public release; distribution unlimited.

NAVAL OCEAN SYSTEMS CENTER
SAN DIEGO, CALIFORNIA 92152

NAVAL OCEAN SYSTEMS CENTER, SAN DIEGO, CA 92152

AN ACTIVITY OF THE NAVAL MATERIAL COMMAND

SL GUILLE, CAPT, USN
Commander

HL BLOOD
Technical Director

ADMINISTRATIVE INFORMATION

The work reported here was performed by members of the EM Propagation Division, Naval Ocean Systems Center, during the period January 1981 through September 1981. It was sponsored by US Army Center for Communication Sciences.

The authors wish to express their indebtedness to Dr. A. D. Spaulding of the Institute of Telecommunication Sciences (ITS) of the National Telecommunications and Information Administration, who gave them complete access to D. H. Zacharisen's files on atmospheric noise numerical maps, provided copies of all D. H. Zacharisen's atmospheric noise numerical mapping computer programs, and provided a data tape containing the original data used to plot the contour maps in CCIR Report 322.

Released by
J. H. Richter, Head
EM Propagation Division

Under authority of
J. D. Hightower, Head
Environmental Sciences Department

UNCLASSIFIED

SECURITY CLASSIFICATION OF THIS PAGE (When Data Entered)

REPORT DOCUMENTATION PAGE		READ INSTRUCTIONS BEFORE COMPLETING FORM
1. REPORT NUMBER NOSC Technical Report 778 (TR 778)	2. GOVT ACCESSION NO.	3. RECIPIENT'S CATALOG NUMBER
4. TITLE (and Subtitle) Development of a Minicomputer Atmospheric Noise Model		5. TYPE OF REPORT & PERIOD COVERED Jan 1981 - Sep 1981 6. PERFORMING ORG. REPORT NUMBER
7. AUTHOR(s) D. B. Sailors R. P. Brown		8. CONTRACT OR GRANT NUMBER(s)
9. PERFORMING ORGANIZATION NAME AND ADDRESS Naval Ocean Systems Center San Diego, CA 92152		10. PROGRAM ELEMENT, PROJECT, TASK AREA & WORK UNIT NUMBERS RDA
11. CONTROLLING OFFICE NAME AND ADDRESS US Army Center for Communications Sciences DRDCO-COM-RY-3 Ft. Monmouth, NJ 07703		12. REPORT DATE 1 May 1982 13. NUMBER OF PAGES 104
14. MONITORING AGENCY NAME & ADDRESS(if different from Controlling Office)		15. SECURITY CLASS. (of this report) UNCLASSIFIED 15a. DECLASSIFICATION/DOWNGRADING SCHEDULE

16. DISTRIBUTION STATEMENT (of this Report)

Approved for public release; distribution unlimited

17. DISTRIBUTION STATEMENT (of the abstract entered in Block 20, if different from Report)

18. SUPPLEMENTARY NOTES

19. KEY WORDS (Continue on reverse side if necessary and identify by block number)

Atmospheric Noise	Numerical map	Noise power
Galactic noise	Fourier series	Fourier analysis
Man-made noise	Universal time	Mini-computer
Computer model	Curves, Statistics, data	
Effective antenna noise-factor	Median atmospheric noise	

20. ABSTRACT (Continue on reverse side if necessary and identify by block number)

A practical but simplified atmospheric noise model for use in estimating system signal-to-noise ratios in micro-mini-computer based HF propagation prediction systems is presented. Numerical mapping techniques were used to represent worldwide atmospheric noise at 1 MHz in 24 numerical maps: one for each of six 4-hour time blocks (in universal time) and each of four 3-month periods. This representation results in a minimum reduction by one-fifth in the number of coefficients necessary in computer memory over that of an earlier model in which the map represented an entire twenty-four hour day.

DD FORM 1 JAN 73 1473 EDITION OF 1 NOV 65 IS OBSOLETE
S/N 0102-LF-014-6601

UNCLASSIFIED

SECURITY CLASSIFICATION OF THIS PAGE (When Data Entered)

20. ABSTRACT (Continued)

The simpler expression for the median noise levels (F_{am}) results in significant savings in computer code and time. Several versions were produced-each with a different number of coefficients (number of harmonics) in the Fourier representation for each time block. The number of coefficients ranged from 192 coefficients per time block for the most accurate versions to 35 coefficients for the least accurate. The accuracies were determined by calculating the rms residual between values of F_{am} used to develop the model and the corresponding values computed from each model. The most accurate model had an average rms error for all times and seasons of 1.25 dB; whereas, the least accurate had an rms error of 4.53 dB. During the worst season, June, July, August, the most accurate model had an rms error of 1.4 dB; whereas, the least accurate had an rms error of 5.63 dB. The CCIR noise data used to generate the models had an average standard deviation of the error at 1 MHz of 5.48 dB and an error of 6.67 dB during June, July, August; the numerical map in use in current HF prediction programs has an average rms error of 1.65 dB and an error of 2.02 dB during June, July and August.

SUMMARY

OBJECTIVE

Develop a practical but simplified atmospheric noise model for use in estimating system signal-to-noise ratios in micro-mini-computer based HF propagation prediction systems.

RESULTS

1. The numerical mapping techniques of Zacharisen and Jones were used to represent worldwide atmospheric noise at 1 MHz.

2. Each four-hour time block (in universal time, UT) for each of four 3-month periods was represented separately rather than for a twenty-four hour day, resulting in 24 numerical maps.

3. This numerical representation results in a minimum reduction by one-fifth of the number of coefficients in computer storage at one time over that used by Zacharisen and Jones for their model.

4. The remaining coefficients would be stored on cassette tape.

5. The simpler expression for the median noise levels results in significant savings in computer code and time.

6. The models produced make use of the frequency dependence model of earlier representations of CCIR Report 322.

7. The average rms error for the Zacharisen and Jones model for all hours and seasons was 1.65 dB; the corresponding error for the CCIR Report 322 data at 1 MHz was 5.48 dB.

8. The average rms error for all times and seasons for a model version using 192 coefficients per time block was 1.25 dB.

9. The average rms error for all times and seasons for a model version with 110 coefficients was 1.60 dB.

10. The two model versions with 77 and 55 coefficients each have an average rms error for all times and seasons of 2.18 dB and 2.94 dB, respectively.

11. The two model versions with 50 and 35 coefficients each have an average rms error for all times and seasons of 3.64 dB and 4.53 dB, respectively.

12. The least accurate season for all model versions was the June, July, and August season.

RECOMMENDATIONS

1. Use the model versions with 192 coefficients in each time block in either Advanced Prophet applications or in large scale HF prediction models.

2. Use the model version with 110 coefficients in each time block in Advanced Prophet applications.

3. Use the model versions with 55 and 77 coefficients each in each time block in either Advanced Prophet applications or Tektronix 4052 mini-computer applications.

4. Use the two model versions with 35 and 50 coefficients each in each time block only for applications for which the memory requirements for the mini-computer demand a sacrifice in the accuracy of the model.

5. Use Fourier series interpolation to obtain F_{am} at 1 MHz for an actual hour of operation.

6. When Fourier series interpolation is not practical, use linear interpolation.

7. At HF calculate noise values for galactic and man-made noise also.

8. Calculate galactic noise only for frequencies above the maximum expected f_oF2.

9. Sum the noise power in watts of the three noise sources and convert back to dB >1 watt.

10. Determine the reliability of the combined 1 MHz models and the frequency dependence model.

11. Determine this reliability as a function of frequency, time of day, geographic location as well as for the maximum longitude and latitude harmonic numbers of the 1 MHz numerical maps.

12. Determine the accuracy of the complete Lucas and Harper model with the same data.

13. Use measured F_{am} data, measured after the data contributing to CCIR Report 322 were measured, as well as data used to develop CCIR Report 322.

ACRONYMS AND SYMBOLS

Where a symbol is shown in both lower case and capital letters, the capital letter is used to represent the equivalent, in decibels, of the quantity denoted by the lower case letter.

atmospheric noise	Noise caused by disturbances in the atmosphere, such as thunderstorms
b, B	Effective receiver noise bandwidth (Hz) ($B = 20 \log_{10} b$)
bias	Average residual
business area	Any area where the predominant usage throughout the area is for any type of business
CCIR	Consultative Committee International Radio
DATA FOUR	A FORTRAN computer program for obtaining the six Fourier coefficients for interpolating from LT to UT
D_l	Value of the average noise power exceeded for 90% of the hours within a time block (dB below the median value for the time block)
D_{la}	D_l value for atmospheric noise
D_{lg}	D_l value for galactic noise
D_u	Value of the average noise power exceeded for 10% of the hours within a time block (dB above the time block median)
D_{ua}	D_u value for atmospheric noise
D_{ug}	D_u value for galactic noise

D_{NU}	Upper decile difference from the median noise of the combined noise
$D_{N\ell}$	Lower decile difference from the median noise of the combined noise
E_e	Expected value of the signal field-strength required for a given grade of service (dB above 1 μV/m)
E_n	Root-mean-square noise field strength for a 1000 Hz bandwidth (dB above 1 μV/m)
f,F	Operating noise factor of a receiving system ($F = 10 \log_{10} f$)
f_a, F_a	Effective antenna noise-factor which results from the external noise power available from a loss-free antenna ($F_a = 10 \log_{10} f_a$)
F_{am}	Median of the hourly values of F_a within a time block
f_c	Noise factor of the antenna circuit (its loss in available power)
FOUR RESD	A FORTRAN program used to determine how many harmonics were necessary to provide an adequate fit for the longitudinal variation
f_r	Noise factor of the receiver
f_t	Noise factor of the transmission line (its loss in available power)
galactic noise	thermal noise that originates outside the earth and its atmosphere

$G_{j,k}(\lambda)$	latitude function $\sin^k\lambda \cos^j\lambda$
J	longitudinal harmonic maximum (number of harmonics N = 2J +1)
k	Boltzmann's constant = $1.38X10^{-23}$ joules per degree Kelvin
K	Latitudinal harmonic maximum (number of harmonics N = K + 1 for j = 8, 9, 10; for $0<j<7$, N = 8)
LT	Local time
man-made noise	Industrial noise
N	Combined median noise from all sources
N_a	Median atmospheric noise F_{am}
NBS	National Bureau of Standards
N_g	Median galactic noise
N_m	Median man-made noise
numerical map	A finite series of mathematical terms, each consisting of a product of a numerical coefficient and an analytic function of the geographic coordinates
$q_{j,k}^{(h)}$	A numerical coefficient representing atmospheric noise for the hour h at a latitudinal harmonic k and longitudinal harmonic j
P	Received signal power available from an equivalent loss-free antenna (dB)
P_n, P_n	Noise power available from an equivalent loss-free antenna

	($P_n = 10 \log_{10} p_n$)
$p_{j,k}^{(h)}$	A numerical coefficient representing atmospheric noise for the hour h at a latitudinal harmonic k and a longitudinal harmonic j
r,R	Signal-to-noise power ratio required ($R = 10 \log_{10} r$)
residential area	Any area used predominantly for single or multiple family dwellings with density of at least two family units per acre and no large or busy highways
residual	Predicted noise minus observed noise
RMS	Root Mean Square
rural area	Locations where land usage is primarily for agricultural or similar pursuits, and dwellings are no more than one every five acres
T_a	Effective antenna temperature in the presence of external noise
T_o	Reference temperature, taken as 288° Kelvin
t_i	Hour angle in degrees
UT	Universal time
V_d	Voltage deviation; the ratio (dB) of the rms voltage to the average noise envelope
V_{dm}	Median value of V_d

$X_h(\lambda,\theta)$	Estimated atmospheric noise at an hour h, latitude λ, longitude θ using numerical map
Y	Diurnal representation of the six values of $X_n(\lambda,\theta)$
$y_{m,n}$	Input value of F_{am} at local time at (λ_m,θ_n)
$y_{m,n}^{(h)}$	Computed values of F_{am} for each of the UT hours h = 0000, 0400, 0800, 1200, 1600, 2000 at (λ_m,θ_n)
UT ANOIS	A FORTRAN computer program that computes values of $y_{m,n}^{(h)}$ of F_{am} using the Fourier coefficients generated by DATA FOUR
UT FOUR	A FORTRAN computer program that calculates the coefficients at each fixed latitude λ_m for each hour and season
UT FOUR3	A FORTRAN computer program that Fourier analyzes the two-dimensional representation produced by UT NEQSOL; it produces one map for each three-month season.
UT NEQSOL	A FORTRAN computer program that determines the coefficients $p_{j,k}^{(h)}$ and $q_{j,k}^{(h)}$ in the two-dimensional representation of F_{am}
θ	Longitude measured eastward from 0°, $0° \leq \theta° 360°$
λ	Latitude, $-90° \leq \lambda \leq 90°$
σ_{D1}	Standard deviation of D_1
σ_{Du}	Standard deviation of D_u
$\sigma_{F_{am}}$	Standard deviation of F_{am}
σ_{NM}	Standard deviation of man-made noise

CONTENTS

ILLUSTRATIONS

TABLES

INTRODUCTION

The determination of the minimum signal level required for satisfactory radio reception in the absence of other unwanted radio signals necessitates a knowledge of the noise with which the wanted signal must compete. There are a number of types of noise that may influence reception. These can be divided into two main categories depending on whether the noise originates in the receiving system or externally to the antenna. External noise can be divided into several types. The most usual types are of atmospheric, galactic and man-made origin. Below about 30 MHz, atmospheric noise usually predominates. The internationally accepted method of predicting atmospheric noise is outlined in International Radio Consultative Committee (CCIR) Report 322[1].

The purpose of this report is to describe the development of a practical but simplified atmospheric noise model for use in estimating system signal-to-noise ratios in micro-mini-computer-based hf propagation prediction systems. Previous numerical representations of atmospheric noise include those of Lucas and Harper[2] and of Zacharisen and Jones[3]. The Lucas and Harper representation at 1 MHz consists of 24 numerical maps: one for each of six 4-hour local time blocks and for each of four 3-month periods. (A numerical map is a finite series of mathematical terms, each consisting of a product of a numerical coefficient and an analytic function of the geographic coordinates.) This model uses 464 coefficients for each time block and 2784 coefficients for a single 3-month period. The frequency dependence is represented by a power series of least squares fit to the frequency dependence curves in CCIR Report 322. The Zacharisen and Jones model is a worldwide representation of 1 MHz atmospheric noise in universal time. The entire day is represented with one set of coefficients, and each 3-month period is represented with only 960 coefficients.

The approach taken to develop an atmospheric noise model suitable for use on a micro-mini-computer was to try to reduce the size of the numerical map representing atmospheric noise at 1 MHz and to represent each four-hour time block separately rather than for a twenty-four hour day. Then, assuming that the micro-computer would have a cassette tape unit, the coefficients for each

four-hour time block for each season would reside on a cassette. Several versions would be produced - each with a different number of coefficients in each time block. The accuracy of these versions was to be determined as a function of the number of harmonics in the representation. A user would choose the version with an error he was willing to accept consistent with the memory space available in his micro-computer.

The numerical mapping techniques of Zacharisen and Jones were used to represent worldwide atmospheric noise at 1 MHz. The data used to model atmospheric noise was the same as used to prepare the local time contour maps in CCIR Report 322[1] and is the same as used to produce the two previous representations of 1 MHz atmospheric noise. The versions produced had their worst error during the summer months of June, July and August. Six atmospheric noise versions were produced: (1) a numerical map with 192 coefficients having an average rms error overall of 1.25 dB and of 1.40 dB during summer; (2) a numerical map with 110 coefficients having an average rms error overall of 1.60 dB and of 1.76 dB during summer; (3) a numerical map with 77 coefficients having an average rms error overall of 2.18 dB and of 2.80 dB during summer; (4) a numerical map with 55 coefficients having an average rms error overall of 2.94 dB and of 3.57 dB during summer; (5) a numerical map with 50 coefficients having an average rms error overall of 3.64 dB and of 5.25 dB during summer; and (6) a numerical map with 35 coefficients having an rms average error overall of 4.53 dB and of 5.63 dB during summer.

The material presented in this report is limited to the development of the 1 MHz model and the determination of its accuracy. Although the frequency dependence model is included in an appendix for completeness the treatment of the reliability of the combined 1 MHz model and the frequency dependence model is left to a subsequent report. The body of the report consists of five main parts: (1) the methods of atmospheric noise prediction; (2) a description of parameters used; (3) the numerical mapping process; (4) determination of the accuracy of the models; and (5) a discussion of the results. Included in the appendices are: (1) world contour maps of 1 MHz atmospheric noise; (2) the frequency dependence model; (3) a FORTRAN computer subroutine of the 1 MHz model; and (4) a computer program for reading and printing the atmospheric noise numerical coefficients.

METHODS OF ATMOSPHERIC NOISE PREDICTION

One of the first methods of worldwide noise prediction was that published in National Bureau of Standards (NBS) Circular No. 462.[4] In this publication noise grade maps and prediction curves were given, indicating the noise level in terms of the minimum required signal strength to assure radio-telephone communication for 90% of the time in the presence of atmospherics.

A more recent publication, NBS Circular No. 557[5], presented the same noise grade maps as used in the previous publication. However, the prediction curves had been revised to show the expected median levels of radio noise during each season instead of required field strength for 90% intelligibility. The method of interpreting the earlier predictions had not been entirely clear, and the new method of presentation was used to remove ambiguities.

An even more recent previous prediction method was contained in CCIR Report 65 (Revised), which was adopted by the CCIR IXth Plenary Assembly, Los Angeles, 1959.[6] The information presented showed the expected values of the average noise power on a worldwide basis throughout the frequency range 10 kHz to 100 MHz, for all times of the day and night, and all seasons of the year. The presentation was revised to show the expected median levels of radio noise during four-hour time blocks for each season. The parameter presented was the median hourly value of the average noise power for each time block, and the variations in this parameter showed the systematic diurnal and seasonal variations of the noise. Variations of the hourly values within a time block were treated statistically, and their extent was indicated by the ratios of the upper and lower decibel values to the median.

Geographic and operating frequency distributions of atmospheric noise from CCIR Report No. 65 were represented numerically by Lucas and Harper for use in computers.[7] Coefficients were tabulated for the worldwide distributions and operating frequency dependence. Representative contour charts of all distributions were shown along with sample longitudinal and latitudinal variations.

The current internationally accepted method of predicting atmospheric noise is outlined in CCIR Report 322.[1] It constituted a comprehensive revision of Report 65. Although the original form of presentation was retained, the Report was improved in the following respects:

- the original predictions were modified to take account more extensive and reliable data;
- statistical information was presented on the accuracy of the modified predictions;
- the fine structure of the noise is described in statistical terms;
- each time block has its own frequency dependence curves and data on noise variability and character;
- methods of using the predictions in the solution of operational problems were presented.

Figures 1-3, a sample of the figures in CCIR Report 322, show the expected median values of atmospheric noise, F_{am} in dB above kT_ob for summer, 1200-1600 hrs local time. The figures are used in the following way. The value of F_{am} for 1 MHz is found directly from the noise charts like Figure 1 for the time block (season and hour) under consideration. Using this value to select the noise grade curve, the value of F_{am} for the required frequency is determined from the curves in Figure 2. The parameters $\sigma_{F_{am}}$, D_u, and σ_{Du} are obtained for the required frequency from the variability curves in Figure 3. If the value of the deviation of an hourly value of F_a from the time block median F_{am} (dB) ($D = F_a - F_{am}$), or the value of σ_D is required for any percentage of time other than 10%, the values can be found by plotting D_u and σ_{Du} on a normal probability paper (with values in dB), and drawing straight lines through 0 dB at 50% and the 10% values. Values at percentages greater than 50% can be determined in the same manner using D_l and σ_{Dl}. Plotted values of V_{dm}, median value of the voltage deviation V_d, are for a bandwidth of 200 kHz.

Since computer methods had become prominent in predicting system performance of high frequency communication circuits, it was only natural that a numerical representation of CCIR Report 322 would be made. The first representation was one due to Lucas and Harper.[2] Their 1 MHz representation consisted of 24 numerical maps: one for each of six 4-hour time blocks (in

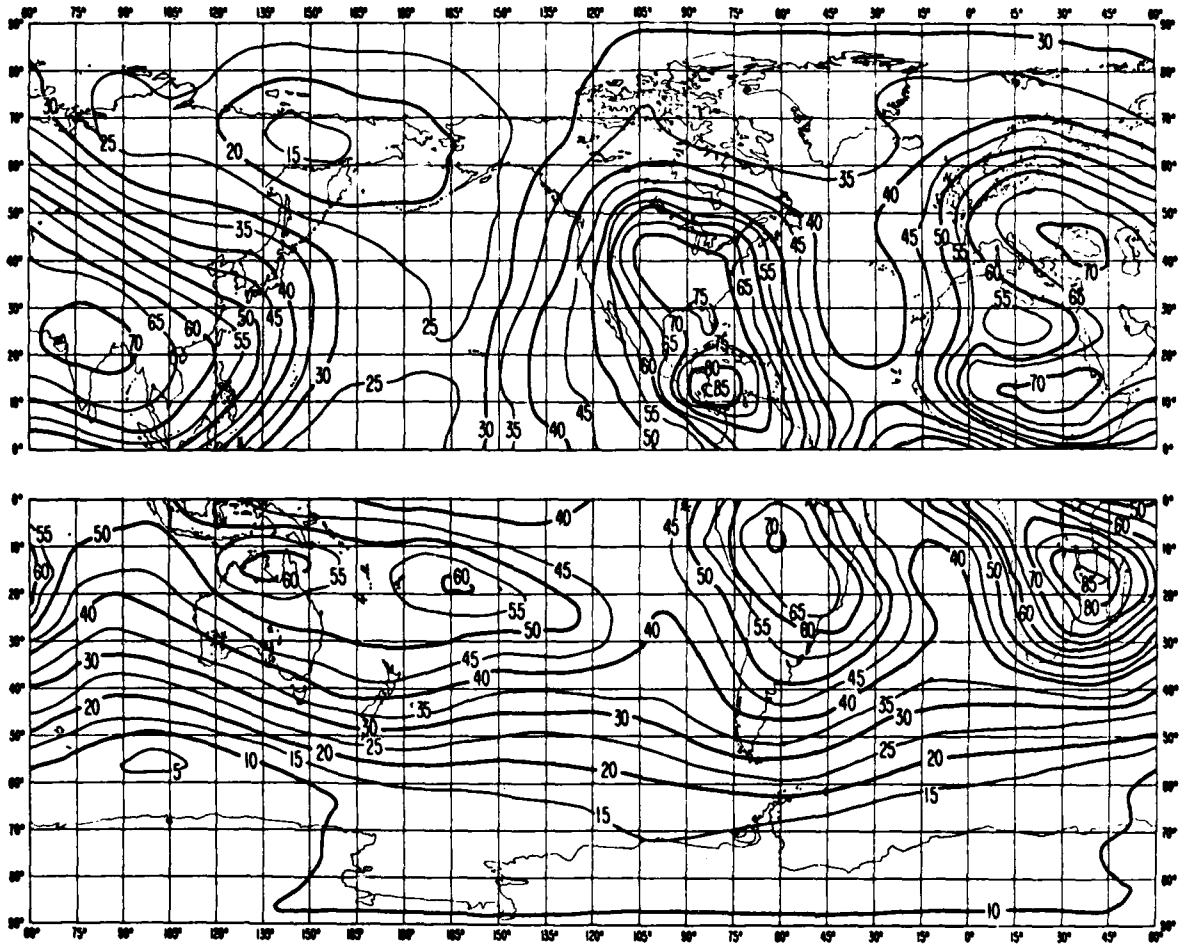

Figure 1. Expected values of atmospheric radio noise, F_{am}, (Summer: 1200-1600 h LT)

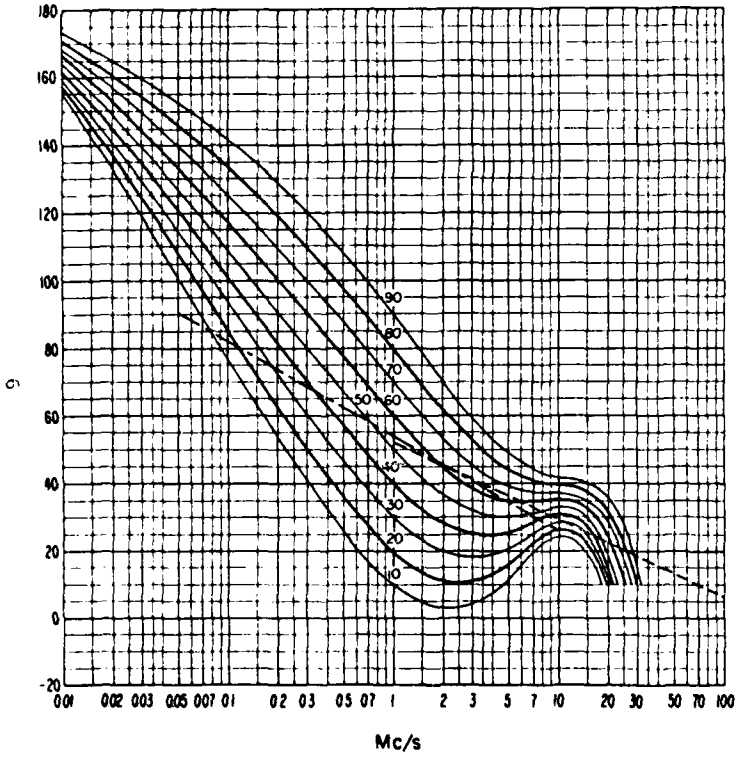

Figure 2. Variation of radio noise with frequency (Summer: 1200-1600 h LT)

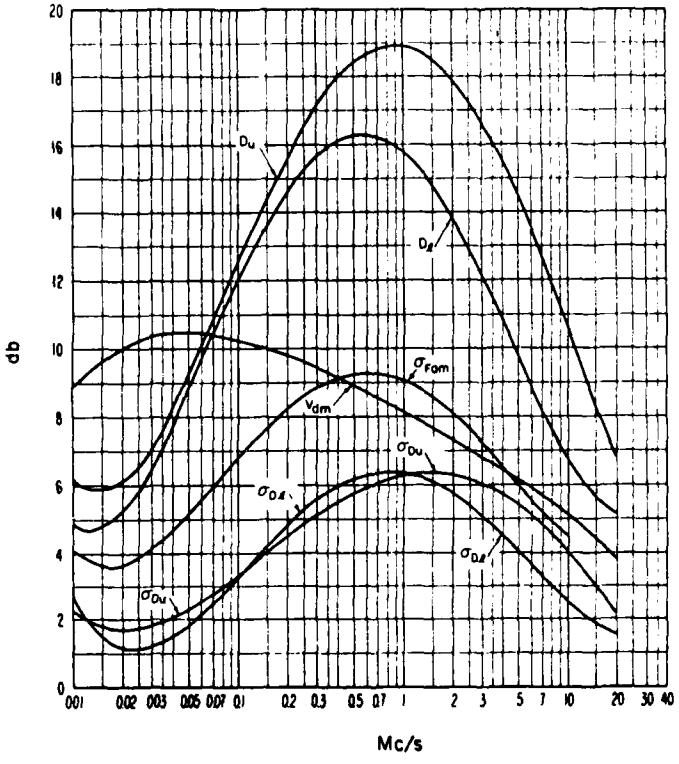

Figure 3. Data on noise variability and character (Summer: 1200-1600 h LT)

B-40701

local time, LT) and each of four 3-month periods. The diurnal variation was obtained by linear interpolation between the numerical map values taken at the central hour of each time block. Seasonal variation was represented by a step function. Both mean and frequency dependence variability were represented by a power series. Zacharisen and Jones developed a representation of the 1 MHz atmospheric noise in universal time (UT).[3] They reduced by two-thirds the number of coefficients necessary. The diurnal variation is represented by a smooth Fourier series (in place of linear interpolation), and the seasonal variation is represented by linear interpolation (instead of a step function).

DESCRIPTION OF PARAMETERS USED

It has been found that no single parameter describing the noise environment is adequate for all types of radio service. Thus, a number of parameters have been defined to evaluate performance of various systems. This section describes noise parameters in common use and gives, where possible, the relationships between them.

The most useful parameter for describing the noise environment is the mean noise power and is the basis of noise predictions. The noise power received from sources external to the antenna is expressed in terms of an effective antenna noise factor, f_a, which is defined by:

$$f_a = p_n/(kT_o b) = T_a/T_o \qquad (1)$$

where

p_n is the noise power available from an equivalent loss free antenna in watts; k is Boltzmann's constant (1.38×10^{-23} joules per degree Kelvin); T_o is the reference temperature 288°K; b is the effective receiver noise bandwidth in Hz; and T_a is the effective antenna temperature in the presence of external noise.

Now, using capital letters corresponding to the lower case letters to denote the ratios in decibels, F_a represents the noise power density per Hz in

decibels above kT_o. F_{am} is the median hourly value of F_a. The parameter p_n expressed in dB above 1 watt becomes:

$$P_n = F_a + B - 204 \text{ dBW} \tag{2}$$

where $10 \log_{10} kT_o = -204$ and $B = 10 \log_{10} b$.

The assessment of the performance of the complete receiving system can be expressed in terms of its operating noise factor, f, which takes into account the external noise as well as noise generated within the receiving system. If it is assumed that the receiver is free from spurious responses and that all elements prior to the receiver are at the reference temperature T_o, then f is given by:

$$f = f_a - 1 + f_c f_t f_r \tag{3}$$

where f_c is the noise factor of the antenna circuit (its loss in available power); f_t is the noise factor of the transmission line (its loss in available power); and f_r is the noise factor of the receiver.

The relation between the noise power, p_n, available from a loss free antenna and the corresponding signal-to-noise ratio, r, at the intermediate frequency output of the receiver, can be derived from the operating noise factor f by:

$$p_n = frkT_o b \tag{4}$$

In decibels (dB), P_n expressed in dB above 1 watt becomes

$$P_n = R + F + B - 204 \text{ dBW} \tag{5}$$

where F is the noise factor f in decibels above kT_o.

The expected value of received power, P_e, required for a particular grade of service during an hour when the antenna noise factor is F_a, is from equation (5)

$$P_e = F_a + R + B - 204 \text{ dBW} \tag{6}$$

where R is the required pre-detection signal-to-noise power ratio for the given bandwidth.

In some cases, it is desirable to deal with the external noise environment in terms of its rms electric field strength, E_n. For a short vertical antenna this is simply related to the noise power factor by

$$E_n = F_a + 20 \log_{10} f_{MHz} - 65.5 \tag{7}$$

where E_n is in dB above 1 μV/m for a 1 kHz bandwidth and f_{MHz} is frequency in MHz. The value of the field strength for any bandwidth b in Hz can be derived by adding (10 $\log_{10}$ b - 30) to E_n. Inserting F_a from equation (6) in equation (7) gives the expected value of the field strength E_e for a short vertical rod:

$$E_e = P_e + 20 \log_{10} f_{MHz} + 108.5 \text{ (dB above 1 μV/m)} \tag{8}$$

where b is in Hz.

NUMERICAL MAPPING PROCESS

In this section we deal with the problem of representing the worldwide geographic variation of the atmospheric noise parameter F_{am} at 1 MHz for a fixed hour of UT and a fixed 3-month season. The procedures described here are those due to Zacharisen and Jones[3]. These procedures were based on numerical methods for representing diurnal and geographic variations of ionospheric data developed by Jones and Gallet.[8,9,10]

The solution to the problem consists of well defined mathematical operations which have been programmed for use on large-scale digital computers. Input to the computer programs are values of F_{am} for a given time block in local time and a 3-month period. The diurnal variation at each grid point is represented by a Fourier analysis of the local time block F_{am} values. Then a Fourier analysis is made of the longitudinal variation for a fixed latitude. Next the worldwide geographic variation of each Fourier coefficient is expanded in a series of functions analogous to surface spherical harmonics. The result then is a two dimensional representation of F_{am} in latitude and longitude at fixed universal times for each season. The relatively small table of coefficients representing F_{am} is referred to as a "numerical map."

BASIC INPUT DATA

The values of F_{am}, used as basic input data to the numerical mapping programs, were the same as those used to prepare the LT contour maps in CCIR Report 322. They were available in binary form on magnetic tape for each of the six time blocks 0000-0400, 0400-0800, 0800-1200, 1200-1600, 1600-2000, and 2000-2400 in LT and for each of the 3-month seasonal periods December-February, March-May, June-August, and September-November.

For a given time block and 3-month period, the values of F_{am} were given at 8,400 grid points (λ_m, θ_n) where

$$\lambda_m = 90 - 1.8(m-1/2),\ m = 1, 2, \ldots, 100, \tag{9}$$

$$\Theta_n = \frac{360}{84}(n - 1/2),\ n = 1, 2, \ldots, 84. \tag{10}$$

Here λ denotes latitude, $-90° \leq \lambda \leq 90°$, and θ denotes longitude measured eastward from 0°, $0° \leq \theta \leq 360°$. The grid point (λ_1, Θ_1) is at 89.1°N and 2.1428571°E. The increment in latitude is 1.8°, and in longitude it is 4.2857143°. The input value of F_{am} at (λ_m, Θ_n) is denoted by $y_{m,n}$.

FOURIER REPRESENTATION OF DIURNAL VARIATION

The Zacharisen and Jones numerical representation of the worldwide atmospheric noise was in universal time (UT). This was done to reduce inconsistencies in the basic input data near the poles that result from the use of local time. Greater computing efficiency was attained with the UT maps since, for most applications, calculations are made for fixed instants of UT. To develop a numerical representation in UT, it was necessary to convert the data from local time to universal time.

The most natural method for representing the diurnal variation is Fourier analysis, since atmospheric noise is periodic in time. Moreover, the trigonometric functions associated with Fourier analysis are automatically orthogonal with respect to equally-spaced points of measurement; hence, the computational problems of least squares fitting are greatly simplified.

The basic data are for the six time blocks 0000-0400, 0400-0800, 0800-1200, 1200-1600, 1600-2000, 2000-2400 in local time. Zacharisen and Jones assumed the data for each time-block could be represented by the central hour, so that the diurnal variation was defined at the 6 hours 0200, 0600, 1000, 1400, 1800, 2200, in LT. We let $y_1, y_2, \ldots, y_6$ denote the six time block values $y_{m,n}$ at λ_m, Θ_n corresponding to the hour angles

$$t_i = 15i - 30,\ i = 2,6,\ldots,22 \tag{11}$$

respectively. By Fourier analysis of the data for these six hours, a continuous diurnal representation is given by

$$Y(t_i) = a_o + \sum_{j=1}^{2} \{a_j \cos jt_i + b_j \sin jt_i\} + a_3 \cos 3t_i \qquad (12)$$

where the Fourier coefficients are given by

$$\left.\begin{aligned} a_o &= \frac{1}{6} \sum_h y_h \\ a_j &= \frac{1}{3} \sum_h y_h \cos jt_1 \\ b_j &= \frac{1}{3} \sum_h y_h \sin jt_i \end{aligned}\right\} \quad j = 1,2 \qquad (13)$$

$$a_3 = \frac{1}{6} \sum_h (-1)^{h-1} y_h$$

Here $\sum_h$ denotes a sum over h = 1, 2, ..., 6. In equation (13) it was assumed that the initial time value was at 0000 rather than 0200 hours. This required a phase shift of 30 degrees in equation (11).

Figures 4-6 are examples of such a Fourier representation. The curves labeled 2.5 harmonics were obtained using equations (11) through (13). The curves labeled 2.0 harmonics are for the case when a_3 was set to zero or only five coefficients were used. As can be seen six data values (shown by ■) are represented exactly by the Fourier representation using the complete set of six coefficients; whereas, the set of five coefficients produce values as much as 5 dB off at the original data points.

By means of the Fourier representation, a computer program, called DATA FOUR, determined these six Fourier coefficients for each of the UT hours h = 0000, 0400, 0800, 1200, 1600, 2000 at each of the 8400 grid points (λ_m, Θ_n) for each season. A second program, called UT ANOIS, computed values of $y_{m,n}^{(h)}$ F_{am} for each of the UT hours h = 0000, 0400, 0800, 1200, 1600, 2000, at each of the 8400 grid points (λ_m,Θ_n) and stored them on magnetic tape. The UT grid points are coincident with that for the LT maps, and each UT grid contains 84 longitude by 100 latitude points.

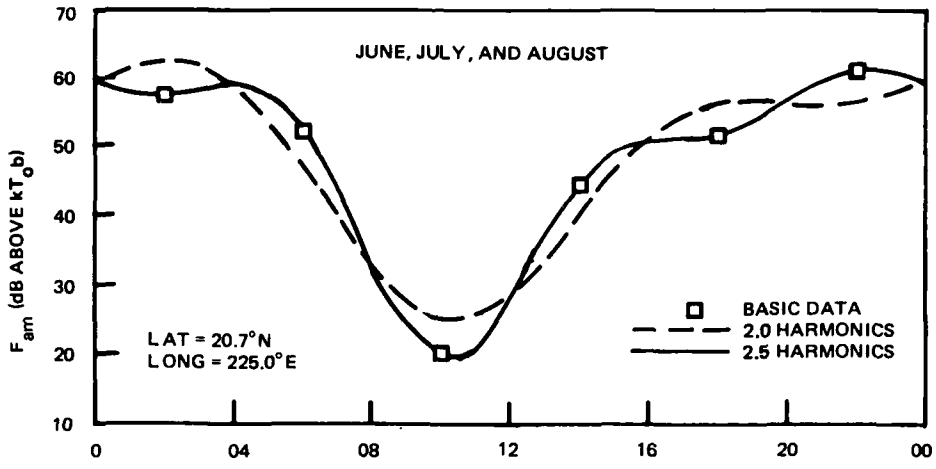

Figure 4. Diurnal variation of basic atmospheric noise data, June, July, August (20.7°N,225.0°E)

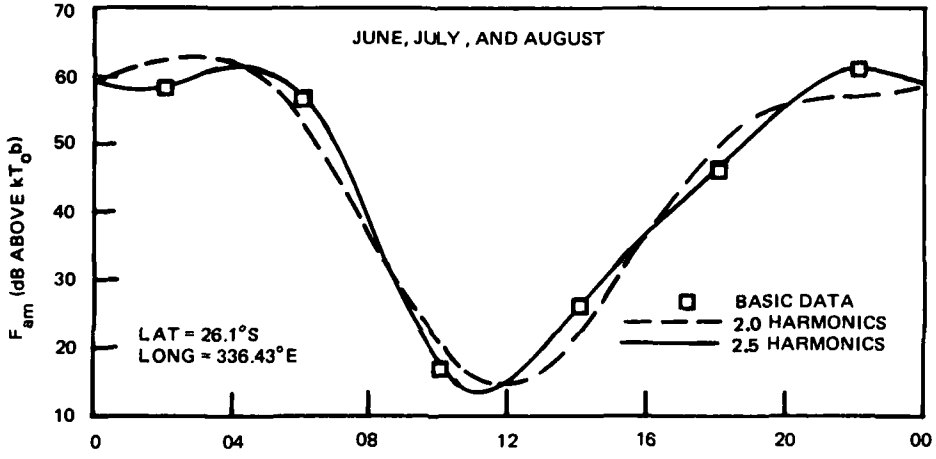

Figure 5. Diurnal variation of basic atmospheric noise data, June, July, August (26.1° S, 336.43°E)

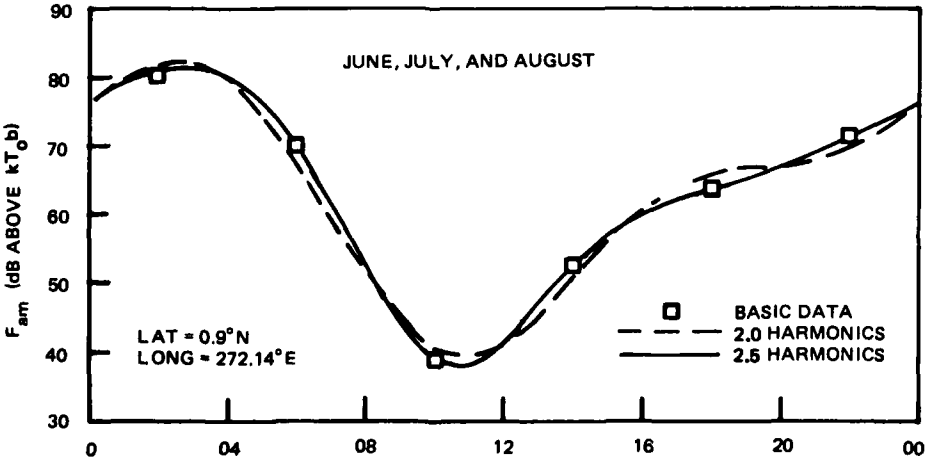

Figure 6. Diurnal variation of basic atmospheric noise data, June, July, August (0.9°N, 272.14°E)

LONGITUDINAL VARIATION FOR FIXED LATITUDE

The first step in representing the worldwide geographic variation of the atmospheric noise parameter F_{am} for a fixed hour of UT and a fixed 3-month season is to hold the latitude λ_m fixed and consider the representation of the periodic function of longitude Θ defined at 84 equally spaced points Θ_n. Zacharisen and Jones Fourier analyzed the data $y^{(h)}_{m,n}$ at the data points (λ_m, Θ_n) using an expression of the form

$$Z_{h,m}(\Theta) = a^{(h)}_{m,o} + \sum_{j=1}^{J} \left[a^{(h)}_{m,j} \cos j\Theta + b^{(h)}_{m,j} \sin j\Theta \right], \tag{14}$$

where J denotes the number of harmonics ($2J + 1 \leq N = 84$). The coefficients are defined by the relationships

$$a^{(h)}_{m,o} = \frac{1}{N} \sum_{n=1}^{N} y^{(h)}_{m,n}$$

$$a^{(h)}_{m,j} = \frac{2}{N} \sum_{n=1}^{N} y^{(h)}_{m,n} \cos j\Theta_n , \tag{15}$$

$$b^{(h)}_{m,j} = \frac{2}{N} \sum_{n=1}^{N} y^{(h)}_{m,n} \sin j\Theta_n .$$

At the outset, it was not known precisely how many harmonics would be needed to provide an adequate fit for the longitudinal variation. Zacharisen wrote a computer program called FOUR RESD to analyze both the mapping residual and the coefficients themselves to aid in the determination of the number of harmonics to be used. The program determines the standard deviation of the

mapping residual for J = 5 to 25 where the residual equals the evaluation of $y^{(h)}_{m,n}$ at each longitude using the Fourier coefficients minus the actual value of $y^{(h)}_{m,n}$. The quantity

$$e_{m,J} = \left[\frac{D^2_{m,J}}{84-2J-1} \right]^{1/2} \tag{16}$$

is used as an estimate of the standard deviation of the residuals, 84-2J-1 being the number of degrees of freedom after subtracting one for each term in equation (14). The square of the residuals is given by

$$D^2_{m,J} = \sum_{n=1}^{84} \left[y^{(h)}_{m,n} - Z_{h,m}(\theta_n) \right]^2 \tag{17}$$

In addition it calculates the average Fourier spectra (means of 100 values). Fourier spectra are calculated using

$$\left[C^{(h)}_{m,j} \right]^2 = \left[a^{(h)}_{m,j} \right]^2 + \left[b^{(h)}_{m,j} \right]^2 . \tag{18}$$

The results indicated to Zacharisen and Jones that the series could be terminated at J=10 resulting in 21 coefficients for each latitude. Rarely did they feel that J need be larger than 17.

Having determined the necessary maximum number of harmonics J for the longitudinal variation, Zacharisen wrote a computer program, called UT FOUR, to calculate the coefficients $a^{(h)}_{m,j}$ and $b^{(h)}_{m,j}$ in equation (14) at each latitude λ_m for each hour h and each season. Fourier coefficients for harmonics up to J=18 were output on a data tape. As these coefficients are orthogonal (the elimination of one does not affect the value of another), the number used in practice can be reduced.

LATITUDINAL VARIATION OF FOURIER COEFFICIENTS

Having determined the longitudinal variation in the equation (14) using $a_{m,j}^{(h)}$ and $b_{m,j}^{(h)}$ for fixed latitudes λ_m, the latitudinal variation of the Fourier coefficients themselves can be represented by series of the form

$$\begin{aligned} a_{h,j}(\lambda) &= \sum_{k=0}^{K} p_{j,k}^{(h)} G_{j,k}(\lambda), \; j = o, 1, \ldots, J=10 \\ b_{h,j}(\lambda) &= \sum_{k=0}^{K} q_{j,k}^{(h)} G_{j,k}(\lambda), \; j = 1,2, \ldots, J = 10, \end{aligned} \tag{19}$$

where the latitude functions $G_{j,k}(\lambda)$ are defined by

$$G_{j,k}(\lambda) = \sin^k \lambda \cos^j \lambda \tag{20}$$

Here λ denotes the geographic latitude $-90° \leq \lambda \leq 90°$. The function $G_{j,k}(\lambda)$ $j \neq 0$ has a built-in constraint at the geographic poles ($\lambda = \pm 90°$) in that the cosine factor is equal to zero. This property resembles that of the classical Legendre polynomials. However orthogonal series of Legendre tend to blow up near the end points.[11] The function given in (20) is as stable at the end points as in the center.

The coefficients $p_{j,k}^{(h)}$ and $q_{j,k}^{(h)}$ were determined by the method of least squares using the FORTRAN program UT NEQSOL.[12,13] The estimates of standard deviations of residuals $E_{j,k}$ and $F_{j,k}$ given as follows

$$E_{j,k} = \left\{ \sum_{m=1}^{100} \left[a_{m,j}^{(h)} - a_{h,j} (\lambda_m)^{*2} \right] / (100-K-1) \right\}^{1/2}$$

$$F_{j,k} = \left\{ \sum_{m=1}^{100} \left[b_{m,j}^{(h)} - b_{h,j} (\lambda_m)^{*2} \right] / (100-K-1) \right\}^{1/2} \qquad (21)$$

were used to measure the goodness of the approximation. Here 100-K-1 is the number of degrees of freedom remaining after subtraction of one degree for each term in the series for $a_{h,j}(\lambda)$ or $b_{h,j}(\lambda)$. Zacharisen and Jones plotted $E_{j,k}$ and $F_{j,k}$ against K for several hours and seasons. They determined that K=9 was a good average cutoff, which was used for harmonics $0 \leq j \leq 7$. For harmonics j = 8, 9, and 10, they choose the cutoff K = 6. This results in 192 coefficients per hour season to represent 8400 data points.

These analyses also showed that an average cutoff of K=6 for all harmonics would result in only a small increase in the variance of the residuals and would provide large reductions in storage of coefficients and in computer time required to evaluate the numerical map. Using K=6 results in 147 coefficients per hour per season to represent F_{am}. However, because the functions used in (19) are not orthogonal, the whole series must be recomputed if terms at the end of the series are to be cut off.

TWO-DIMENSIONAL GEOGRAPHIC REPRESENTATION

Thus far we have described a representation of the two-dimensional geographic representation of F_{am} at 1 MHz for a fixed UT hour h and season. This representation has the form

$$X_h(\lambda, \theta) = \sum_{k=0}^{K} p_{o,k}^{(h)} G_{o,k}(\lambda)$$

$$+ \sum_{j=1}^{J} \left\{ \left(\sum_{k=0}^{K} p_{j,k}^{(h)} G_{j,k}(\lambda) \right) \cos j\theta \right. \tag{22}$$

$$\left. + \left(\sum_{k=0}^{K} q_{j,k}^{(h)} G_{j,k}(\lambda) \right) \sin j\theta \right\}$$

where K=9 for $0 \leq j \leq 7$, K=6 for j = 8, 9, 10, and J = 10. $G_{j,k}(\lambda)$ is given by equation (20). The coefficients $p_{j,k}^{(h)}$ and $q_{j,k}^{(h)}$ are found using UT NEQSOL as described in the previous section for 6 hours of UT, h=0000, 0400, 0800, 1200, 1600, 2000 for each 3-month season.

Zacharisen and Jones carried the mapping progress one step further. The numerical coefficients from UT NEQSOL were Fourier analyzed in UT by a program called UT FOUR3, producing one map for each three-month season. They originally used six coefficients for this purpose, but later dropped the highest order time harmonic coefficient. Their final map was 192 x 5 = 960 coefficients.

DETERMINATION OF MODEL ACCURACY

The approach taken in the development of the model was that several versions would be produced - each with a different number of coefficients representing F_{am} in each time block. Then the accuracy of these versions was to be determined as a function of the number of harmonics in the representation (number of coefficients). The user would choose the version with an error he would be willing to accept consistent with the memory space available in his micro-mini-computer.

There are two methods for assessing the accuracies of the models. The first would be to study the residuals between values $y_{m,n}^{(h)}$ of F_{am} and corresponding values computed from the numerical map using equation (22). The second would be to produce UT contour maps of F_{am} in dB above $kT_o b$. Examination of the geographical detail for each of the versions would indicate differences between the various choices.

In the comparisons to follow, the accuracies are given in terms of the longitudinal harmonic number J and the latitudinal harmonic number K. Table 1 gives the number of coefficients as a function of these maximum harmonic numbers.

	NUMBER OF COEFFICIENTS		
J	K = 9	K = 6	K = 4
10	192	147	105
9	178	133	95
8	164	119	85
7	150	105	75
6	130	91	65
5	110	77	55
4	90	63	45
3	70	49	35
2	50	35	25
1	30	21	15

Table 1. Number of Coefficients as a Function of the Longitude and Latitude Maximum Harmonic Numbers

MAPPING RESIDUALS

To develop a sufficient knowledge about the capabilities of the various versions of the representation of F_{am} possible, residuals were computed between values $y^{(h)}_{m,n}$ of F_{am} and corresponding values computed from numerical maps using equation (22). The term residual is used with the following meaning:

$$\text{residual} = (\text{predicted value}) - (\text{observed datum}). \tag{23}$$

Certain statistical measures of this term have proved useful in past studies in comparing predicted and observed data. These include the average residual (av. res.) and the root mean square residual (rms res.). The average residual locates the center of the distributions of error and is often referred to as the bias in the estimate. The root mean square residual is a measure of the dispersion in the error. In fact, the rms res. is the standard deviation of the error about the origin (zero bias) and is related to the standard deviation about the mean according to

$$\sigma^2 = \nu_2 - \nu_1^2 \tag{24}$$

where ν_2 is the mean square error (the square of the rms error) and ν_1 is the bias. When the bias is small or nearly zero, then the standard deviation and the rms error are nearly the same. Otherwise, the rms error is larger than the standard deviation.

The sampling of $y^{(h)}_{m,n}$ consisted of values at a rectangular array defined by the intersections of 42 equally spaced longitudes and 30 equally spaced latitudes between $\lambda = 81°N$ and $\lambda = 81°S$, or about one-sixth of the original grid of 100 latitude by 84 longitude $y^{(h)}_{m,n}$ data points. Since residuals at the high latitudes $|\lambda| > 81°$ were considerably larger, they were omitted from these computations.

For comparison, Table 2 gives the rms error for Zacharisen and Jones model.[3] Examination of the table reveals that the rms error is largest during the summer months of June, July and August. The largest dispersion in the rms error with time occurs during the spring months of March, April and May. The bias for the Zacharisen and Jones model is for all practical purposes zero.

Hour (UT)	December January February	March April May	June July August	September October November
0000	1.66	1.35	2.07	1.43
0400	1.53	1.34	2.11	1.45
0800	1.71	1.57	2.08	1.57
1200	1.84	1.74	1.94	1.69
1600	1.54	1.42	1.93	1.49
2000	1.41	1.30	1.97	1.28
Average	1.62	1.45	1.01	1.49
Std. Dev.	0.15	0.17	0.08	0.14

Table 2. RMS Residual in dB of the Zacharisen and Jones Model.

The initial comparison was for the maximum number of harmonics K for the latitudinal variation equal 9. The maximum number of harmonics J for the longitudinal variation was varied from 1 to 10. The bias was found to be practically zero. Figure 7 shows how the average rms error in dB varies with longitudinal harmonic number J; the average is the average over the six hours of the day. In the figure winter means December, January, February; spring means March, April, May; summer means June, July, August; and fall means September, October, November. For J equal 5 through 10 there is little

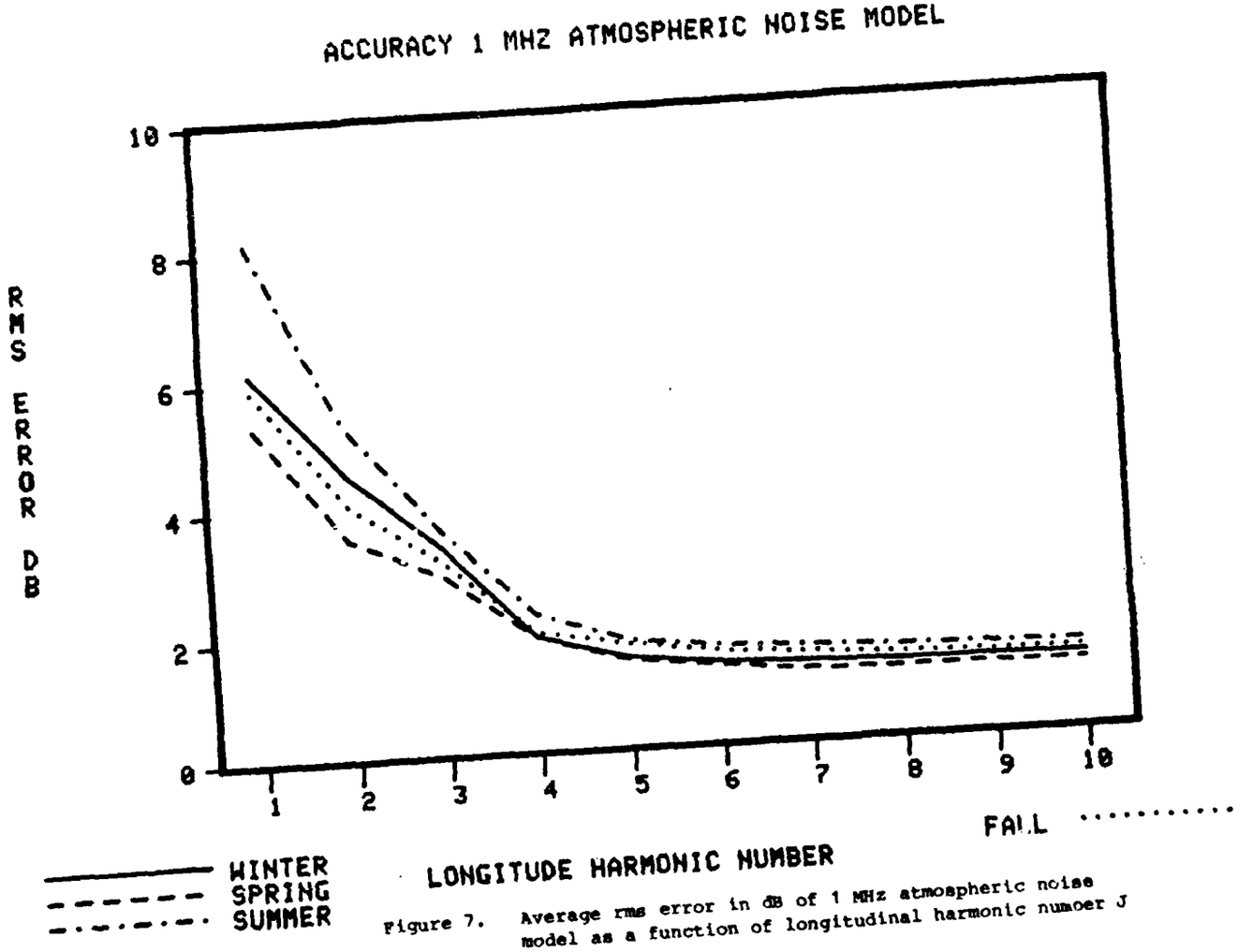

Figure 7. Average rms error in dB of 1 MHz atmospheric noise model as a function of longitudinal harmonic numoer J (K=9)

variation in the rms error except for the seasonal difference. Below J=5 there is a rapid increase of rms error with decreasing J. In fact at J=1, the summer has an rms error of 8.2 dB. Figure 8 gives the standard deviations with time of the rms error. The standard deviation does not vary appreciably for J=5 to J=10 but rapidly increases with decreasing J below 5.

The next step was to assess the effect of allowing the maximum number of harmonics K for the latitudinal variation to vary. Since the functions used in the latitudinal variation are not orthogonal, it was necessary to run the computer program UT NEQSOL for each value of K being considered. In addition coefficients previously determined for K=9, coefficients were also calculated for K=6 and K=4. These were then used to determine the residuals as a function of longitudinal harmonic number J and season. In all cases the bias was practically zero. Figures 9-12 present the average rms error over time as a function of longitudinal harmonic number. Figure 9 is for the winter season of December, January, and February; figure 10 is for the spring season of March, April and May; figure 11 is for the summer season of June, July, and August; and figure 12 is for the fall season of September, October, and November. In all of the figures, there are two apparent effects. The first is in the region for J=5 to J=10. In this range the variation is mainly due to changing K. The effect of changing J is not as pronounced here as below J=5. The change caused by varying K is not consistent from season to season; the change is most pronounced in the winter and summer season. Here again it is not linear. During winter it changes slower than during the summer months. Below J=5, even though the average rms error increases with decreasing value of K, the main effects are caused by decreasing J. This is particularly true at J=2 and below.

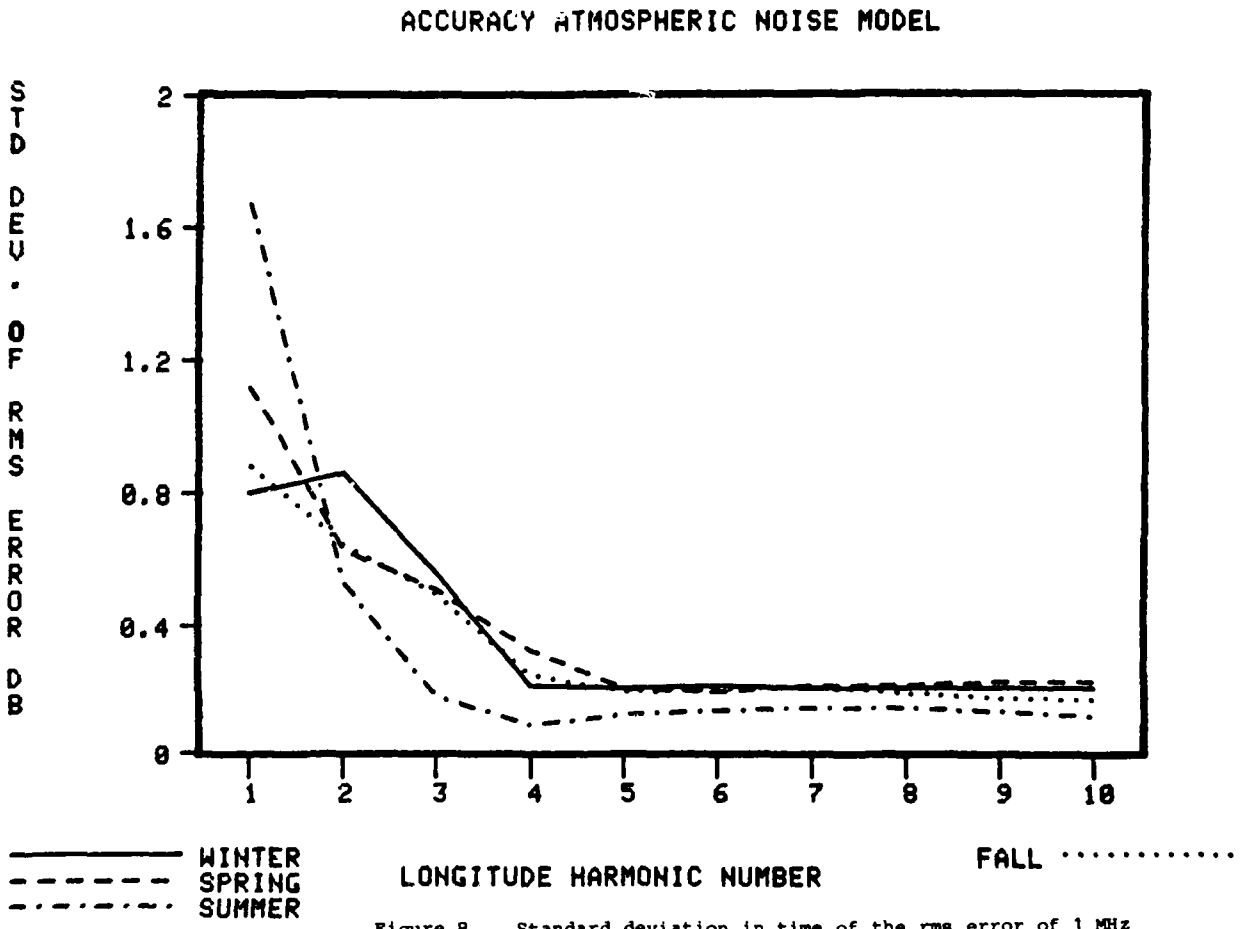

Figure 8. Standard deviation in time of the rms error of 1 MHz atmospheric noise model as a function of longitudinal harmonic number J (K=9)

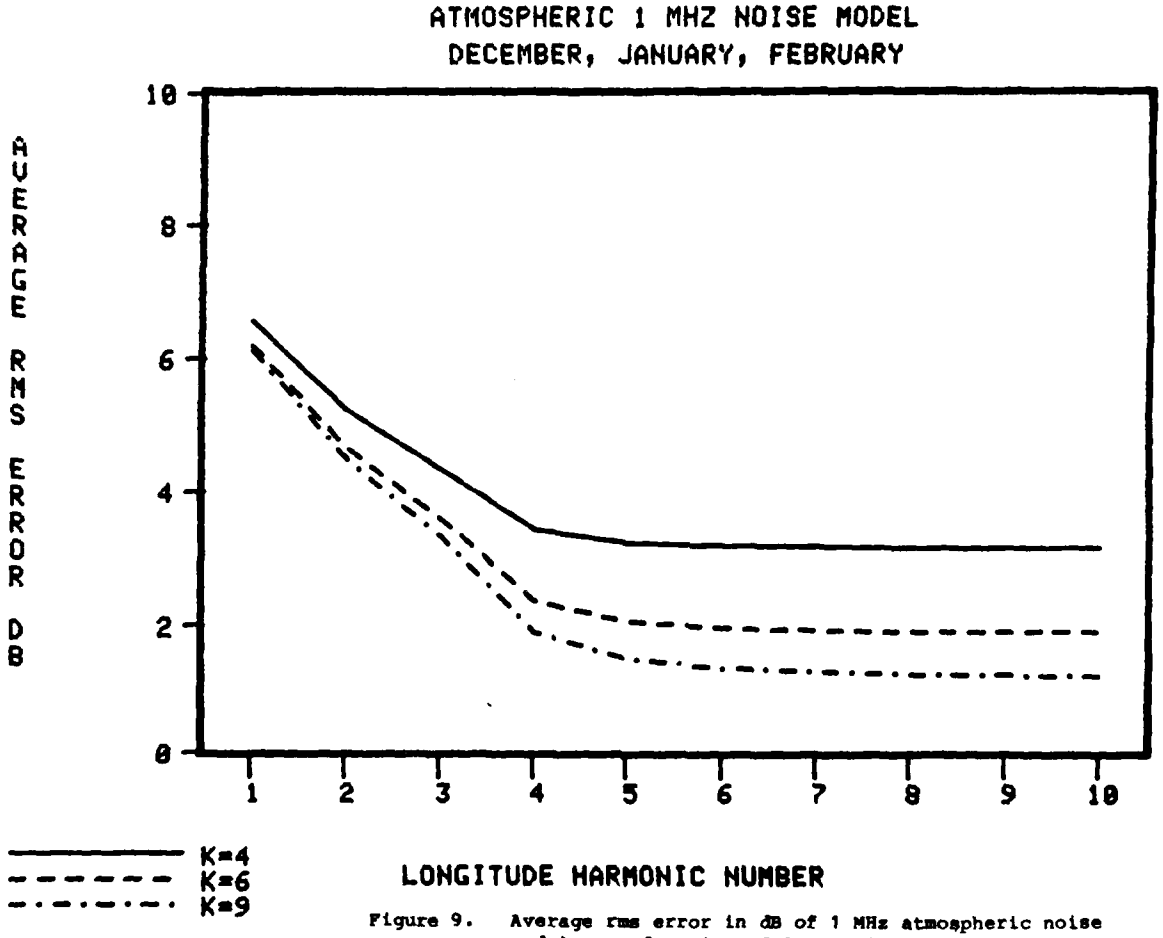

Figure 9. Average rms error in dB of 1 MHz atmospheric noise model as a function of latitudinal and longitudinal harmonic numbers, December, January, February

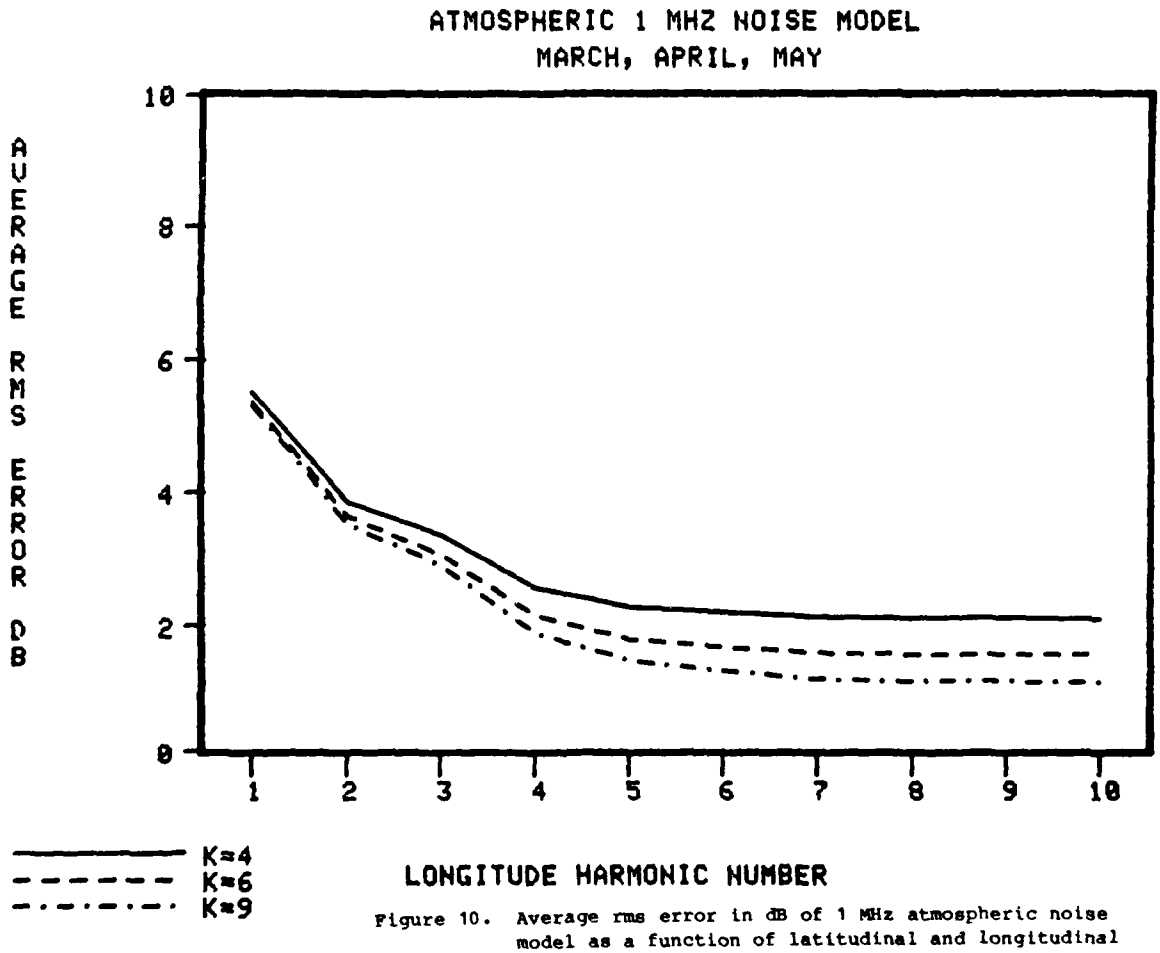

Figure 10. Average rms error in dB of 1 MHz atmospheric noise model as a function of latitudinal and longitudinal harmonic numbers, March, April, May

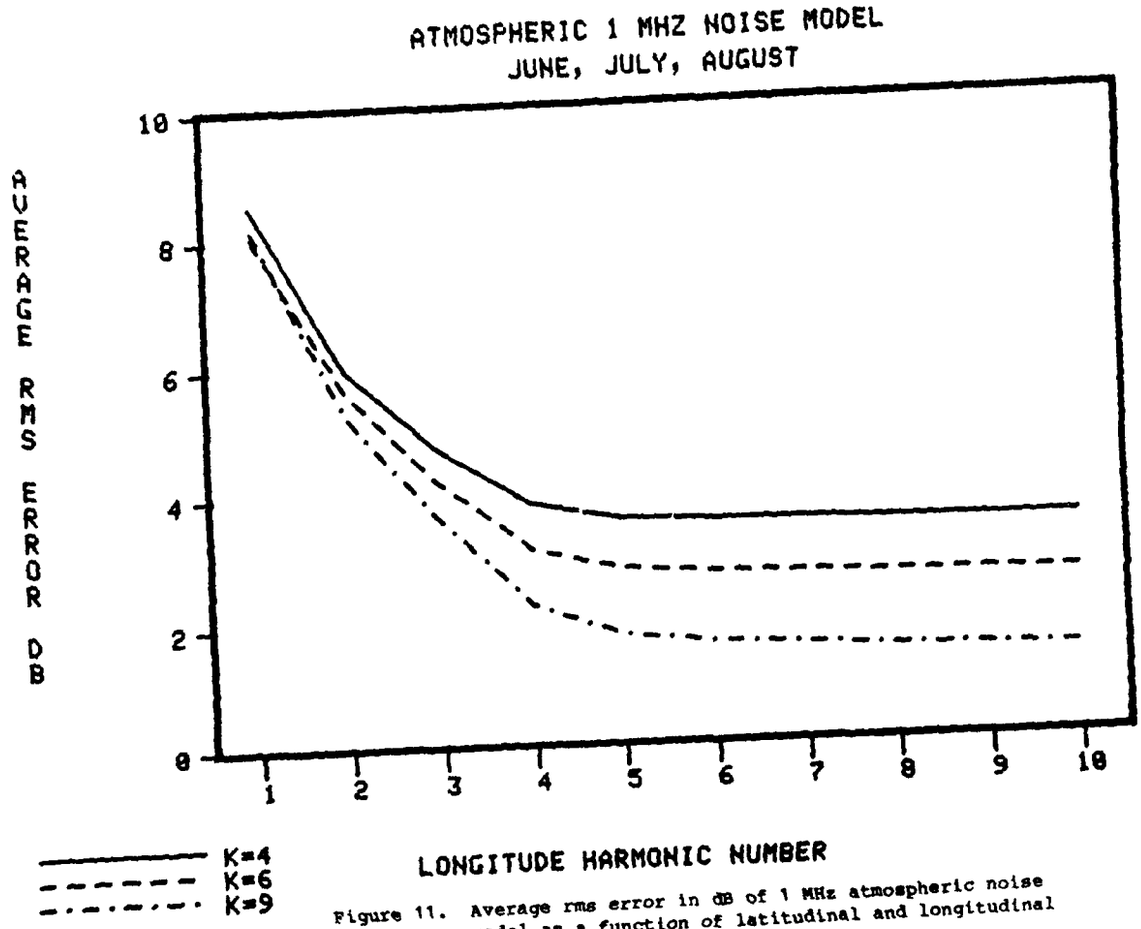

Figure 11. Average rms error in dB of 1 MHz atmospheric noise model as a function of latitudinal and longitudinal harmonic numbers, June, July, August

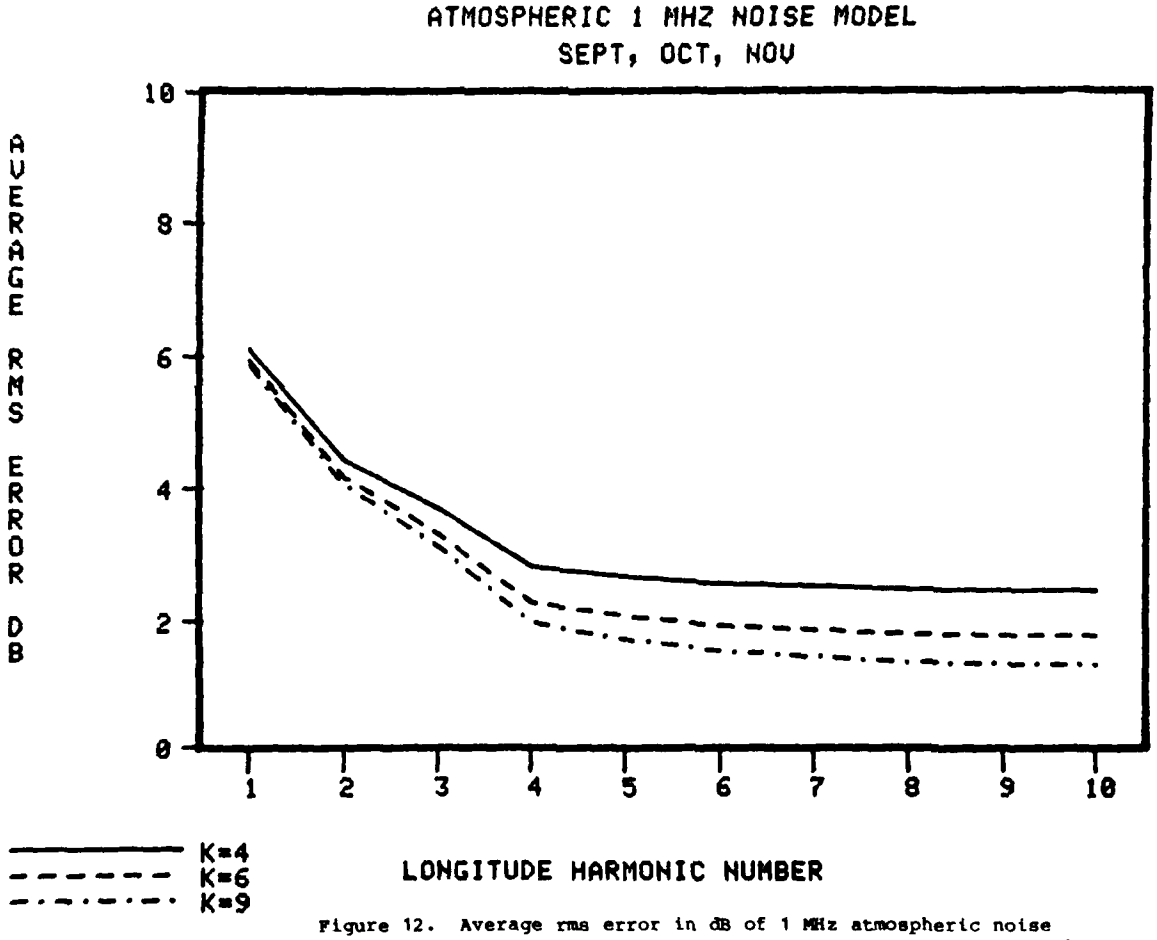

Figure 12. Average rms error in dB of 1 MHz atmospheric noise model as a function of latitudinal and longitudinal harmonic numbers, September, October, November

WORLD MAP CONTOURS

Using a computer evaluation of the numerical maps, one can produce UT contour maps of F_{am} in dB above $KT_o b$ directly on a plotter. This is particularly useful in making choices between the various models. Examination of the geographical detail will reveal missing contours of importance. The absence of contours of high level would be particularly significant.

Contour maps were plotted for the hours 0000 and 1200 during the seasons December, January, February and June, July, August. A contour map was drawn for each harmonic number combination of J=10 and K=9; of J=5 and K=9,6,4; and of J=2 and K=9,7. A contour plot was also drawn for each hour and season for the Zacharisen and Jones model. Figures 13-19 are for hour=0000 during June, July, and August. Because the residual analysis showed this hour and season to have a particularly high rms error, it was chosen to illustrate the effects of reducing the number of coefficients. A contour map is also included for the Zacharisen and Jones model for the same hour and season. The remaining contour maps are presented in Appendix A.

Figure 13 is for the Zacharisen and Jones model, and Figure 14 is for the model with J=10, K=9. There is slightly more detail in Figure 14 in the equatorial region. In particular there is a contour in Figure 14 of 10 dB/kTb missing in Figure 13. Also, in the left portion of Figure 13 for the Zacharisen and Jones model, the detail is smoothed out more. In the northern polar regions there is a break in the 20 dB/kTb contour level in Figure 14 missing in Figure 13. Figure 15 for J=5, K=9 is very much like that for the Zacharisen and Jones model except it has a little more detail in the polar region.

As the number of harmonics is reduced further, the high level contours begin to disappear. In Figure 16 for J=5, K=6 two high level contours disappeared -- a 85 $dB/kT_o b$ and a 90 $dB/kT_o b$ in the equatorial region. Also a 20 $dB/kT_o b$ contour level curve disappeared in the northern polar region. In Figure 17 for J=5, K=4; there is a considerable loss of detail on the righthand in the equatorial region. Both Figures 18 for J=2, K=9 and 19 for J=2 and K=6, show a loss of detail over the whole contour plot from the previous versions. This is more noticeably true in the latter.

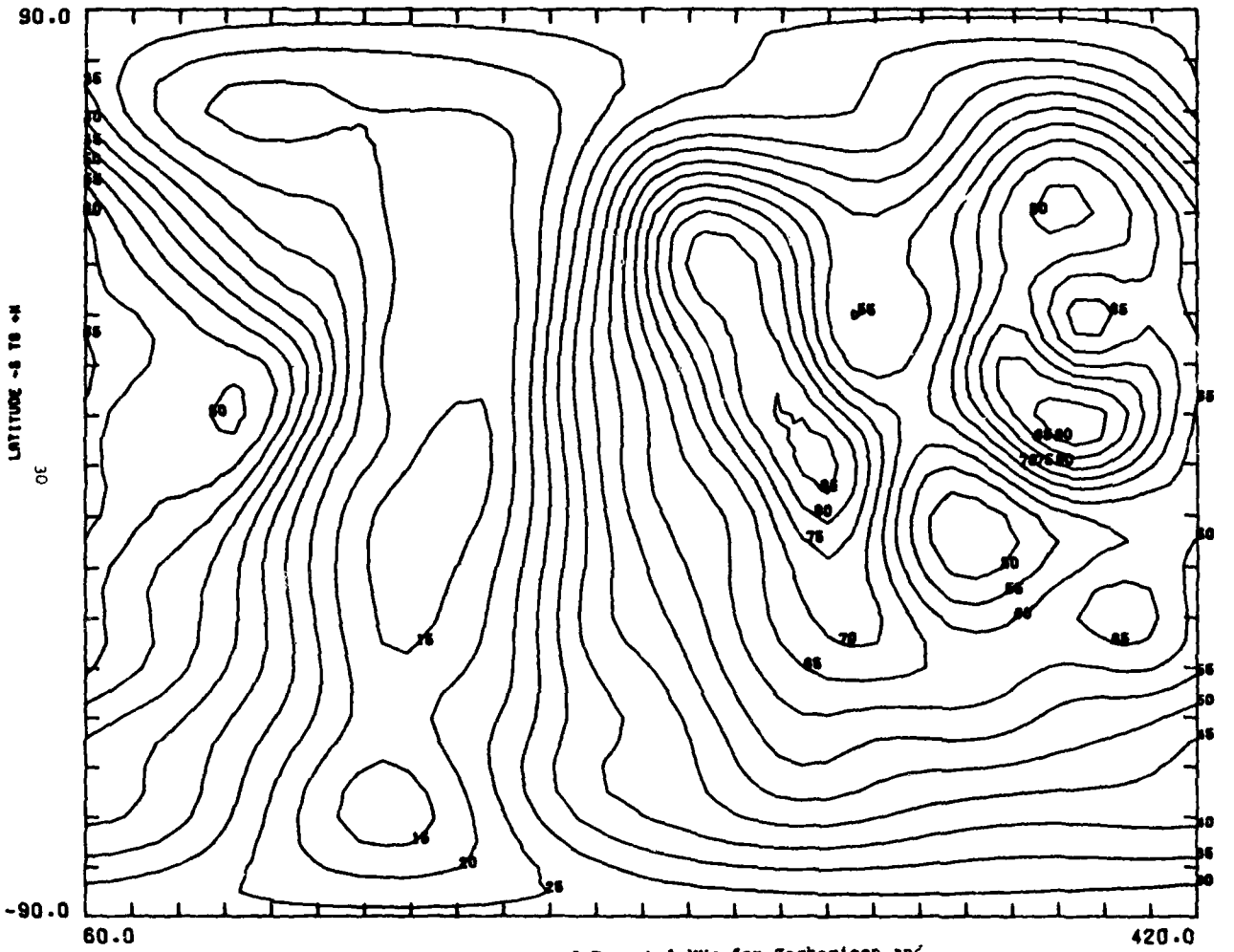

Figure 13. World contour map of F_{am} at 1 MHz for Zacharisen and Jones model for June, July, August 0000 hrs UT

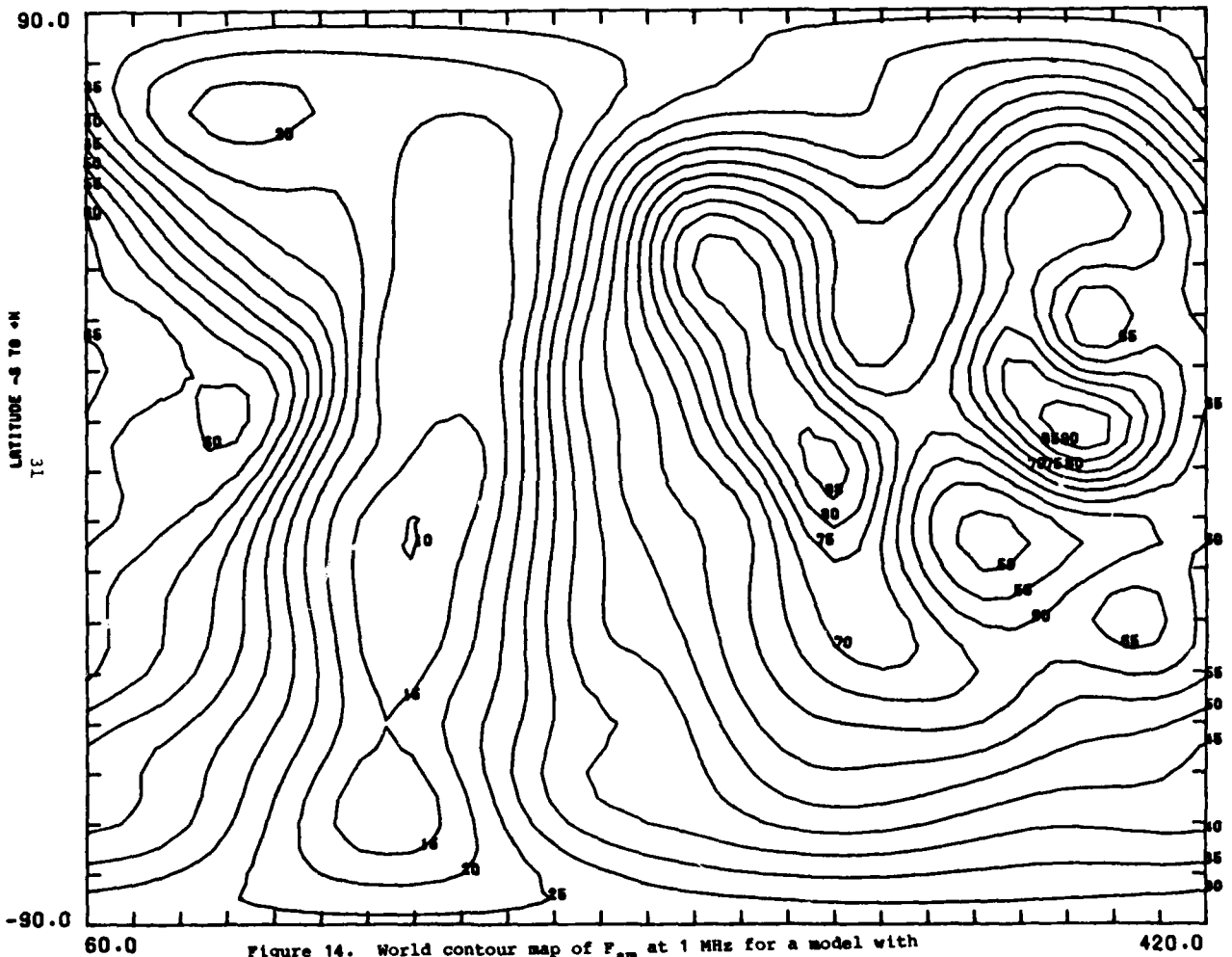

Figure 14. World contour map of F_{am} at 1 MHz for a model with 192 coefficients per time block (J=10, K=9) for June. July, August 0000 hrs UT

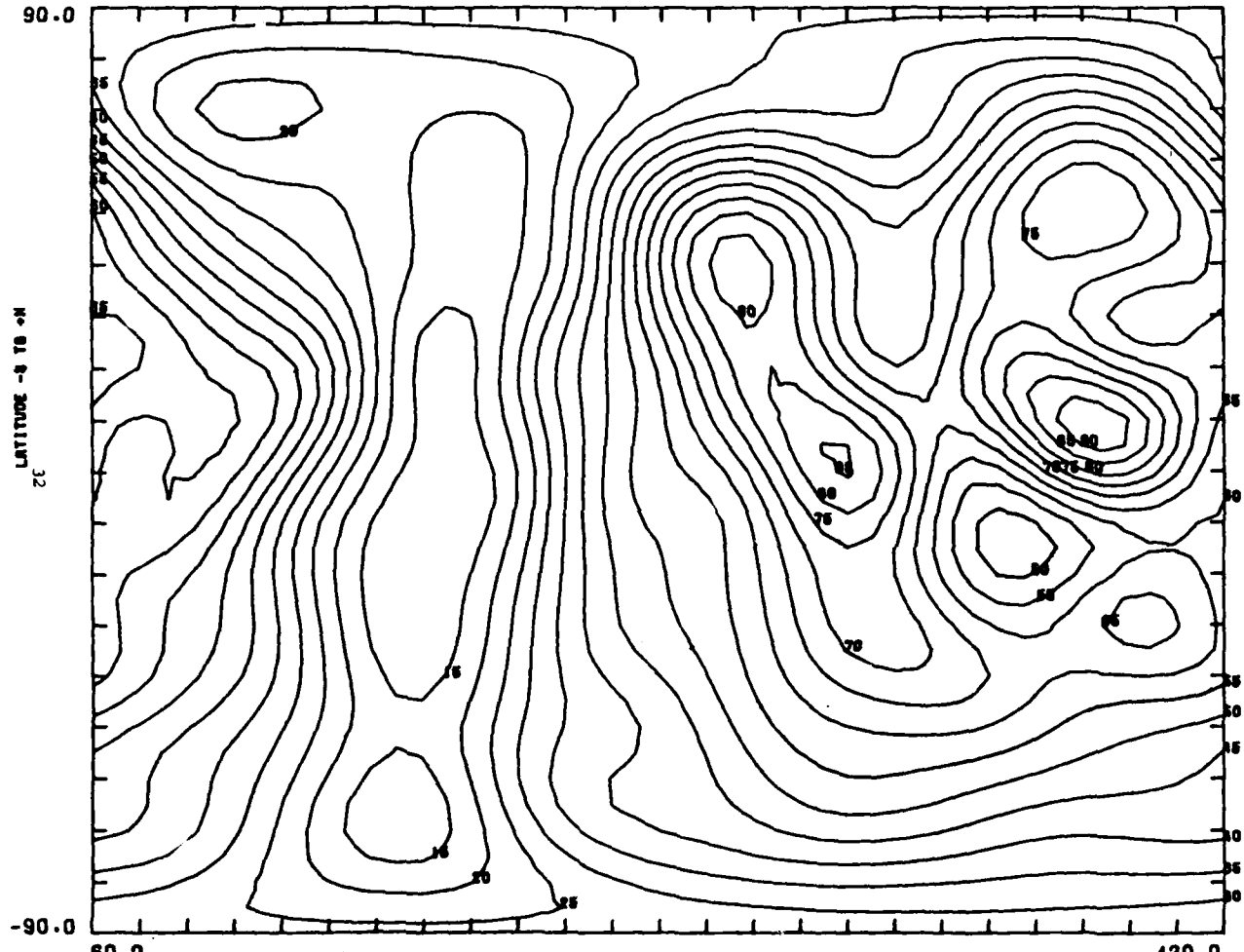

Figure 15. World contour map of F_{am} at 1 MHz for a model with 810 coefficients per time block (J=5, K=9) for June, July, August 0000 hrs UT

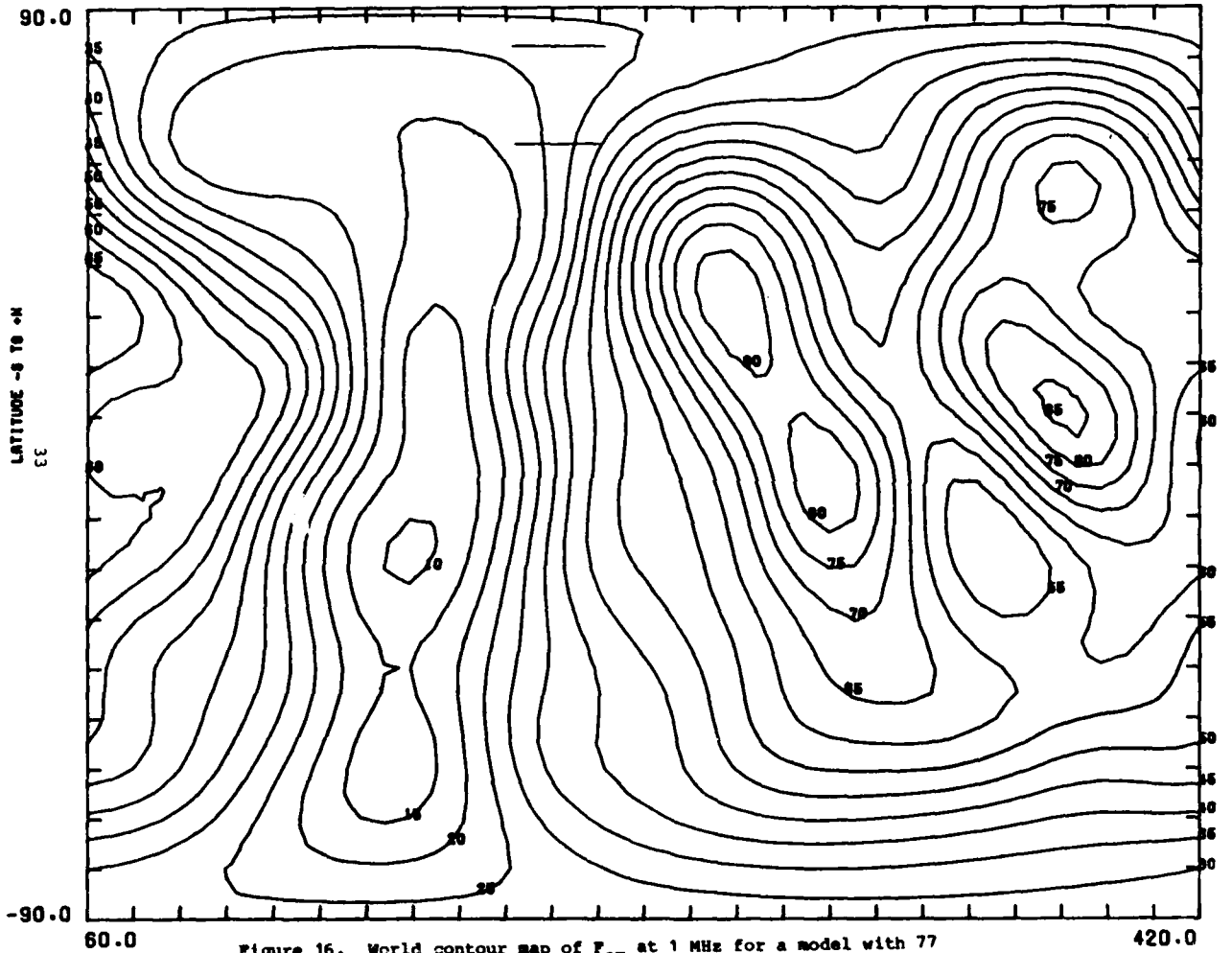

Figure 16. World contour map of F_{am} at 1 MHz for a model with 77 coefficients per time block (J=5, K=6) for June, July, August 0000 hrs UT

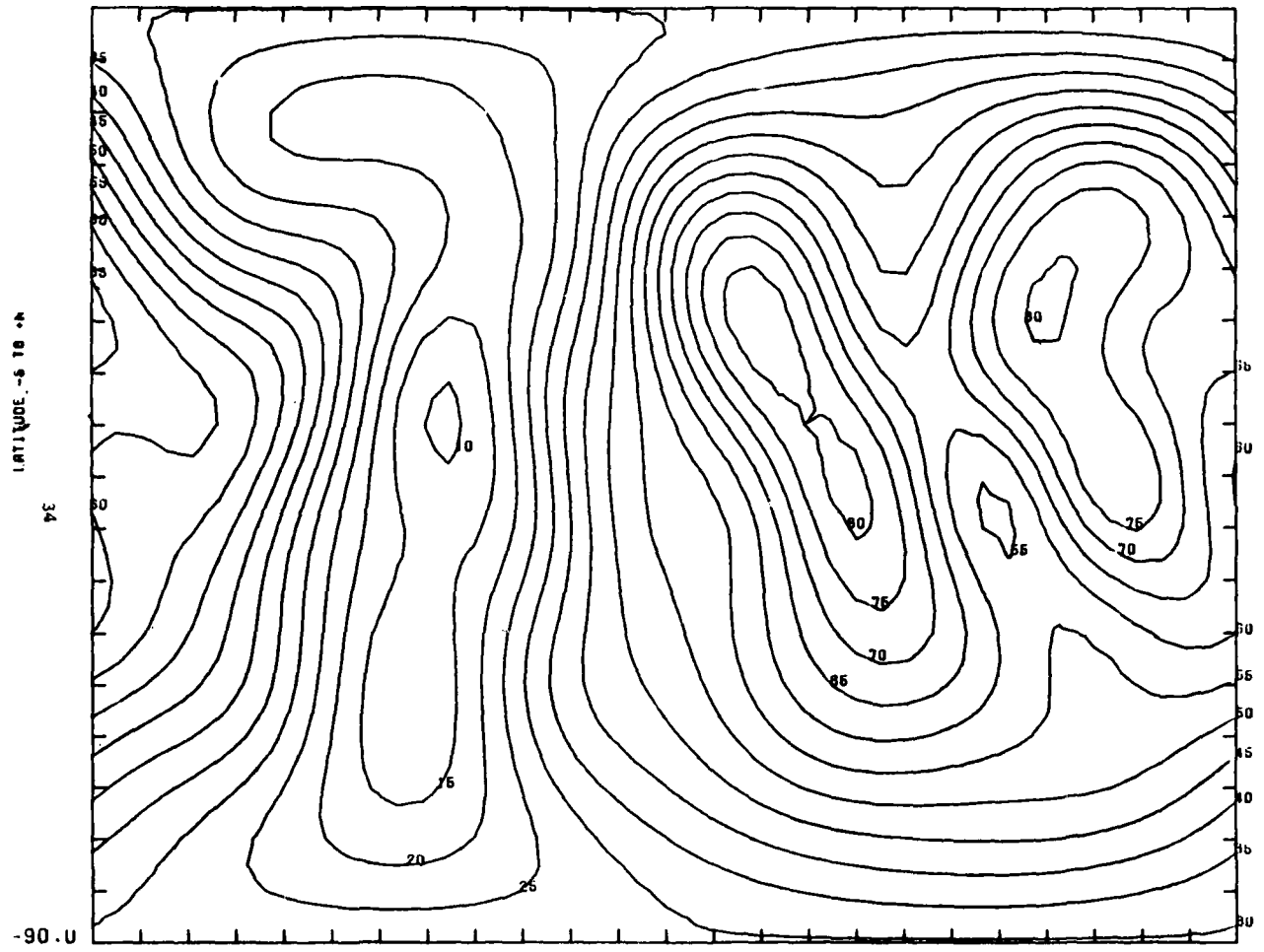

Figure 17. World contour map of F_{am} at 1 MHz for a model with 55 coefficients per time block (J=5, K=4) for June, July, August 0000 hrs UT

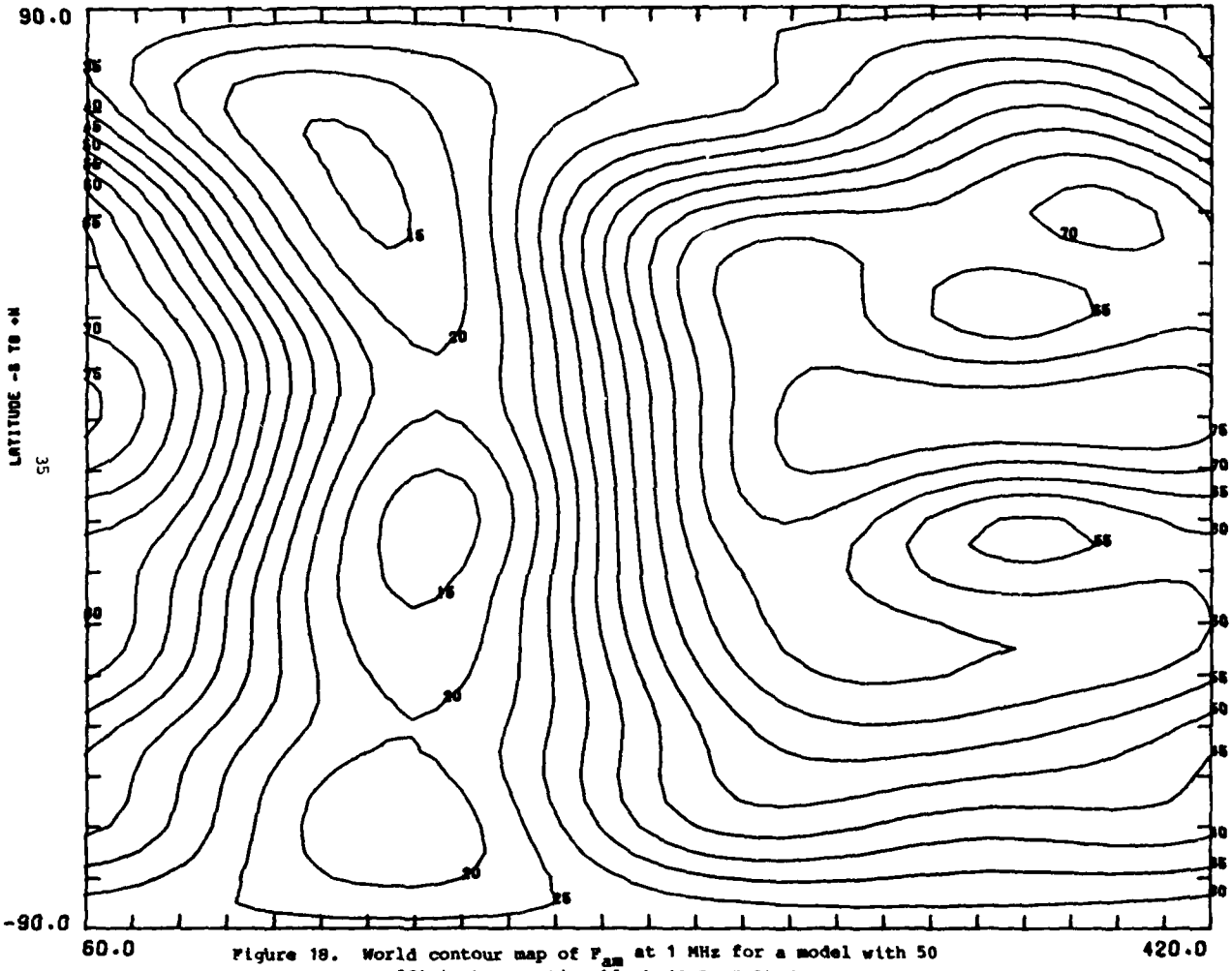

Figure 18. World contour map of F_{am} at 1 MHz for a model with 50 coefficients per time block (J=2, K=9) for June, July, August 0000 hrs UT

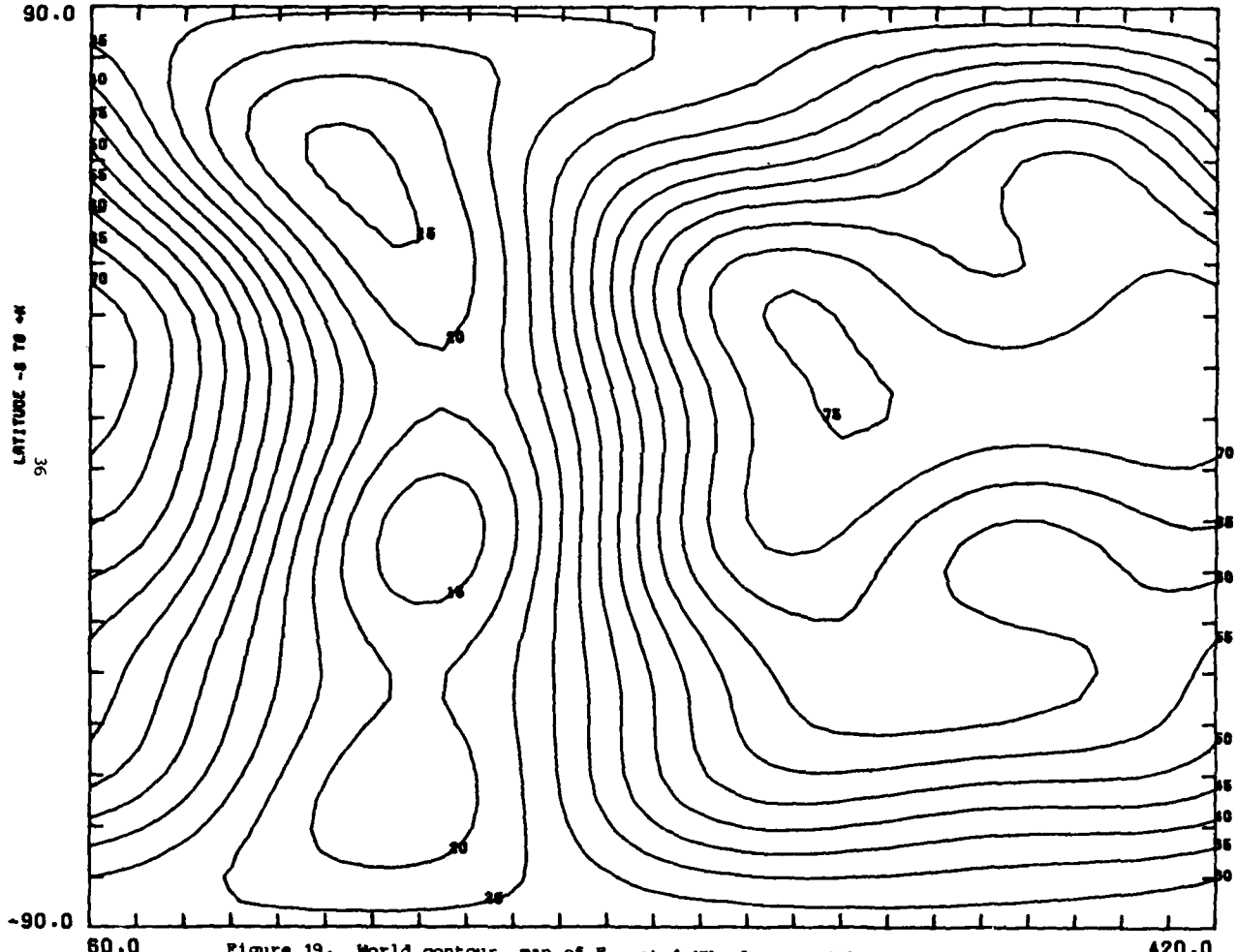

Figure 19. World contour map of F_{am} at 1 MHz for a model with 35 coefficients per time block (J=2, K=6) for June, July, August 0000 hrs UT

DISCUSSION OF RESULTS

This report presented the development of several minicomputer atmospheric noise models. This was done using the Zacharisen and Jones numerical mapping techniques. Several versions were produced -- each with a different number of coefficients representing F_{am} in each time block. The accuracies of these versions were presented in the previous section as a function of the number of harmonics in the representation (number of coefficients). The user then can choose the version with an error he could accept consistent with the memory space available in his micro-mini-computer.

It is the purpose of this section to provide some guidance in the selection of a model, to review methods available for interpolation between time blocks, and to describe how these model values of F_{am} can be used with values of F_{am} produced by models of man-made noise and galactic noise.

CHOICE OF MODEL

In addition to the memory space available in a particular minicomputer, several other factors would influence the choice of a noise model. These include the accuracy of the CCIR 322 noise data used to generate the models, the accuracy of the Zacharisen and Jones model, and the accuracy of the noise models.

Accuracy of CCIR 322 Noise Data

In the previous section the accuracy of the noise model was determined by determining the residuals with the data used to generate the models. These data were the same as those used to generate the contour plots in CCIR Report 322. Hence the accuracy of these data has some bearing on the choice of models. If the rms residual is low compared to the error of the CCIR 322 data, then it is probably an acceptable model. However, if it is nearly equal to or larger than that for the CCIR 322 noise data, then combined errors would be a better indicator of the actual error in the model.

The error in the values of F_{am} presented in CCIR Report 322 is given for each time block for each season as $\sigma_{F_{am}}$. It appears as a curve as a function of frequency like Figure 3.

Hour LT	December January February	March April May	June July August	September October November
00-04	4.6	3.7	5.6	3.9
04-08	4.2	5.0	7.0	4.5
08-12	4.5	6.0	7.7	4.9
12-16	4.8	6.3	9.0	6.0
16-20	4.7	4.5	5.9	4.4
20-24	5.3	3.9	4.8	4.3
Average	4.68	4.90	6.67	4.67

Table 3. Standard Deviation (dB) of F_{am} Values ($\sigma_{F_{am}}$) at 1 MHz from CCIR Report 322.

Table 3 gives values of σ_{Fam} at 1 MHz for each of the seasons and time blocks. It also gives the average over time of σ_{Fam}. Note that there is considerably more error in CCIR Report 322 in the June, July, August season. Hence a slight increase in rms residual in a model for this season might not be as important as the error in the data used to generate the model.

Accuracy of Zacharisen and Jones Model

In the previous section, Table 2 gave the rms error for the Zacharisen and Jones model. Table 4 given below gives the average rms error for the Zacharisen and Jones model along with the average error for the CCIR 322 data. Examination of the table shows the error in the Zacharisen and Jones model is well below that of the CCIR 322 data. Because the bias in the Zacharisen and Jones model is nearly zero, its rms error is approximately equal to the standard deviation of the residuals. Assuming that the rms residual of F_{am} of this model and the standard deviation of F_{am} values used to generate the model are independent, then the total error in the model is given by the square root of the sums of the squares of the two errors. This is also given in Table 4.

Season	December January February	March April May	June July August	September October November
Average rms residual (dB)	1.62	1.45	2.02	1.49
Average $\sigma_{F_{am}}$ at 1 MHz	4.68	4.90	6.67	4.67
Combined	4.95	5.11	6.97	4.90

Table 4. Comparison of the Accuracy of the Zacharisen and Jones Atmospheric Noise Model and the standard deviation of F_{am} values used to generate the model.

Accuracy of Minicomputer Models

Table 5 compares the accuracy of the several minicomputer models and that of the standard deviation $\sigma_{F_{am}}$ used to generate the models. The table gives the number of coefficients per time block and the longitude and latitude maximum harmonic numbers J and K, respectively. As can be seen from the table, a large number of coefficients (i.e., 192 of 110) results in a rms error much lower than that of the CCIR 322 data. Whereas, a small number of coefficients (i.e., 50 and 35) results in a rms error approaching that of the CCIR 322 F_{am} values. Between these two extremes are the models with 77 and 55 coefficients, respectively. The model with 55 coefficients appears to be a good model when a small number of coefficients is desired. Note that the model for 192 coefficients per time block is more accurate than the Zacharisen and Jones model, and that the model using 110 coefficients is more accurate than the Zacharisen and Jones model except during the September, October, November season.

Number of Coefficients	J	K	December January February	March April May	June July August	September October November
192	10	9	1.21	1.10	1.40	1.29
110	5	9	1.48	1.44	1.76	1.71
77	5	6	2.05	1.78	2.80	2.07
55	5	4	3.24	2.28	3.57	2.67
50	2	9	4.51	3.52	5.25	4.05
35	2	6	4.68	3.64	5.63	4.16
average $\sigma_{F_{am}}$ at 1 MHz from CCIR Report 322			4.68	4.90	6.67	4.67

Table 5. Accuracy of Minicomputer Atmospheric Noise Models.

INTERPOLATION WITH TIME

Because there is a separate numerical map of F_{am} for each of the UT hours h = 0000, 0400, 0800, 1200, 1600, 2000, it is often necessary to interpolate between these hours to get F_{am} at a particular receive site.

An alternate approach to the standard linear interpolation, would be to use a finite Fourier series for interpolation in much the same way that the LT data were converted to UT data points. The main difference here is that the formula for the hour angle given in equation (11) is replaced by

$$t_i = 15\ i \qquad , i = 0, 4, 6, \ldots, 20. \tag{25}$$

By Fourier analysis of $F_{am}^{(h)}$ for these six hours, a continuous diurnal representation is given by

$$Y(t_i) = a_o + \sum_{j=1}^{2} \{a_j \cos jt_i + b_j \sin jt_i\} + a_3 \cos 3\ t_i \tag{26}$$

where the Fourier coefficients are given by

$$\left.\begin{aligned} a_o &= \frac{1}{6} \sum_h F_{am}^{(h)} \\ a_j &= \frac{1}{3} \sum_h F_{am}^{(h)} \cos j\ t_i \\ b_j &= \frac{1}{3} \sum_h F_{am}^{(h)} \sin j\ t_i \\ a_3 &= \frac{1}{6} \sum_{h=1}^{6} (-1)^{h-1} F_{am}^{(h)} \end{aligned}\right\} \quad j=1,2 \tag{27}$$

Here $\sum_h$ notes a sum over h = 0000, 0400, 0800, 1200, 1600, and 2000. Having obtained the coefficients in (27), then (26) can be used for the hours $0° \leq t_i \leq 360°$ or $0 \leq i \leq 24$.

MODEL USE WITH OTHER NOISE SOURCES

In the HF band where these models are intended to be used, there are three principal types of environmental noise:

(1) atmospheric from thunderstorms and other types of disturbed weather
(2) cosmic (galactic noise)
(3) man-made

To assess the effect of radio noise on a receiver system it is necessary to calculate the combined noise power available from an equivalent loss free antenna.

Atmospheric

Atmospheric noise as calculated by these models is usually the dominant type of noise at HF, especially in the lower portion of the band. It is also the most erratic of the three major types of noise. It may change over wide limits as a function of location, frequency, bandwidth, time of day, season, solar activity, and azimuthal direction. Although in the presence of local storms atmospheric noise may be an important factor at almost any frequency; it is the ability of noise from distant thunderstorms to propagate over long distances that makes it so important at HF and below. Because ionospheric absorption is high during the daytime, the contribution from distant sources is reduced, and local sources become important. Because of the strength of propagated noise from distant storms at night, the diurnal maximum occurs at night - even for locations in the earth's major source regions.

For the purposes of combining the component noise into one, denote atmospheric noise at a particular frequency by N_a and its variability by D_{ua} and D_{la}.

Cosmic

Cosmic noise is thermal noise that originates outside the earth and its atmosphere. It includes both solar radio noise and noise from interstellar space.

The low frequency cutoff of cosmic noise is determined by the peak density of the ionosphere; radio waves of frequency less than the critical frequency of the F-region cannot penetrate to the earth. Cosmic noise starts to become an important factor near the frequencies where propagated atmospheric noise drops due to lack of ionospheric support and absorption. Because the existence of cosmic noise at the ground depends upon the critical frequency of the F-region, it is necessary to estimate the critical frequency in order to determine whether cosmic noise should be considered. On the other hand, it is not desirable to insert a major portion of an HF skywave prediction program in a minicomputer to see whether galactic noise should be considered. Because cosmic noise is rarely the dominant type of noise for an HF system in the ambient environment except at the highest frequencies and at very quiet receiving sites, it suffices to determine the maximum expected median f_oF2 for low, moderate, and high sunspot levels for each season. This was accomplished by examining contour plots of f_oF2 for sunspot numbers, 10, 110, and 160.[14-17] The maximum contour value for each month was determined for each sunspot level. Then the average of the three monthly values was chosen as the value to be used for the maximum expected median f_oF2. The values so determined are presented in table 6. These values are to be interpolated for the actual sunspot number, and cosmic noise is then to be considered if the operating frequency is above this interpolated frequency.

Sunspot Number	December January February	March April May	June July August	September October November
10	11.3	12.3	10.0	12.0
110	15.0	15.3	13.7	16.7
160	16.0	16.0	14.0	17.3

Table 6. Maximum Median MUF(ZERO)F2

At times when it is possible to see the galaxy at the operating frequency, the median galactic noise is given for a short vertical electric dipole above a perfectly conducting ground screen by

$$N_g = 52.0 - 23.0 \log_{10} f \qquad (28)$$

where

N_g = expected median value of the galactic noise in a 1 Hz band --dB > 1 watt

f = operating frequency -- MHz.[1]

The variability of galactic noise (D_{ug} and D_{lg}) can be taken to 2 dB about the median.

Man-made Noise

At certain receiving locations, unintended man-made radio noise may be the predominant external noise with which the communication system must compete. It may arise from any number of sources, such as power lines, industrial machinery, ignition systems, etc., and thus it may have wide geographic and short term variations. Because it propagates primarily by the ground wave and along power lines, its range of effects is limited and its average value depends primarily on the location of the receiving site relative to the sources.

A major advance in environmental noise level documentation was made when workers at the U. S. Department of Commerce Institute for Telecommunications Sciences (ITS) used the same measurement system to obtain noise data in the band 250 kHz to 250 MHz with a short vertical antenna near ground at various sites in the United States.[18] Three environmental categories were designated: rural, residential, and business. Rural areas were defined as locations where land usage is primarily for agricultural or similar pursuits, and dwellings are no more than one every five acres. Residential areas (urban or suburban) were defined as any area used predominantly for single or multiple family dwellings with a density of at least two family units per acre and no large or busy highways. A business area was defined as any area where the predominant usage throughout the area is for any type of bsiness (shopping centers, main streets or highways lined with various business enterprises, etc.). Further limited measurements relate to parks and university campuses (which generally have less vehicular traffic, electrical equipment and other types of noise sources than business or residential areas) and relate to interstate highways (where the main source is ignition noise).

The results of the measurements were analyzed statistically and least-squares fits for F_{am} were obtained. In all cases results were consistent with a linear variation of the median value, F_{am}, with frequency f of the form

$$N_m = c - d \log_{10} f \qquad (29)$$

with f expressed in MHz, and c and d taking the values given in table 7. Using the data given by Spaulding and Disney,[18] Hagn and Sailors[19] found that the time and location variability of man-made noise could be represented by a simple Gaussian model. The standard deviations for this model are given in table 8.

Environmental Category	c	d
Business	76.8	27.7
Interstate Highways	73.0	27.7
Residential	72.5	27.7
Parks and University Campuses	69.3	27.7
Rural	67.2	27.7

Table 7. Values of the constant c and d in the Equation for F_{am} for Man-Made Noise

Freq. (MHz)	Business		Residential		Rural	
	F_{am}	σ_{NM} (dB)	F_{am}	σ_{NM} (dB)	F_{am}	σ_{NM} (dB)
1.00	76.8	6.3	72.5	6.5	67.2	9.5
2.50	65.8	12.4	61.5	10.4	56.2	10.2
5.00	57.4	9.2	53.1	8.4	47.8	9.4
10.00	49.1	7.7	44.8	6.1	39.5	6.8
20.00	40.8	8.7	36.5	8.3	31.2	6.9
48.00	30.2	11.1	25.9	8.8	20.6	4.5

Table 8. Summary of Man-Made Noise Model Parameters.

Combination of Noise

When the noise received is due to several different sources, the component noise will combine into one, taking the different phases into account. In this case, these phases are independent and continuously variable. Hence, the noise power in watts can be summed. The resultant median noise is given by

$$N = 10 \log_{10} (10^{N_a/10} + 10^{N_g/10} + 10^{N_m/10}) \quad (30)$$

where N_a is the atmospheric noise in a 1 Hz band -- dB above 1 watt. Figure 20 shows the quadratic addition chart for two signals. If two noise sources are within 3 dB of each other, then an additional 1.76 dB of noise is received. On the other hand, if the two sources are within only 6.02 dB of each other, the additional noise is 0.976 dB. Finally, if the two sources are separated by 12.04 dB, the additional noise due to a second source would be 0.26 dB.

The upper and lower decile differences from the median noise are found also by summing the upper and lower deciles of the noise in watts, converting the deciles back to decibels, and subtracting the median noise. The resulting expressions are:

$$D_{NU} = |10 \log_{10}(10^{(N_a + D_{ua})/10} + 10^{(N_g + D_{ug})/10} + 10^{(N_m + 1.28\sigma_{NM})/10}) - N| \quad (31)$$

$$D_{N\ell} = |10 \log_{10}(10^{(N_a + D_{la})/10} + 10^{(N_g + D_{lg})10} + 10^{(N_m + 1.28\sigma_{Nm})/10}) - N| \quad (32)$$

where D_{ua} and D_{la} are the upper and lower deciles of atmospheric noise. The results of equations (31) and (32) can be used to determine circuit reliability.

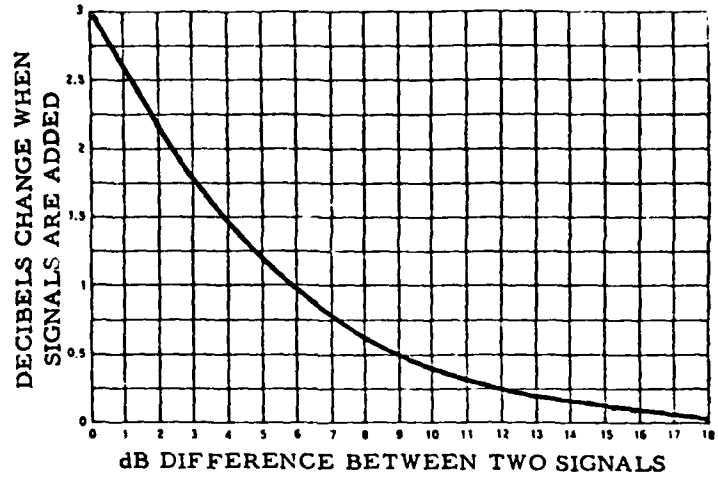

Figure 20. Quadratic addition chart for two signals in dB

CONCLUSIONS

Practical but simplified atmospheric noise models were developed for use in estimating system signal-to-noise ratios in micro-mini-computer based HF propagation prediction systems. The numerical mapping techniques of Zacharisen and Jones were used to represent worldwide atmospheric noise at 1 MHz. Each four-hour time block was represented separately rather than for a twenty-four hour day. This resulted in 24 numerical maps: one for each of six 4-hour time blocks (in universal time, UT) and each of four 3-month periods. This method provided a numerical representation of atmospheric noise with a minimum reduction (by one-fifth) from the number of coefficients used by Zacharisen and Jones in computer storage at one time. The remaining coefficients would be stored in the computer's cassette tape unit. The simpler expression for the median noise levels (F_{am}) results in significant savings in computer code and time. Several versions were produced-each with a different number of coefficients (number of harmonics) in the Fourier representation in each time block. The models produced make use of the frequency dependence model of earlier representations of CCIR Report 322.

The accuracy of these model versions was determined as a function of the number of harmonics in the representation. The average (bias) and rms residual was determined between values of F_{am} used to develop the model and the corresponding values computed from each numerical model. In all cases the bias was nearly zero. The significance of the rms residual was determined by comparing the value of each version to the published accuracy of the CCIR 322 noise data used to generate the models.

The average rms error for the Zacharisen and Jones model for all hours and seasons was 1.65 dB. Its worst season; June, July, and August; had an rms error of 2.02 dB. The corresponding rms errors for the CCIR data were 5.48 dB and 6.97 dB, respectively. The Zacharisen and Jones model rms error is much smaller than the CCIR 322 data.

The average rms error for all times and seasons for the model using 192 coefficients per time block was 1.25 dB. Its worst season was the June, July, August season, which had an rms error of 1.4 dB. These errors were well below that of the CCIR 322 noise data and are even less than that of the Zacharisen

and Jones model. The most suitable application for this version would be in Advanced Prophet applications or in a large scale HF prediction model.

The average rms error for all times and seasons for the versions with 110 coefficients was 1.60 dB. For the June, July, August season the error was 1.76 dB. These error figures were well below that of the CCIR 322 data and were slightly less than that of the Zacharisen and Jones model. The reason this model had better accuracy than the Zacharisen and Jones model was that it retained more time information. The most suitable application for this version would be use in Advanced Prophet applications.

The two versions with 77 and 55 coefficients each had an average rms error for all times and seasons of 2.18 dB and 2.94 dB, respectively. During June, July, August, these two versions had a rms error of 2.8 dB and 3.57 dB, respectively. These error figures were still reasonably below that of the CCIR 322 noise data. These models would be suitable for both Advanced Prophet applications and for applications using Tektronix 4052 type mini-computers.

Finally, the two versions with 50 and 35 coefficients each had an average rms error for all times and seasons of 3.64 dB and 4.53 dB, respectively. During June, July, August, these two versions had a rms error of 5.25 dB and 5.63 dB, respectively. These error figures have begun to approach the average rms error of 5.23 dB for the CCIR 322 noise data. These versions would be most suitable for applications for which the memory requirements for the mini-computer demand a sacrifice in the accuracy of the model.

RECOMMENDATIONS

As a result of this study, the following recommendations are made:

1. Fourier series interpolation should be used to obtain F_{am} at 1 MHz for an actual hour of operation;

2. When Fourier series interpolation is not practical, then linear interpolation should be used;

3. Because other noise sources are present at HF, these noise values should also be determined;

4. Galactic noise should only be calculated for frequencies above the maximum expected f_oF2 given herein as a function of sunspot number and season;

5. The formula provided should be used for combining the values of man-made, galactic, and atmospheric noise;

6. The reliability of the combined 1 MHz models and the frequency dependence models should be determined;

7. This reliability should be determined as a function of frequency, time of day, geographic location as well as the maximum longitude and latitude harmonic numbers of the 1 MHz numerical maps;

8. The accuracy of the complete Lucas and Harper Model[2] should be determined with the same data;

9. This reliability analysis should make use of data measured after the data contributing to CCIR Report 322 were measured as well as for data used to develop CCIR Report 322.

REFERENCES

1. International Radio Consultative Committee 10th Plenary Assembly, Geneva 1963, Report 322; World Distribution and Characteristics of Atmospheric Radio Noise Data, International Telecommunications Union, Geneva, 1964.

2. National Bureau of Standards Technical Note 318, A Numerical Representation of CCIR Report 322 High Frequency (3-30 MC/s) Atmospheric Radio Noise Data, by D. L. Lucas and J. D. Harper, Jr. 1965.

3. Office of Telecommunications ITS Research Report 2, World Maps of Atmospheric Radio Noise in Universal Time, by D. H. Zacharisen and W. B. Jones, October (1970).

4. National Bureau of Standards Circular 462, Ionospheric Radio Propagation, June 25, 1948.

5. National Bureau of Standards Circular 557, Worldwide Radio Noise Levels Expected in the Frequency Band 10 Kilocycles to 100 Megacycles, by W. Q. Crichlow, D. F. Smith, R. N. Norton, and W. R. Corliess, August 25, 1955.

6. International Radio Consultative Committee IXth Plenary Assembly, Los Angeles, 1959, Report 65; Revision of Atmospheric Radio Noise Data, International Telecommunications Union, Geneva 1959.

7. National Bureau of Standard Report 7615, A Numerical Representation of Atmospheric Radio Noise in Band 7, by D. L. Lucas and J. D. Harper, Jr., April 12, 1961.

8. Jones, W. B., and Gallet, R. M., "Representation of Diurnal and Geographic Variations of Ionospheric Data by Numerical Methods," J. Res. NBS, Vol. 66D, pp 419-438, July-August 1962.

9. Jones, W. B. and Gallet, R. M., "Methods for Applying Numerical Maps of Ionospheric Characteristics," J. Res. NBS, Vol 66D, pp 649-662, November-December 1962.

10. Jones, W. B. and Gallet, R. M., "The Representation of Diurnal and Geographic Variations of Ionospheric Data by Numerical Methods," Telecommunications Journal, Vol. 29, pp 129-149, 1962.

11. Lanczos, C., "Trigonometric Interpolation of Empirical and Analytical Functions", J. Math. Phys. (Cambridge, Mass.), Vol. 17, pp 144-245, 1938.

12. Environmental Science Service Administration Tech. Rept IER 25-ITSA 25, Application of Numerical Methods of Mapping to Astronomical Surface Photometry, by W. B. Jones, D. L. Obitts, R. M. Gallet, and G. deVaucouleurs, February 1967.

13. National Bureau of Standards Report 8783, A Method and Computer Program for Fitting Large Sets of Data with Functions of Several Variables by Least Squares, by D. L. Obitts, March 25, 1965.

14. Office of Telecommunications, Telecommunications Research and Engineering Report 13, Ionospheric Predictions, Vol. 1, The Estimation of Maximum Usable Frequency from World Maps of MUF(ZERO)F2, MUF(4000)F2 and MUF(2000)E, edited by M. Leftin, Septembe 971.

15. Office of Telecommunications, Telecommunications Research and Engineering Report 13, Ionospheric Predictions, Vol. 2, Maximum Usable Frequencies MUF(ZERO)F2, MUF(4000)F2, MUF(2000)E for a Period of Minimum Solar Activity, R_{12} = 10, by W. M. Roberts and R. K. Rosich, September 1971.

16. Office of Telecommunications, Telecommunications Research and Engineering Report 13, Ionospheric Predictions, Vol. 3, Maximum Usable Frequencies MUF(ZERO)F2, MUF(4000)F2, MUF(2000)E for a Maximum Solar Activity Period of an Above Average Solar Cycle, R_{12} = 110, by W. M. Roberts and R. M. Rosich, September 1971.

17. Office of Telecommunications, Telecommunications Research and Engineering Report 13, Ionospheric Predictions, Vol. 4, Maximum Usable Frequencies MUF(ZERO)F2, MUF(4000)F2, MUF(2000)E for a Maximum Solar Activity Period of an Above Average Solar Cycle, R_{12} = 160, by W. M. Roberts and R. M. Rosich, September 1971.

18. Office of Telecommunications Report 74-38, Man-Made Noise Part 1: Estimates for Business, Residential, and Rural Areas, by A. D. Spaulding and R. T. Disney, June 1974.

19. Hagn, G. H. and Sailors, D. B., Empirical Models for Probability Distributions of Short-term Environmental Man-Made Levels, paper presented at 3rd Symposium and Technical Exhibition on Electromagnetic Compatibility, Rotterdam, May 1-3, 1979.

APPENDIX A

WORLD CONTOUR MAPS OF 1 MHz ATMOSPHERIC NOISE

UT contour maps of F_{am} in dB above KT_ob are particularly useful in making choices between the various 1 MHz atmospheric noise models. The absence of contours of high level or the lack of geographical detail is particularly significant.

The June, July, August season and December, January, February season were chosen to illustrate the effects of reducing the number of coefficients. Contour maps were drawn for the UT hours 0000 and 1200. A contour map was drawn for each harmonic number combination of J=10 and K=9; of J=5 and K=9, 6, 4; and J=2 and K=9, 7. A contour plot was also drawn for each hour and season for the Zacharisen and Jones model. Figures 13-19 in the main body of the report are for the hour = 0000 during June, July, and August. The remaining contour maps are presented here in figures A1-A21.

Figures A1 through A7 are for December, January, February at 0000 hours UT. Figure A1 is for the Zacharisen and Jones model. The remaining six figures are for the six versions of the 1 MHz atmospheric noise model presented in the main text.

Figures A8 through A14 are for December, January, February at 1200 hours UT. Figure A8 is for the Zacharisen and Jones model, and Figures A9-A14 are for the six model versions.

Figures A15 through A21 are for June, July, August at 1200 hours UT. Figure A15 is for the Zacharisen and Jones model, and Figures A16-A21 are for the six model versions being compared.

The same type of variation from contour map to contour map reported on Figures 13-14 also occurs here. For the map versions with J=10, K=9, there is slightly more detail in the equatorial and polar regions than in the Zacharisen and Jones model. The model for J=5, K=9 is very much like that for the Zacharisen and Jones model except there is a little more detail in the

polar regions. As the number of harmonics is reduced further, the high level contours begin to disappear. In the June, July, and August season, this change occurs even with higher order harmonics. For the J =2, K = 9 and for the J = 2, K = 6 cases, there is a loss of detail over the whole contour plot from the versions with larger harmonics.

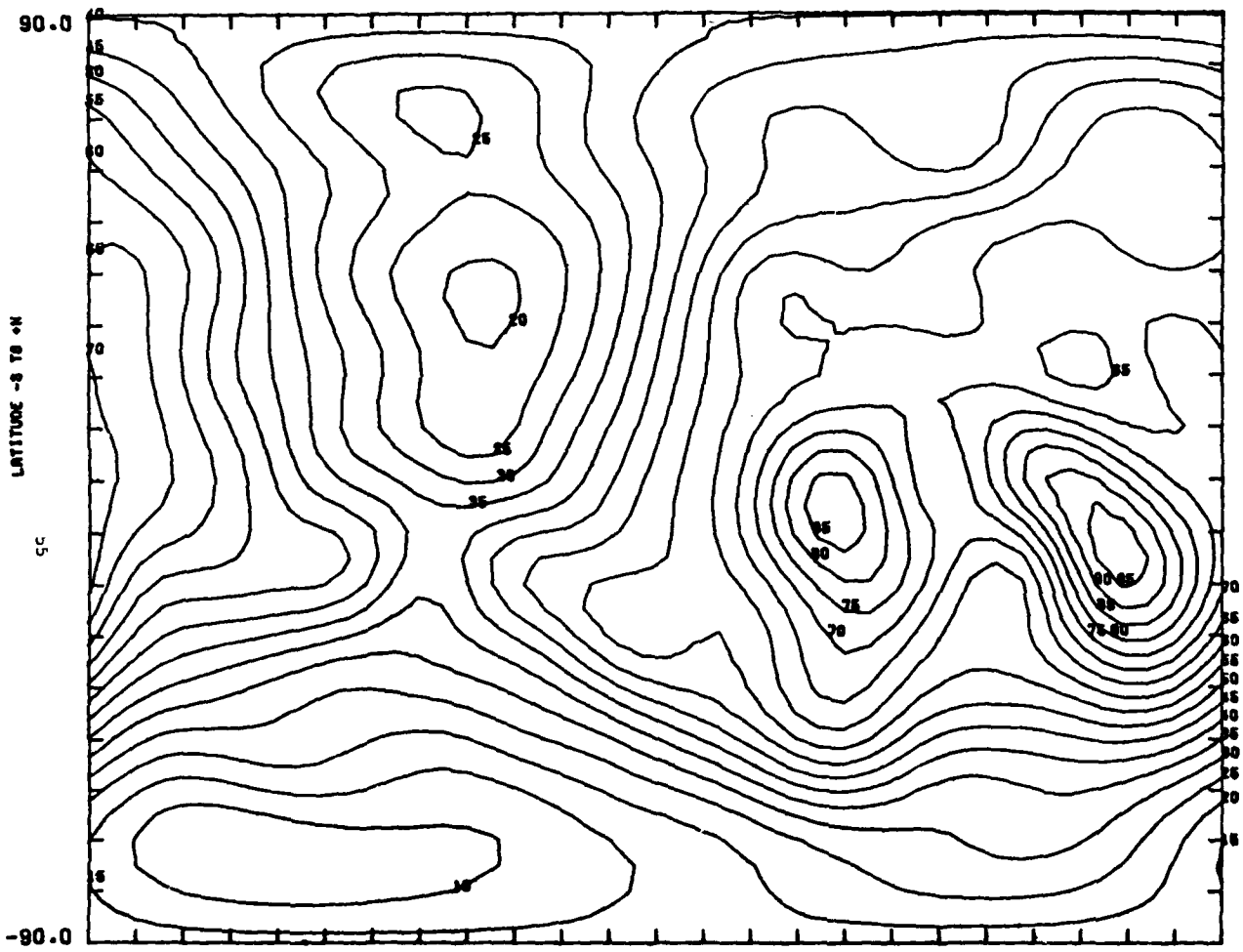

Figure A1 World contour map of F_{am} at 1 MHz for Zacharisen and Jones model for December, January, February 0000 hrs UT

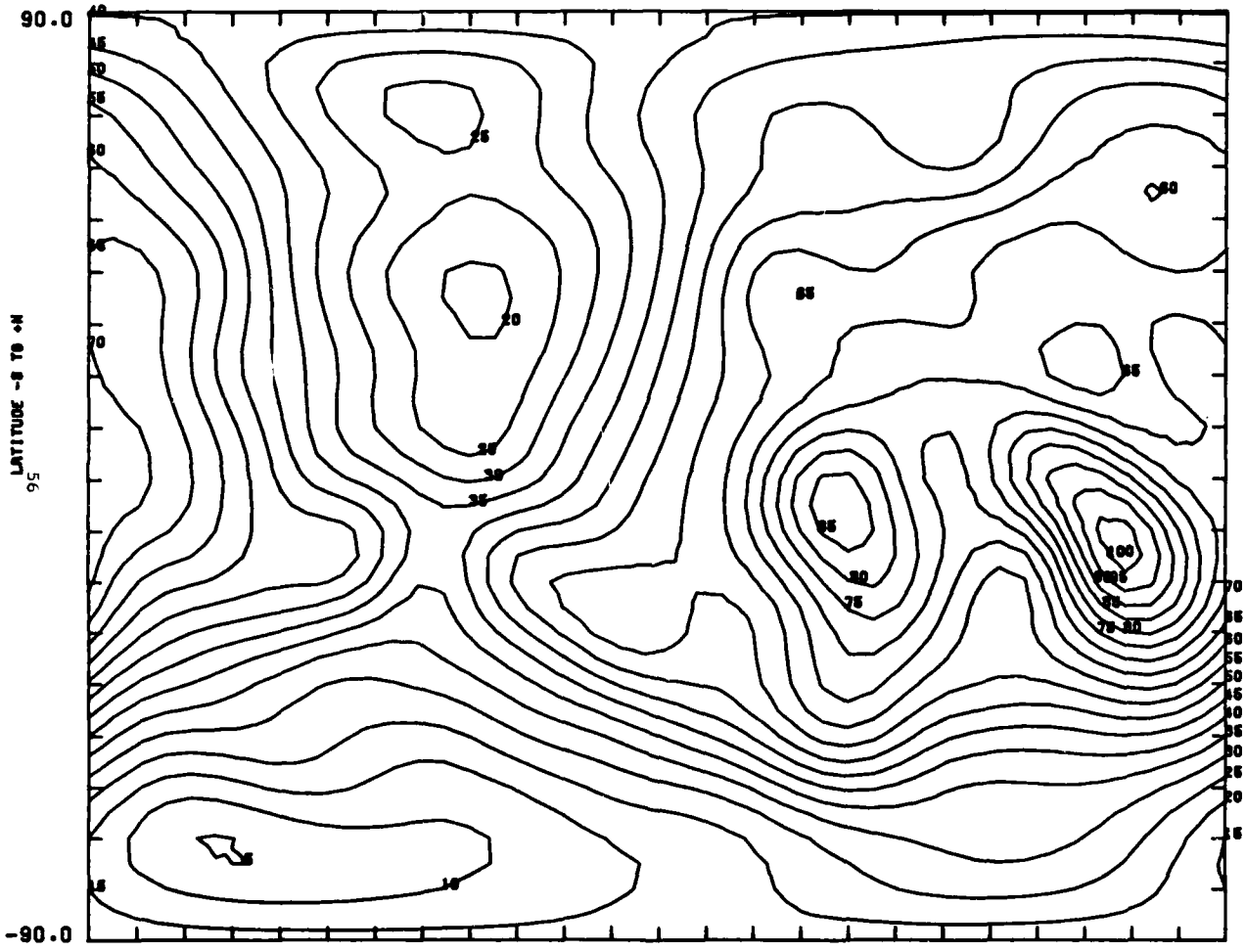

Figure A2 World contour map of F_{am} at 1 MHz for a model with 192 coefficients per time block (J=10, K=9) for December, January, February 0000 hrs UT

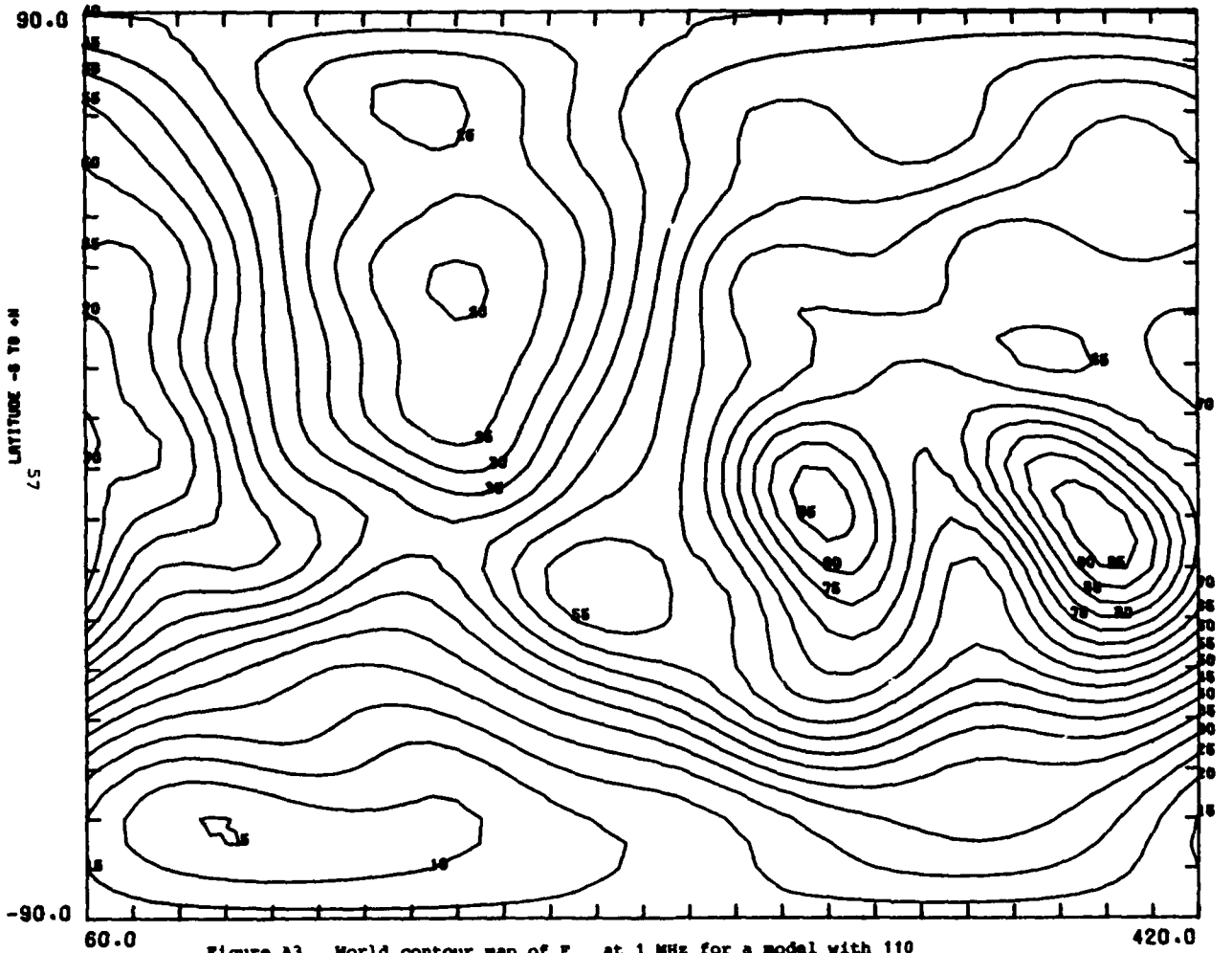

Figure A3 World contour map of F_{am} at 1 MHz for a model with 110 coefficients per time block (J=5, K=9) for December, January, February 0000 hrs UT

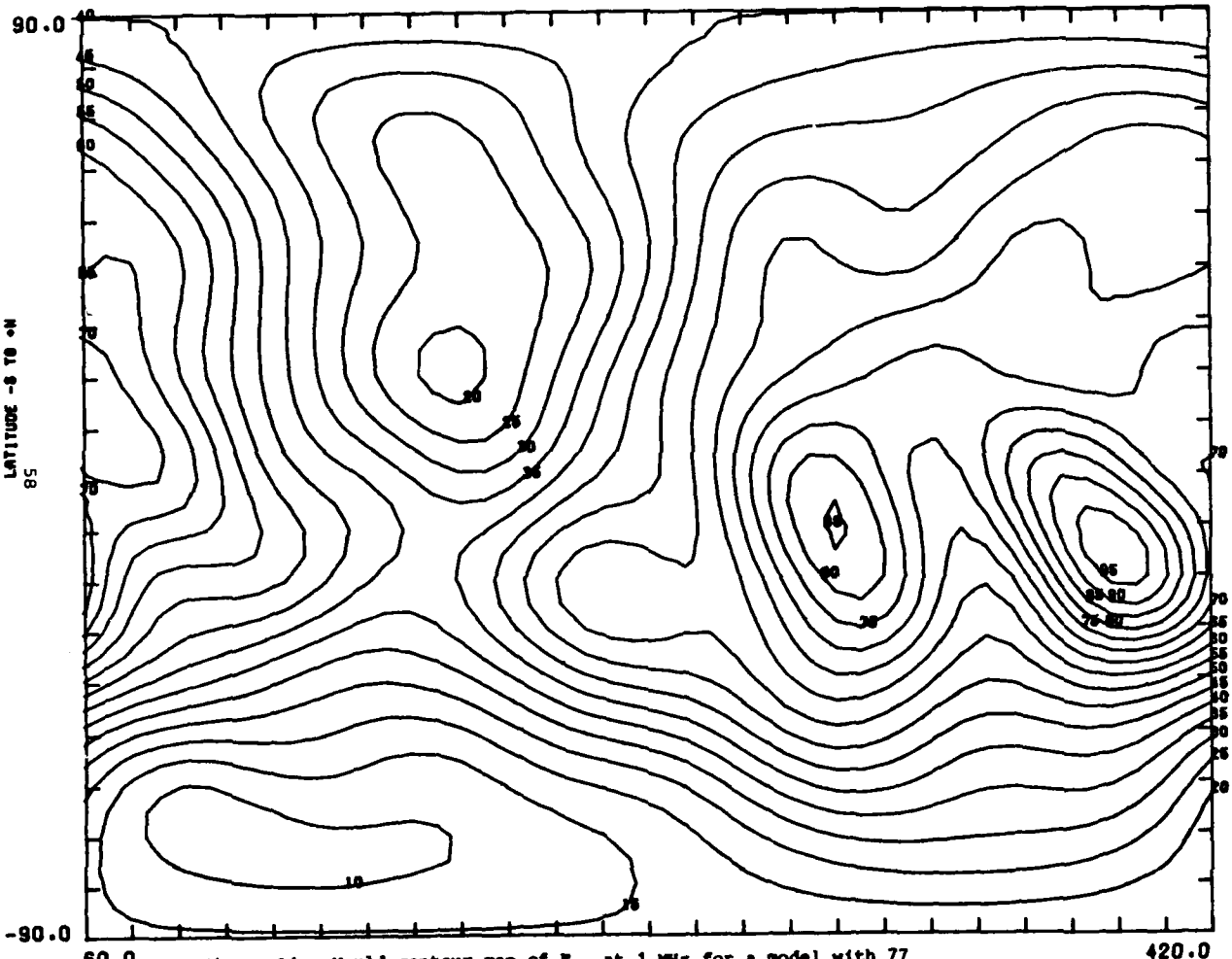

Figure A4 World contour map of F_{am} at 1 MHz for a model with 77 coefficients per time block (J=5, K=6) for December, January, February 0000 hrs UT

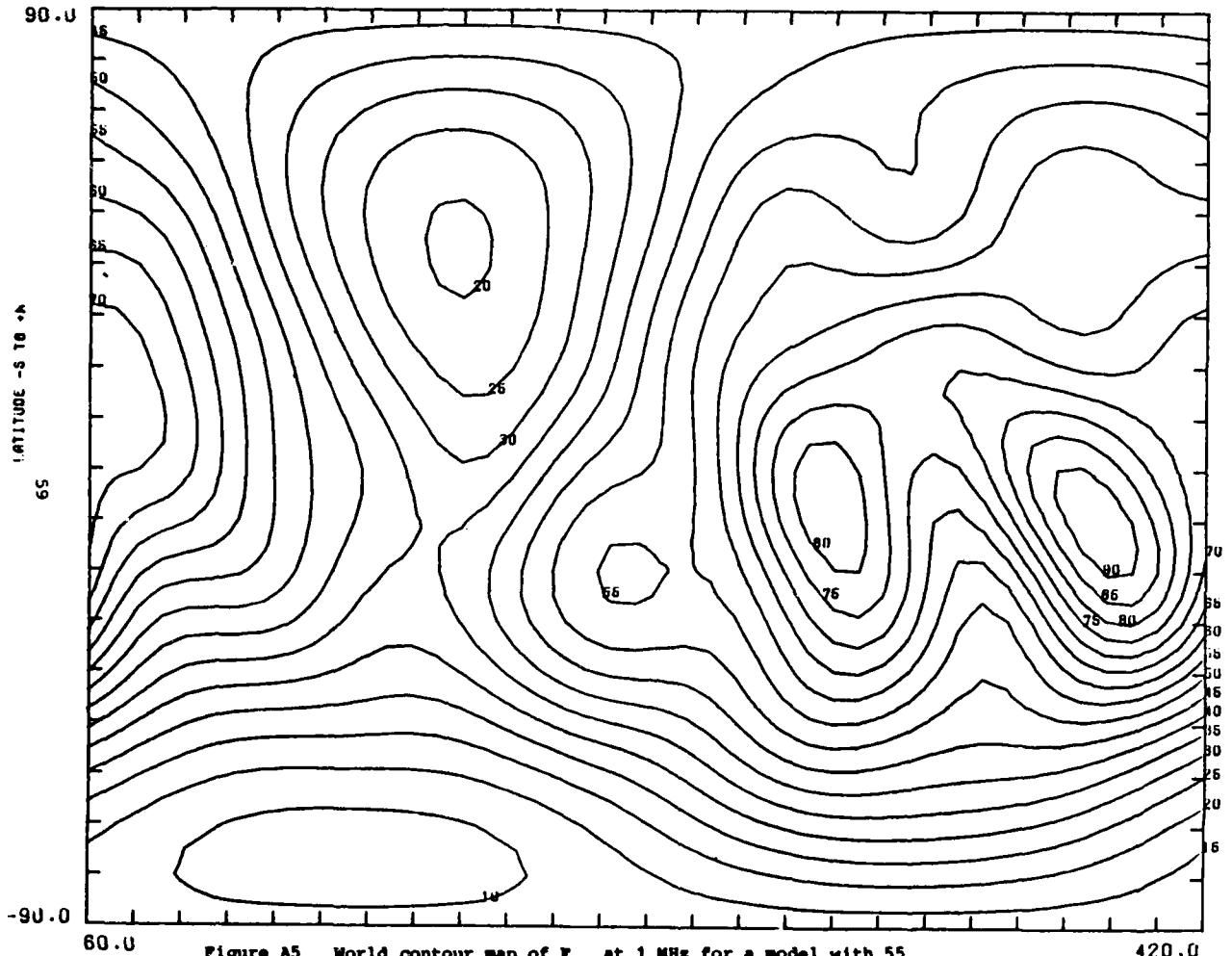

Figure A5 World contour map of F_{am} at 1 MHz for a model with 55 coefficients per time block (J=5, K=4) for December, January, February 0000 hrs UT

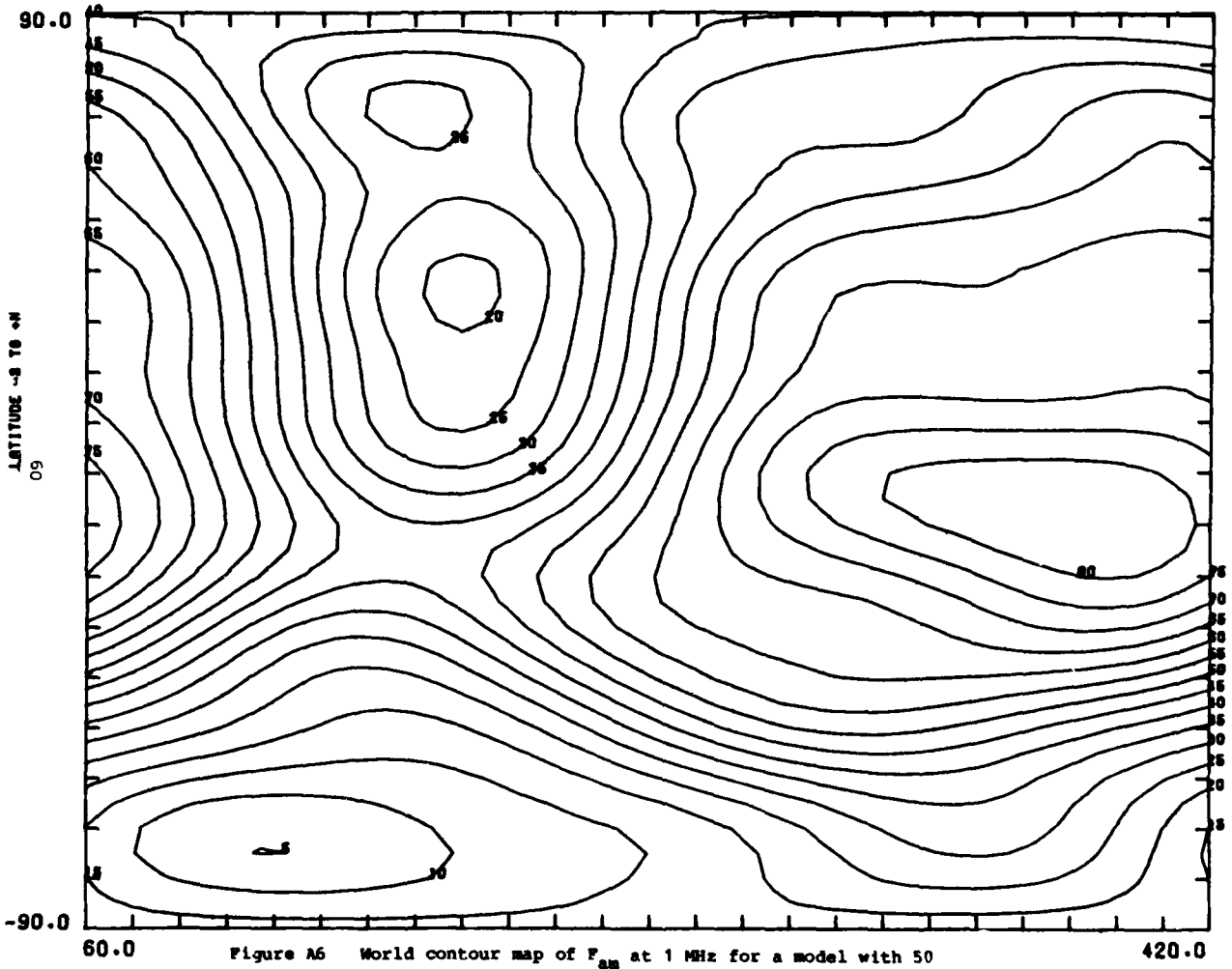

Figure A6 World contour map of F_{am} at 1 MHz for a model with 50 coefficients per time block (J=2, K=9) for December, January, February 0000 hrs UT

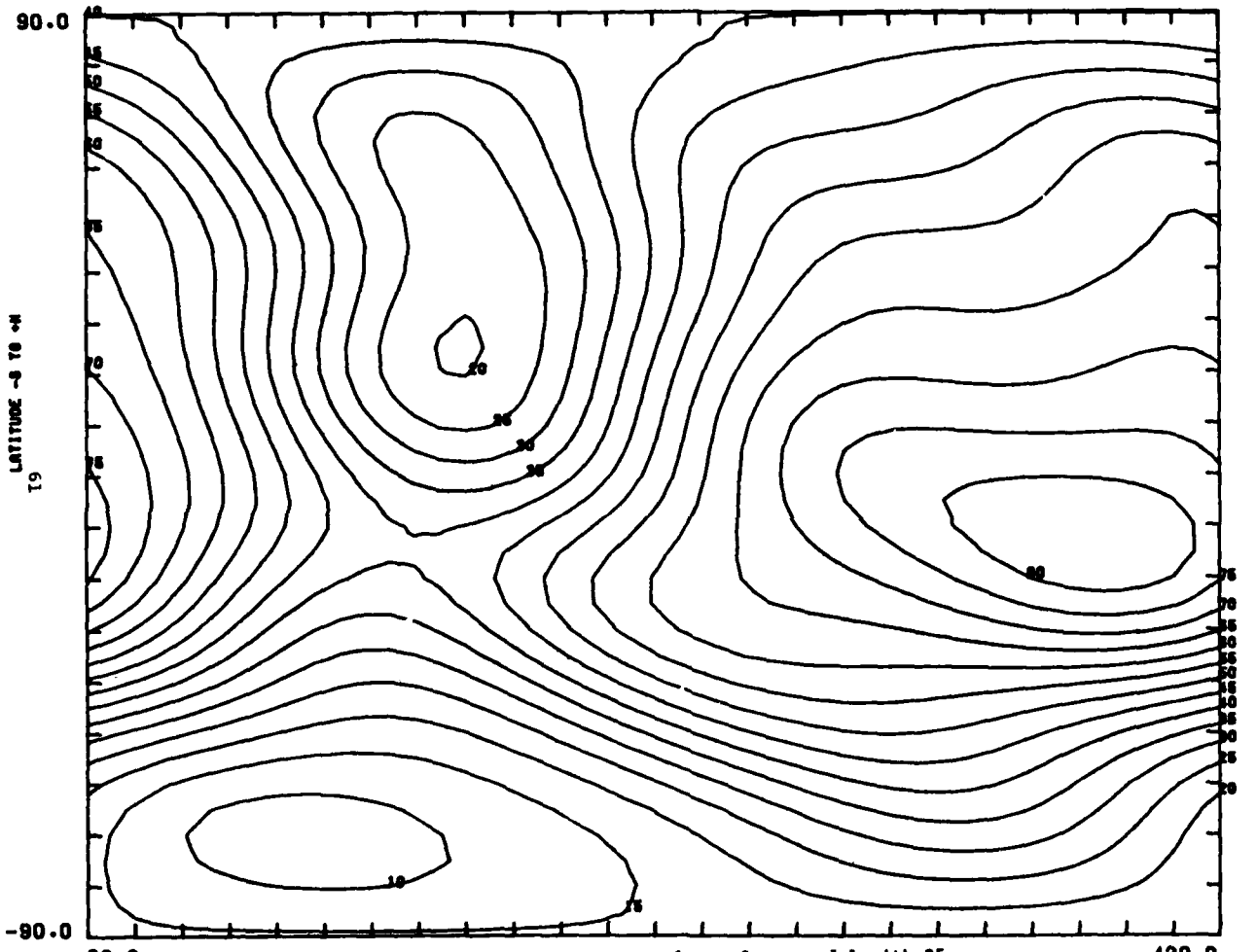

Figure A7 World contour map of F_{am} at 1 MHz for a model with 35 coefficients per time block (J=2, K=6) for December, January, February 0000 hrs UT

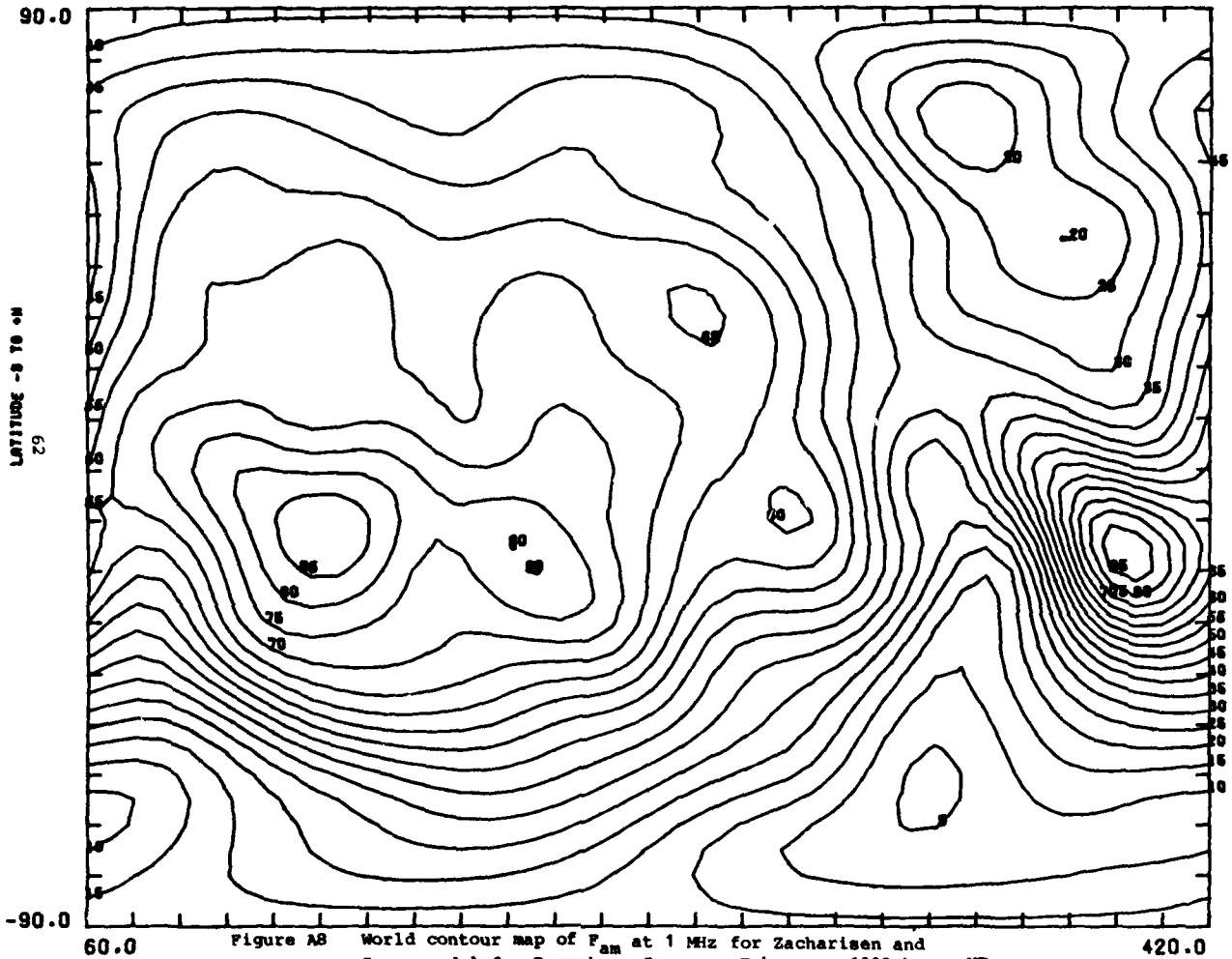

Figure A8 World contour map of F_{am} at 1 MHz for Zacharisen and Jones model for December, January, February 1200 hrs UT

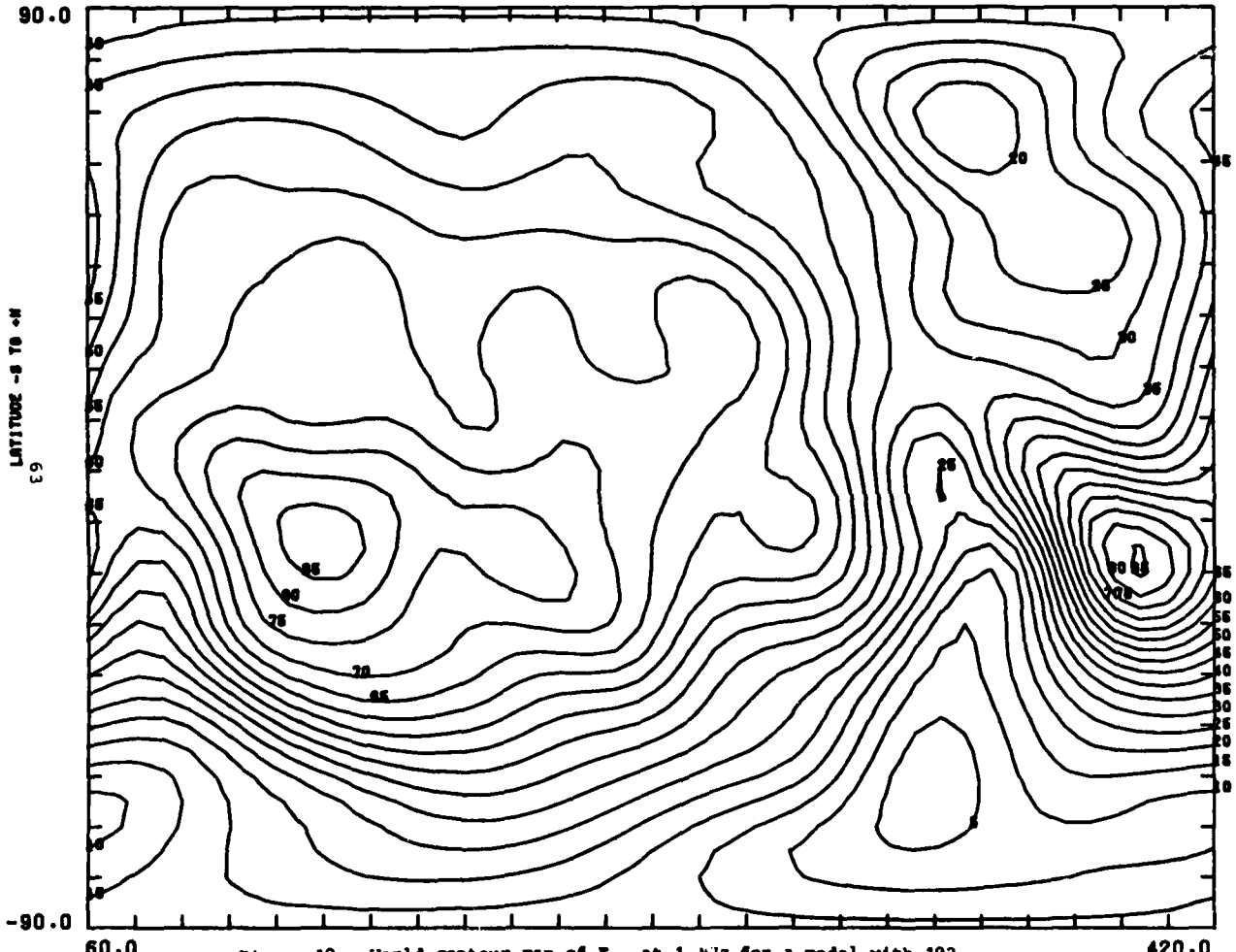

Figure A9 World contour map of F_{am} at 1 MHz for a model with 192 coefficients per time block (J=10, K=9) for December, January, February 1200 hrs UT

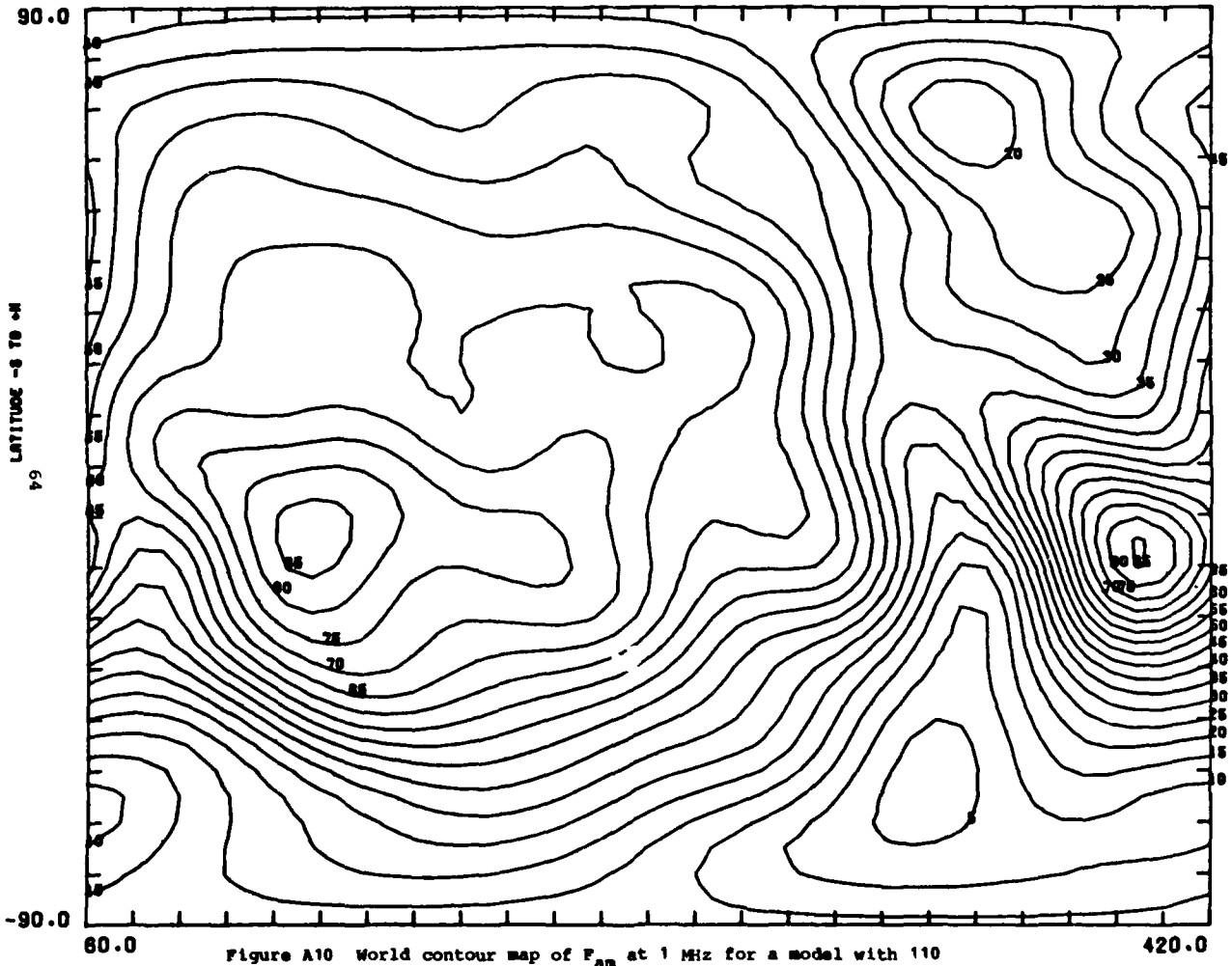

Figure A10 World contour map of F_{am} at 1 MHz for a model with 110 coefficients per time block (J=5, K=9) for December, January, February 1200 hrs UT

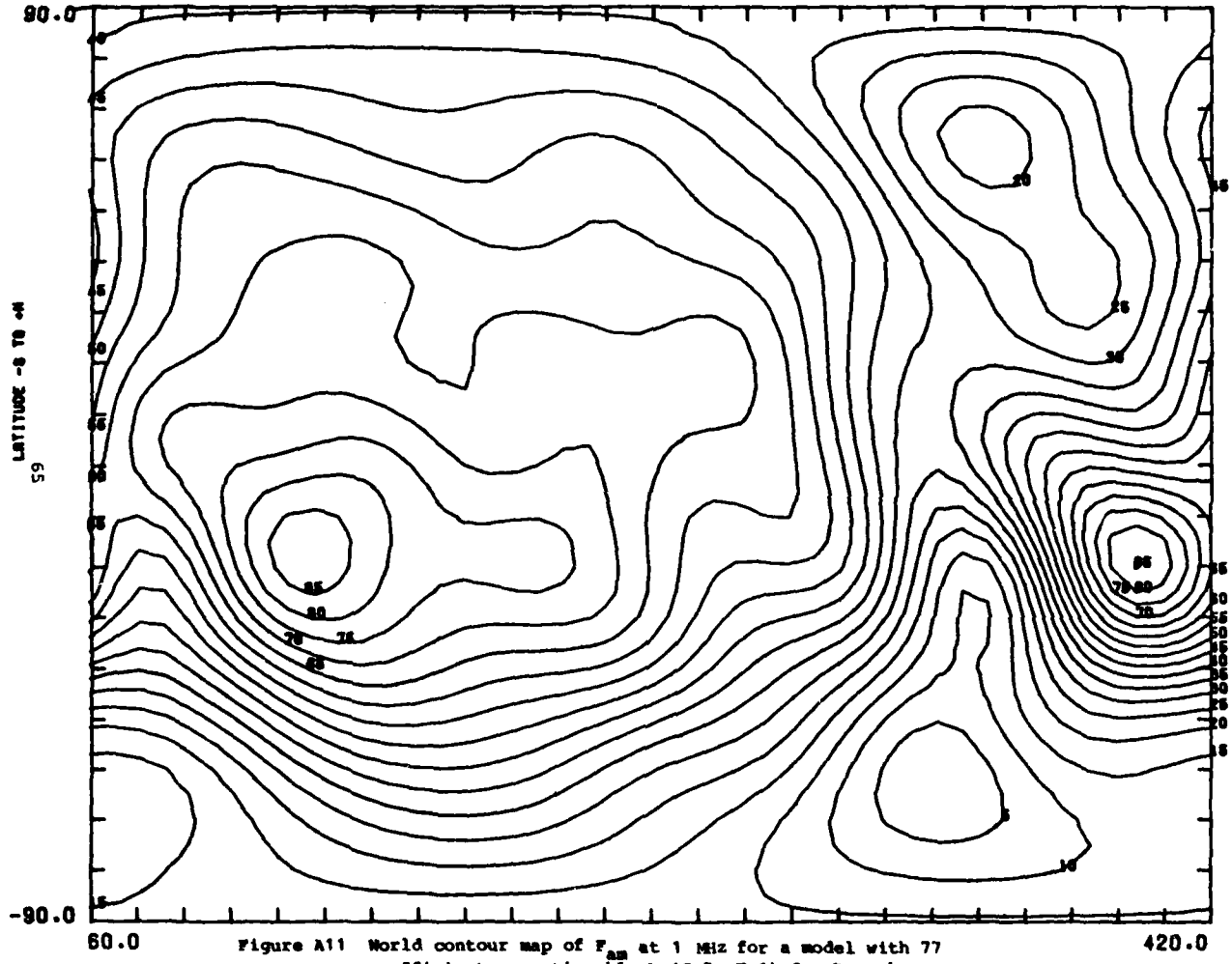

Figure A11 World contour map of F_{am} at 1 MHz for a model with 77 coefficients per time block (J=5, K=6) for December, January, February 1200 hrs UT

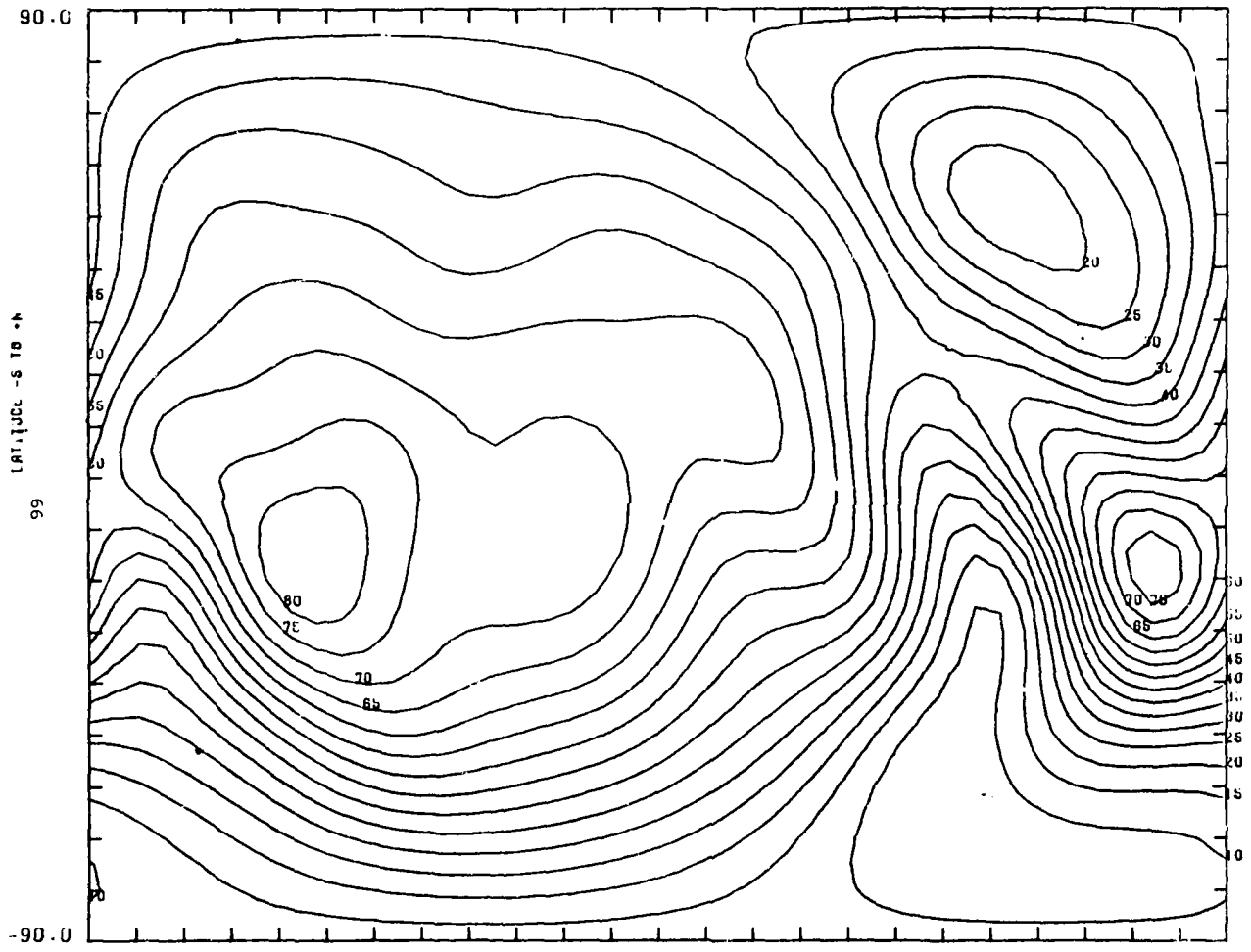

Figure A12 World contour map of F_{am} at 1 MHz for a model with 55 coefficients per time block (J=5, K=4) for December, January, February 1200 hrs UT

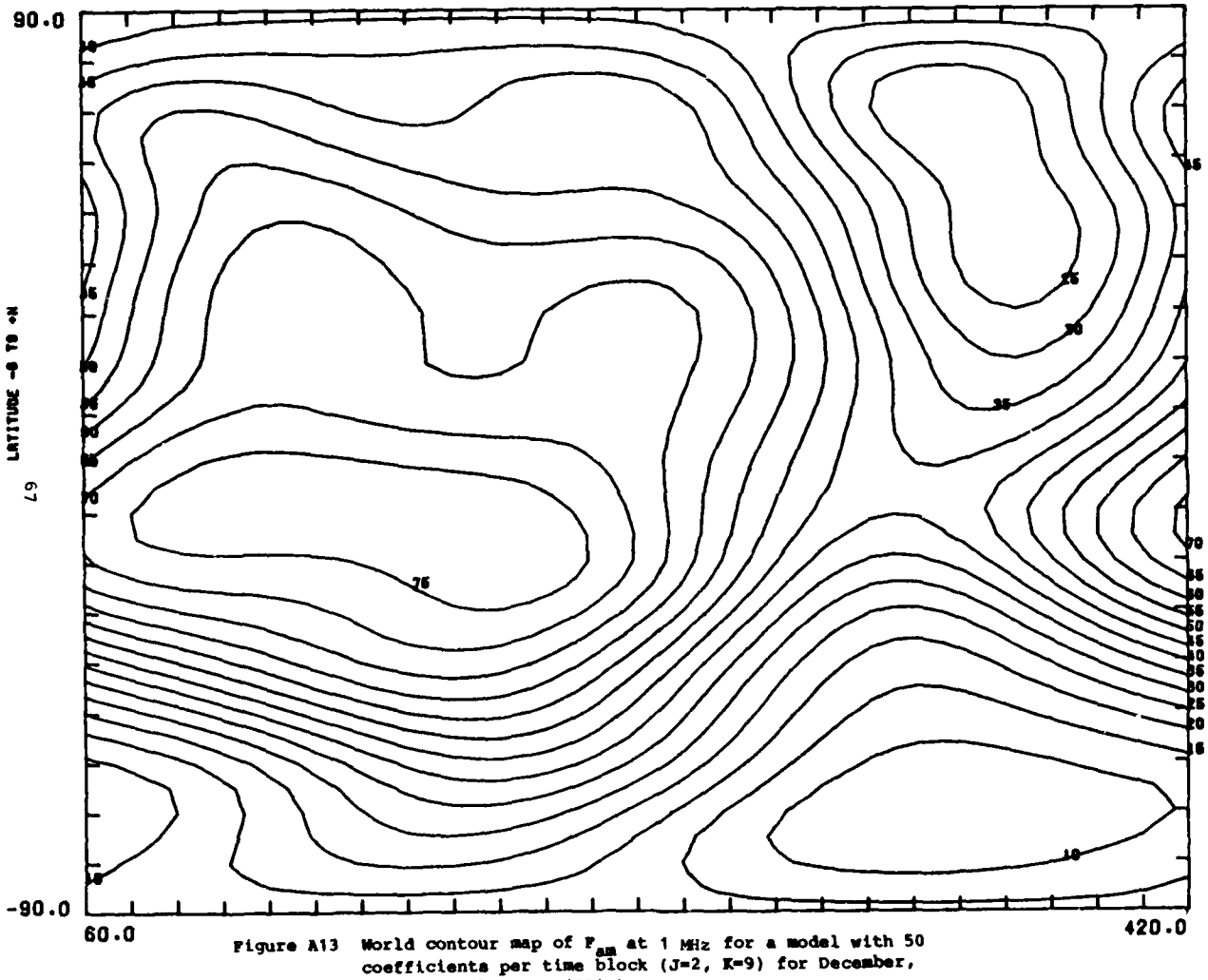

Figure A13 World contour map of F_{am} at 1 MHz for a model with 50 coefficients per time block (J=2, K=9) for December, January, February 1200 hrs UT

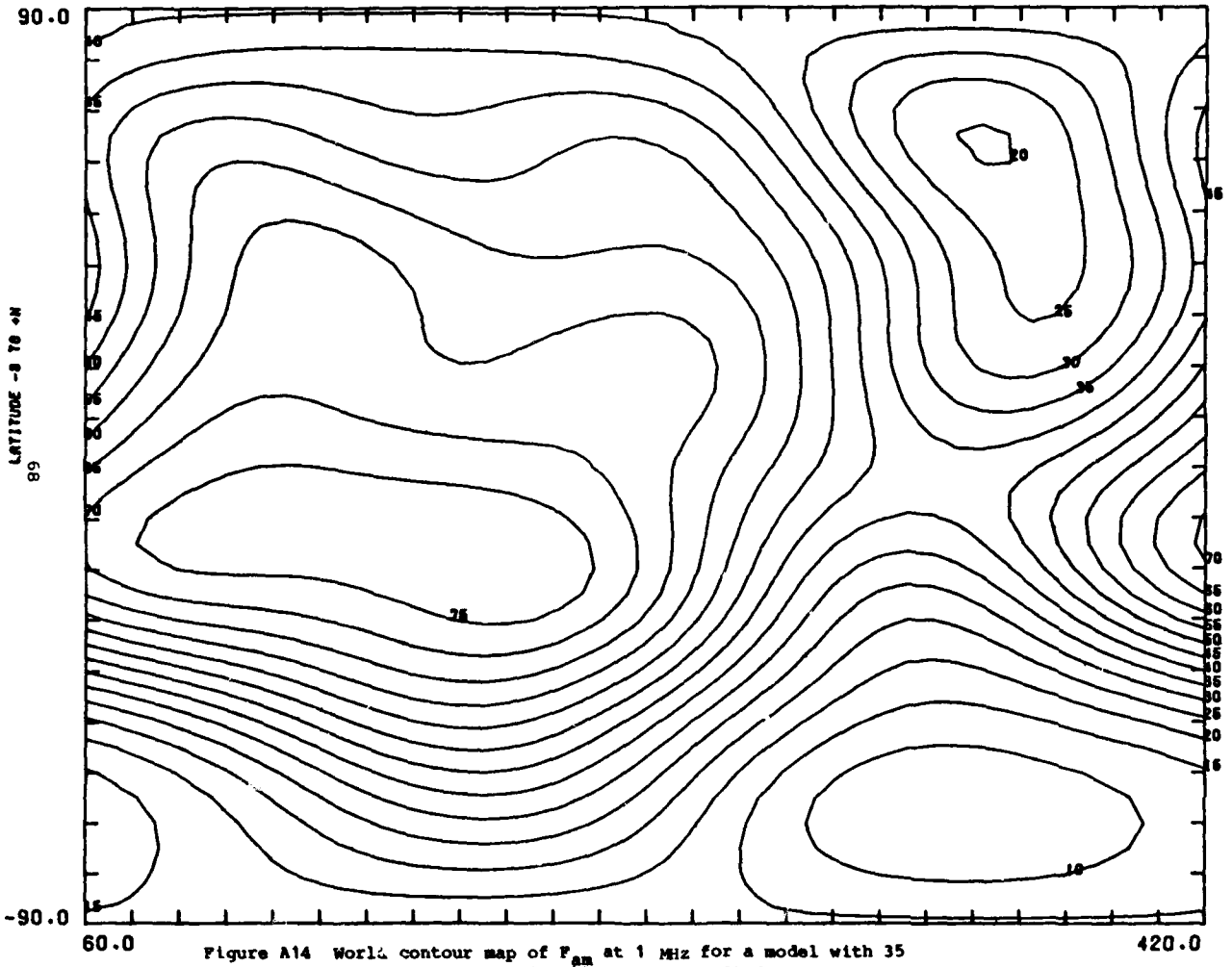

Figure A14 World contour map of F_{am} at 1 MHz for a model with 35 coefficients per time block (J=2, K=6) for December, January, February 1200 hrs UT

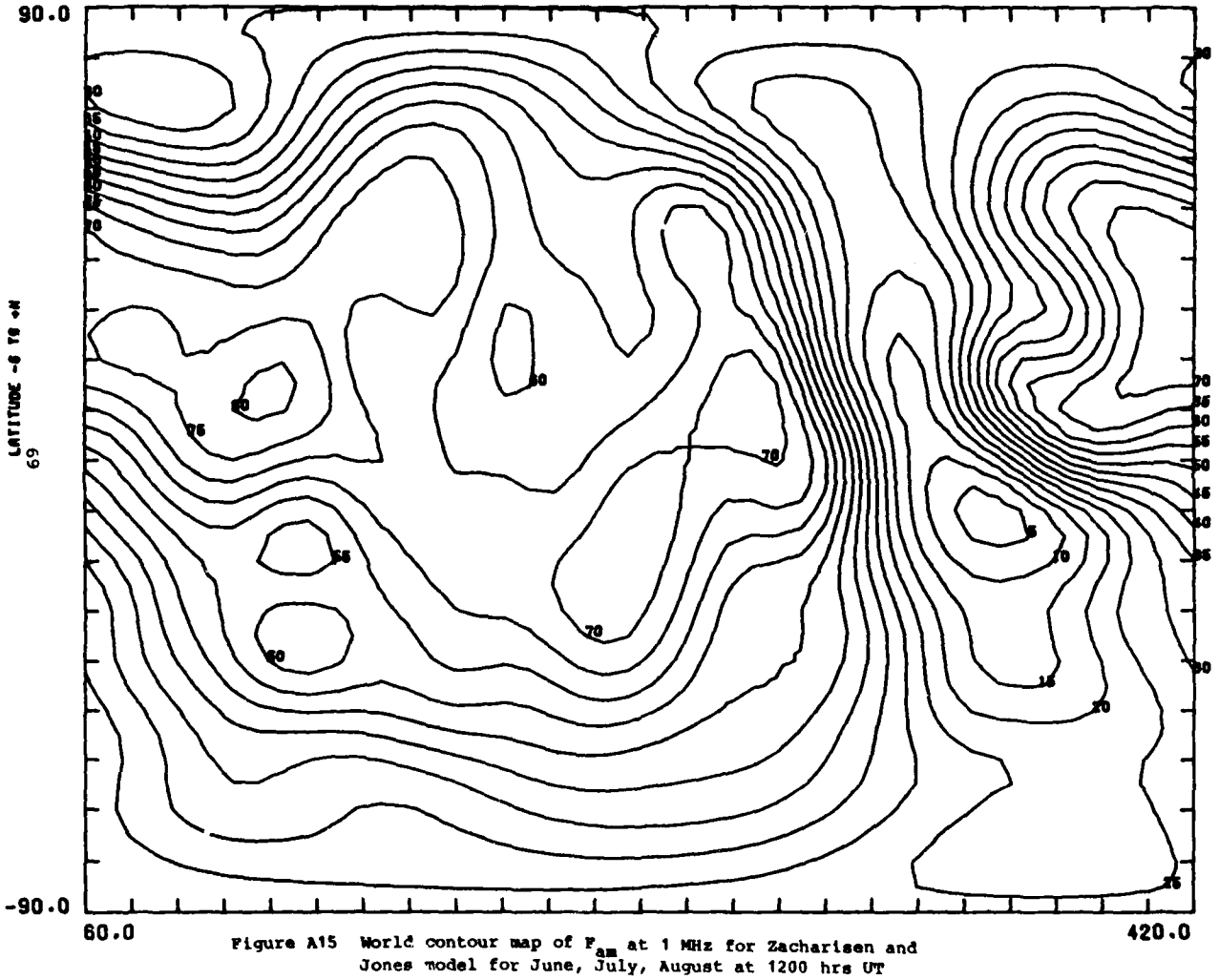

Figure A15 World contour map of F_{am} at 1 MHz for Zacharisen and Jones model for June, July, August at 1200 hrs UT

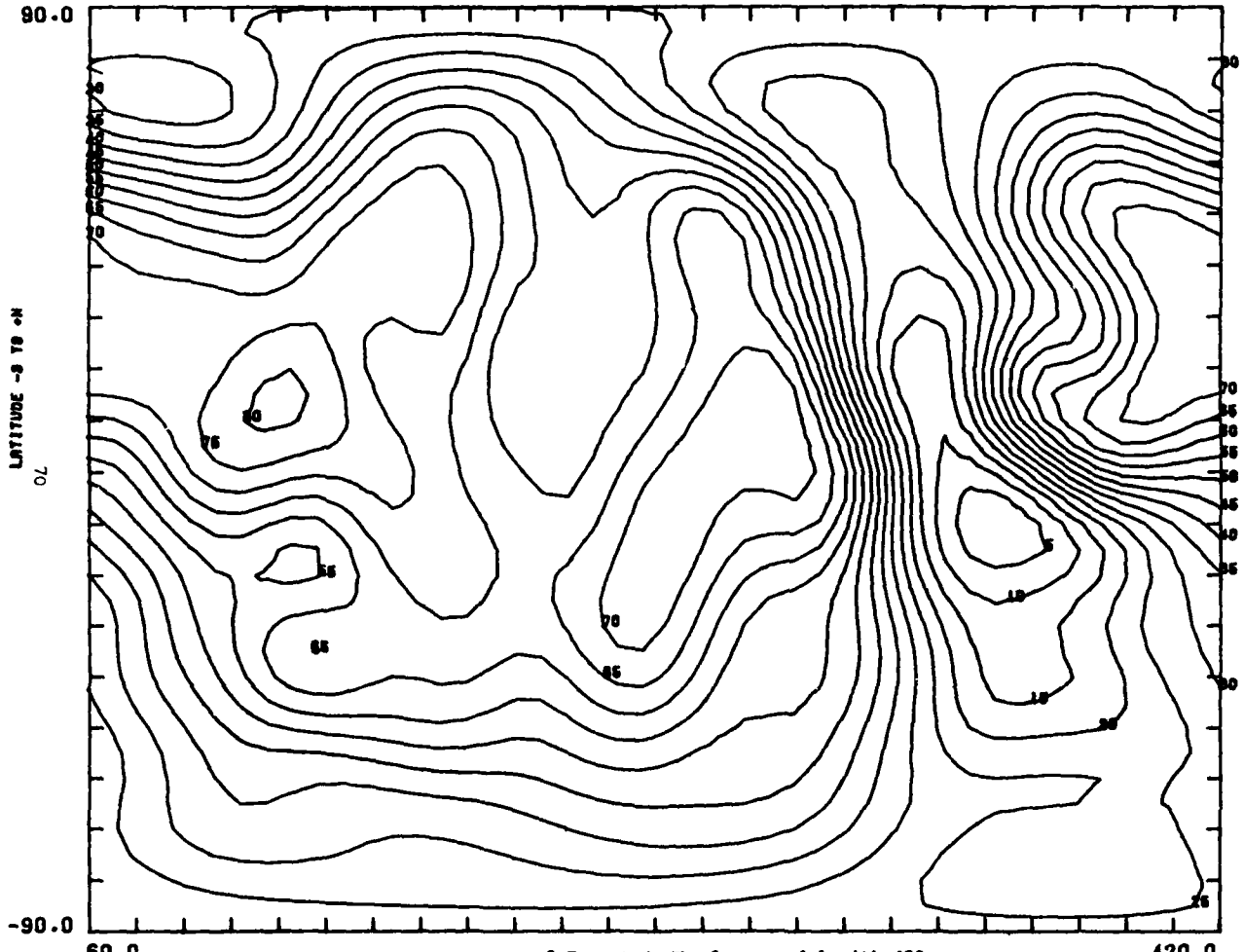

Figure A16 World contour map of F_{am} at 1 MHz for a model with 192 coefficients per time block (J=10, K=9) for June, July, August 1200 hrs UT

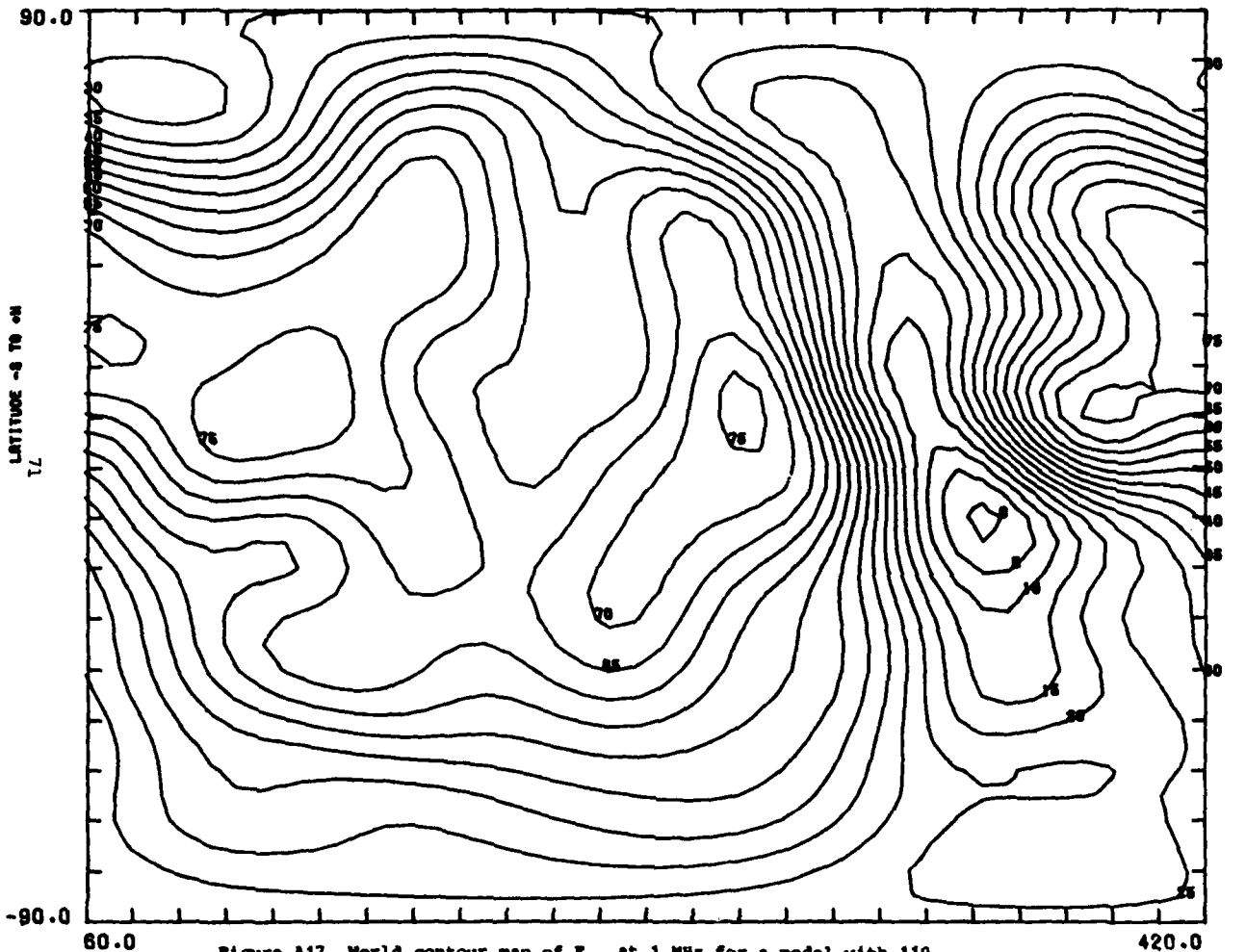

Figure A17 World contour map of F_{2m} at 1 MHz for a model with 110 coefficients per time block (J=5, K=9) for June, July, August 1200 hrs UT

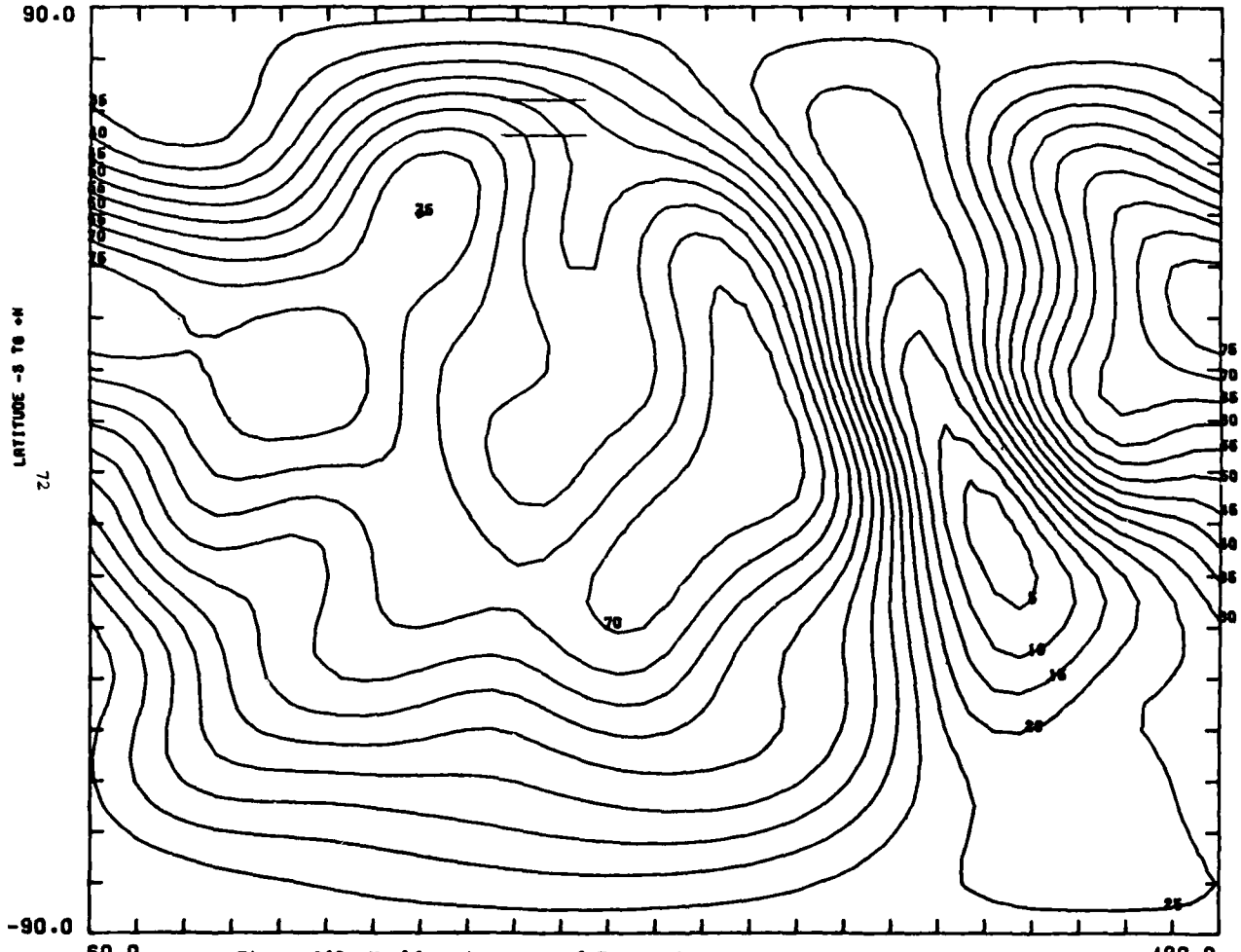

Figure A18 World contour map of F_{am} at 1 MHz for a model with 77 coefficients per time block (J=5, K=6) for June, July. August 1200 hrs UT

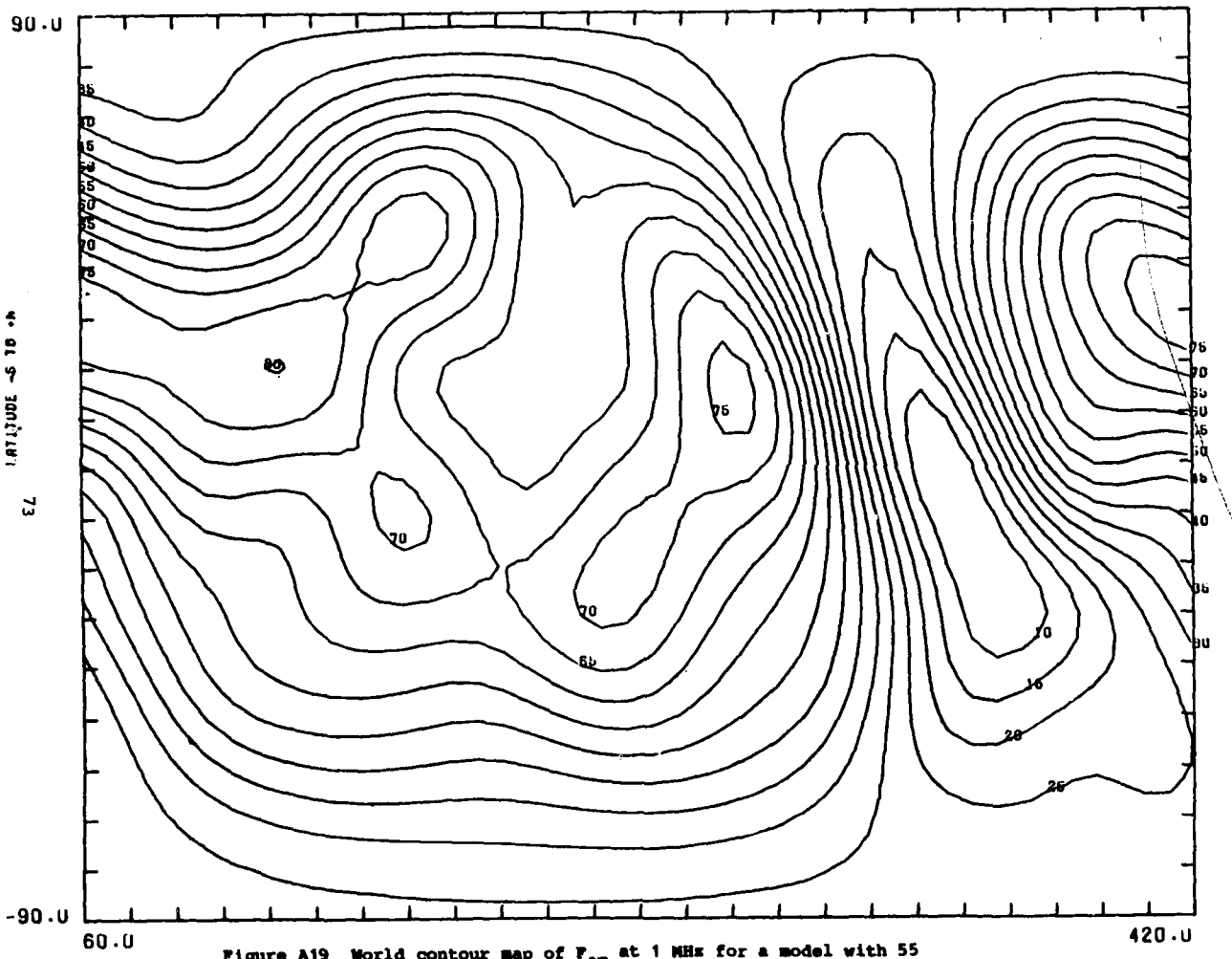

Figure A19 World contour map of F_{am} at 1 MHz for a model with 55 coefficients per time block (J=5, K=4) for June, July, August 1200 hrs UT.

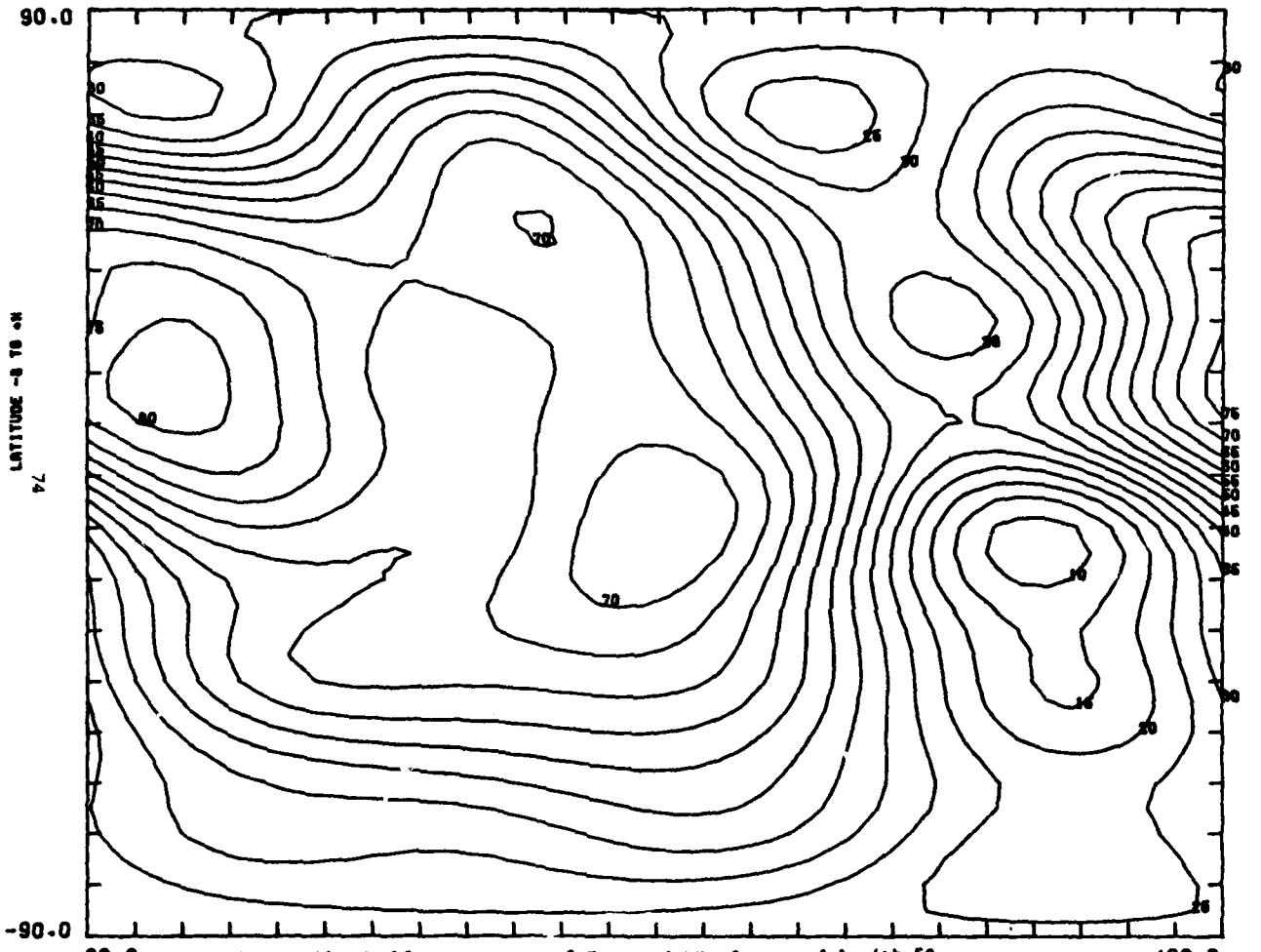

Figure A20 World contour map of F_{am} at 1 MHz for a model with 50 coefficients per time block (J=2, K=9) for June, July, August 1200 hrs UT

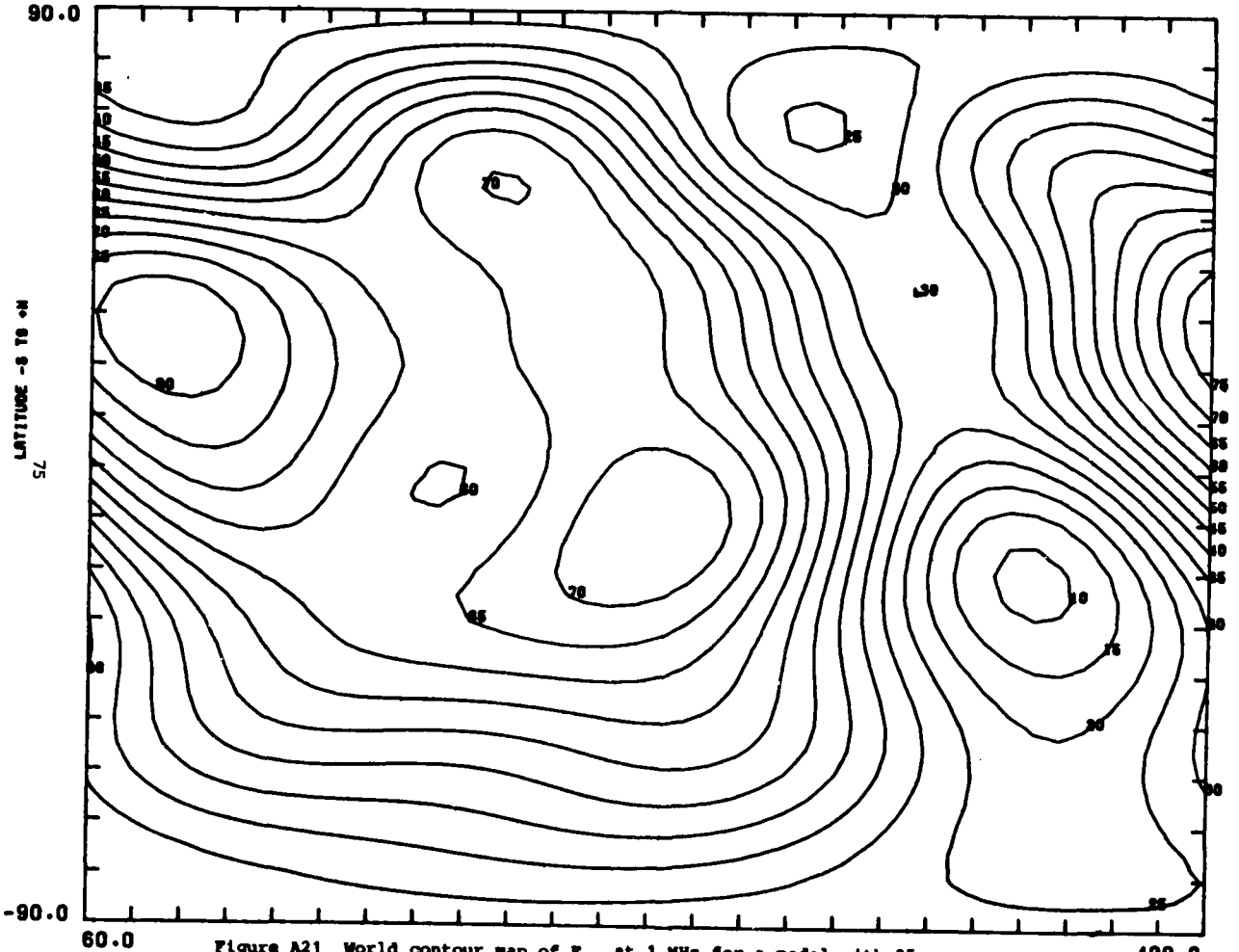

Figure A21 World contour map of F_{am} at 1 MHz for a model with 35 coefficients per time block (J=2, K=6) for June, July. August 1200 hrs UT

APPENDIX B

REPRESENTATION OF FREQUENCY DEPENDENCE AND VARIABILITY OF ATMOSPHERIC NOISE

PURPOSE

To determine the value of F_{am} for atmospheric noise for a given time and frequency and its variability.

NUMERICAL METHOD

The frequency Dependence curves given in CCIR Report 322 were fitted by Lucas and Harper using least squares.[2] The result is a power series of the form

$$Y(X,N) = A_1(N) + A_2(N)\,X + A_3(N)\,X^2 + \ldots + A_7(N)\,X^6 \qquad \text{(B-1)}$$

where

$$A_i(N) = b_{i,1}\,N,\ i = 1, \ldots, 7 \qquad \text{(B-2)}$$

N = amplitude of the hourly median 1 MHz atmospheric noise (dB>kT_ob), and

$$X = \frac{8 \times 2^{\log_{10} f} - 11}{4}, \qquad \text{(B-3)}$$

where f is the operating frequency in MHz. Equation (B-1) is subject to the constraint Y(-3/4,N) = N (i.e., the frequency variation of the 1 MHz value must be zero).

The CCIR Report 322 curves representing the decile values of the distributions were generated by a least square fit by Lucas and Harper to the function

$$Y(X) = A_1 + A_2 X + A_3 X^2 + A_4 X^3 + A_5 X^4 \qquad \text{(B-4)}$$

where $X = 10 \log_{10} f$ and f is the operating frequency in MHz.

STRUCTURE

SUBROUTINE GENFAM(RLAT, NTB, FREQ, ANOS, ATNO, DU, DL, GU, SIGU, SIGL, SIGM)

Formal Parameters

RLAT	Geographic latitude in radians (+N,-S)
NTB	Time band index
FREQ	Frequency in MHz
ANOS	1 MHz atmospheric noise for time of interest
ATNO, DU, DL	Atmospheric noise and deciles at desired freque cy
SIGU, SIGL, SIGM	Standard deviation of deciles and mean noise

Related Algorithms

An algorithm called XINTER provides the interpolation time band indices for use with GENFAM and the linear interpolation fraction for a given UT.

SUBROUTINE XINTER (TIMER, ITIME, NTB, ABCT)

Formal Parameters

TIMER	Time -- either local or universal
ITIME	Time type index -- 1 for LT, 2 for UT
NTB	First time band index for interpolation
NTX	Second time band index for interpolation
ABCT	Fraction for interpolation

Usage

For use with GENFAM it is necessary to determine the LT corresponding to the UT of interest at the receive site. Then XINTER is called. Next two calls are made to GENFAM -- one with NTB, one with NTX (1 i.e., with NTB atmospheric noise is ATNO; with NTX atmospheric noise is ATNX). Then the atmospheric noise at a hour LT corresponding UT is

$$ATMNO = ATNO + (ATNX - ATNO) * ABCT \quad (B-5)$$

In the same manner the upper and lower deciles are given by

$$DUA = DU + (DUX - DU) * ABCT \quad (B-6)$$

and

$$DLA = DL + (DLX - DL) * ABCT \quad (B-7)$$

ADDITIONAL COMMENTS

The listings given for GENFAM and XINTER in Figures B1-B2 are in the Harris FORTRAN 66 language. The Harris FORTRAN 66 language is a super set of USA standard FORTRAN X3.9 - 1966. Except for changes made in GENFAM to make it run on the Harris mini-computer, GENFAM given here is the same subroutine found in many HF prediction programs.

AD-A117 851 NAVAL OCEAN SYSTEMS CENTER SAN DIEGO CA F/G 4/1
DEVELOPMENT OF A MINICOMPUTER ATMOSPHERIC NOISE MODEL.(U)
MAY 82 D B SAILORS, R P BROWN
UNCLASSIFIED NOSC/TR-778 NL

```
      SUBROUTINE GENFAM (RLAT,NTR,FREQ,ANOS,ATNO,DU,DL,SIGU,SIGL,SIGM)  MUA03100
C     CALCULATES THE FREQUENCY DEPENDENCE OF THE MEDIAN
C     1 MHZ ATMOSPHERIC NOISE AND ITS ASSOCIATED DECILE VALUES AND
C     STANDARD DEVIATION OF THE MEDIAN AND UPPER AND LOWER DECILES
C     OF THE ATMOSPHERIC NOISE.
C        RLAT=GEOGRAPHIC LATITUDE IN RADIANS(+N,-S)
C        NTR=TIME BAND INDEX
C        FREQ=FREQUENCY IN MHZ
C        ANOS=1 MHZ ATMOSPHERIC NOISE
C        ATNO,DU,DL=ATMOSPHERIC NOISE AND DECILES AT DESIRED FREQ
C        SIGU,SIGL,SIGM=STD. DEVIATIONS OF DECILES AND MEAN NOISE
      IMPLICIT REAL*6 (A-H,O-Z)
      DIMENSION V(5)                                                    MUA03101
      COMMON /ONE/ DUD(5,12,5),FAM(14,12)
      IF (FREQ .GT. 30) GO TO 6                                         MUA03105
      F20=ALOG10(20.0)                                                  MUA03106
      F=ALOG10(FREQ)                                                    MUA03107
      ITR=NTR                                                           MUA03108
      IF (RLAT.LT.0.0) ITR=ITR+6                                        MUA03109
      X=-0.75                                                           MUA03110
1     PZ=0.0                                                            MUA03111
      PX=0.0                                                            MUA03112
      DO 2 I=1,7                                                        MUA03113
      PZ=X*PZ+FAM(I,ITR)                                                MUA03114
2     PX=X*PX+FAM(I+7,ITR)                                              MUA03115
      IF (X.NE.-0.75) GO TO 3                                           MUA03116
      CZ=ANOS*(2.0-PZ)-PX                                               MUA03117
      X=(A.0*2.0**F-11.0)/4.0                                           MUA03118
      GO TO 1                                                           MUA03119
3     ATNO=CZ*PZ+PX                                                     MUA03120
      IF(F.GT.F20) F=F20                                                MUA03121
      DO 5 I=1,5                                                        MUA03122
      Y=0.0                                                             MUA03123
      IF(I.EQ.5.AND.F.GT.1.0) F=1.0                                     MUA03124
      DO 4 J=1,5                                                        MUA03125
4     Y=F*Y+DUD(J,ITR,I)                                                MUA03126
5     V(I)=Y                                                            MUA03127
      DU=V(1)                                                           MUA03128
      DL=V(2)                                                           MUA03129
      SIGU=V(3)                                                         MUA03130
      SIGL=V(4)                                                         MUA03131
      SIGM=V(5)                                                         MUA03132
      RETURN                                                            MUA03133
6     ATNO = -10                                                        MUA03134
       DU = 0                                                           MUA03135
       DL = 0                                                           MUA03136
       SIGU= 0                                                          MUA03137
      SIGL = 0                                                          MUA03138
       SIGM = 0                                                         MUA03139
        RETURN                                                          MUA03140
      END                                                               MUA03141
```

Figure B1 Listing of GENFAM, frequency dependence model of atmospheric noise

```
      SUBROUTINE XINTER(TIMER,ITIME,NTB,NTX,ABCT)
C     PROVIDES INTERPOLATION INDICES AND FRACTION FOR SAME
C     TIMER=TIME--EITHER LOCAL OR UNIVERSAL TIME
C     ITIME=TIME TYPE INDEX--1 FOR LT, 2 FOR UT
C     NTB=FIRST TIME BAND INDEX
C     NTX=SECOND TIME BAND INDEX
C     ABCT=FRACTION FOR INTERPOLATION
      IMPLICIT REAL*6 (A-H,O-Z)
      CC=TIMER
      NTB=CC/4.0+1.0
      IF(NTB .GT. 6) NTB=6
      TM=4*NTB-2+ITIME
      ABCT=ABS(CC-TM)/4.0
      NTX=NTB-1
      IF(CC .GT. TM) NTX=NTB+1
      IF(NTX .GT. 6) NTX=1
      IF(NTX .LT. 1) NTX=6
      RETURN
      END
```

Figure B2 Listing of XINTER, an algorithm for determining linear interpolation indices and fraction for same

APPENDIX C

FORTRAN SUBROUTINE OF THE 1 MHZ ATMOSPHERIC NOISE MODEL

PURPOSE

To calculate the value of F_{am} for atmospheric noise for a given time at 1 MHz.

NUMERICAL METHOD

The two-dimensional geographic representation of F_{am} for the hours 0000, 0400, 0800, 1200, 1600, and 2000 for each season is given by

$$X_h(\lambda, \Theta) = \sum_{k=0}^{K} P_{o,k}^{(h)} G_{o,k}(\lambda) + \sum_{j=1}^{J} \left[\left(\sum_{k=0}^{K} P_{j,k}^{(h)} G_{j,k}(\lambda) \right) \cos j\Theta + \left(\sum_{K=0}^{K} q_{j,k}^{(h)} G_{j,k}(\lambda) \right) \sin j\Theta \right] \quad \text{(C-1)}$$

where maximum longitudinal harmonic number, k, is 9 for $0 \leq j \leq 7$ and is 6 for $j = 8, 9, 10$, and where J is the longitudinal maximum harmonic. The latitude functions $G_{j,k}(\lambda)$ are defined by

$$G_{j,k}(\lambda) = \sin^k \lambda \cos^j \lambda \quad \text{(C-2)}$$

Here λ denotes latitude, $-90° \leq \lambda \leq 90°$, and θ denotes longitude measured eastward from 0°, $0° \leq \theta \leq 360°$.

The coefficients $p_{j,k}^{(h)}$ and $q_{j,k}^{(h)}$ were found using the numerical mapping techniques developed by Zacharisen and Jones.[3] The procedure is described in the main body of the report. The actual number of coefficients used depends on the memory space available and the application.

STRUCTURE

The model consists of two subroutines - EVALGK and EVAL4 listed in Figures C1-C2. The first evaluates the $G_{j,k}(\lambda)$ functions and the resulting summation of the product of $G_{j,k}(\lambda)$ and $p_{j,k}^{(h)}$ and $q_{j,k}^{(h)}$ in equation (C-1) at a fixed latitude (e.g., $\sum_{k=0}^{K} p_{j,k}^{(h)} G_{j,k}(\lambda)$). The latter subroutine completes the evaluation of F_{am} in equation (C-1) at a fixed longitude using the Fourier coefficients generated in EVALGK.

SUBROUTINE EVALGK(FLAT, MAXG, NH)

Formal Parameters

FLAT	Geographic latitude in degrees (+N, -S)
MAXG	Maximum latitudinal harmonic K+1
NH	Maximum longitudinal harmonic J

SUBROUTINE EVAL4(FLON, NH, OMEGA)

Formal Parameters

FLON	Geographic longitude in degrees eastward from 0°
NH	Maximum longitudinal harmonic J
OMEGA	Estimated value of F_{am} for given latitude, longitude, and time of day
COMMON	/A/ D(21,10),DK(21),DR

Formal Parameters

D(21,10)	Set of numerical coefficients representing F_{am}
DK(21)	Resultant Fourier coefficients calculated in EVALGK
DR	Degrees to radians constant (0.01745329252)

RELATED ALGORITHMS

An algorithm called XINTER provides the interpolated time band indices for use with these two subroutines. Using XINTER it is possible to linearly interpolate between the UT hours 0000, 0400, 0800, 1200, 1600, and 2000. ITIME should be set equal to 2. XINTER and its usage are described in appendix B.

ADDITIONAL COMMENTS

The listings given for EVALGK and EVAL4 are in the Harris FORTRAN 66 language. The Harris FORTRAN 66 language is a super set of USA FORTRAN X3.9 1966.

The listings given here are for J=10 and K=9. For other versions of the numerical map it may be necessary to make minor changes to the subroutines. The dimensioning in the common block A for D should be (2*NH+1, K+1) and DK should be (2*NH+1). In EVAL4 the dimensioning for FCOS and FSIN should be (2*NH+1).

```
      SUBROUTINE EVALGK(FLAT,MAXG,NH)
C     EVALUATES THE GK FUNCTION.
      IMPLICIT REAL*6 (A-H,O-Z)
      COMMON /A/ D(21,10),DK(21),DR
      NF=2*NH+1
      MAX = MAXG
      TLAT = FLAT * DR
      TSIN =SIN(TLAT)
      TCOS = COS(TLAT)
      DO 1  I=1,NF
      JTERM=I/2
      SUM = 0.0
      IF(I .GE. 16) MAXG=7
      DO 2  K=1,MAXG
      KK=K-1
      SUM = SUM + D(I,K) * (TSIN **KK) * (TCOS ** JTERM)
2     CONTINUE
1     DK(I) = SUM
      MAXG=MAX
      RETURN
      END
```

Figure C1 Listing of EVALGK, an algorithm for obtaining 1 MHz atmospheric noise.

```
      SUBROUTINE EVAL4 (FLON,NH,OMEGA)
C     EVALUATES FOURIER COEFFICIENTS FOR A FIXED LATITUDE
      IMPLICIT REAL*8 (A-H,O-Z)
      COMMON /A/ D(21,10),DK(21),DR
      DIMENSION FCOS(21),FSIN(21)
      SUM = DK(1)
      RAD = DR * FLON
      CF = COS(RAD)
      FCOS(1) = CF
      SF = SIN(RAD)
      FSIN(1) = SF
      DO 1  I=2,NH
      FCOS(I) = CF * FCOS(I - 1) - SF * FSIN(I - 1)
1     FSIN(I) = CF * FSIN(I - 1) + SF * FCOS(I - 1)
      DO 2  J=1,NH
2     SUM = SUM + DK(2* J) * FSIN(J) + DK(2 * J + 1) * FCOS(J)
      OMEGA = SUM
      RETURN
      END
```

Figure C2 Listing of EVAL4, an algorithm for obtaining 1 MHz atmospheric noise

APPENDIX D

A COMPUTER PROGRAM FOR READING AND PRINTING THE ATMOSPHERIC NOISE NUMERICAL COEFFICIENTS

Purpose

To read into a computer the atmospheric noise coefficients, generated by UT NEQSOL, and to print these coefficients in tabular listings.

Method

The number of cards produced by UT NEQSOL depends on the value of K, the maximum latitudinal harmonic. Each card contains an index identifying the season and hour, an index identifying the longitudinal harmonic, an index identifying the beginning latitudinal harmonic on the card, and four Fourier coefficients. It produces three cards for the first ten latitudinal coefficients for J .LT. 16 and two for J .GE. 16. This results in 342 cards per season when K=9 and 252 when K=4 or 6.

Input

The input consists of:

1) An alphanumerical title card (columns 1-78)

2) A card with J, K+1, season number, and a control index to control the end of the program.

3) The set of coefficient cards.

Each subsequent season is placed after the one preceding it. The variable names and format of the input are given as follows:

1)	NTITLE	13A6	Title to be printed
2)	NH	I10	J
	MAXG	I10	K+1 (e.g., 10 for K=9)
	NSEAS	I10	Season number (1 through 4)
	NEND	I10	.GE.10 will halt program

OUTPUT

The output looks like that shown in Figure D-1. Across the top is the title. Then hours 0000,0400,0800,1200,1600, and 2000 appear as column headings. Each column is for a particular hour UT. On the left are values of j and k. Each row is for a combination of the values of j and k. The first row is for j=1 and k=1. Subsequent rows are for increasing k values up to 10. Then j is incremented and k starts again at 1. This process continues until both j and k reach their maximum value (2*J+1 and K+1).

COMMENT

Since UT NEQSOL considers J to be 10, the printout provided by this program continues until j equals 10. Some of the models described in the main body of the report only have a J equal 5. As all the longitudinal coefficients are orthogonal, the longitudinal coefficients for j values greater than 2*J+1 can be ignored for that model.

```
C       READS THE NUMERIAL COEFFICIENTS FROM UT NEOSOL
C       AND PRINTS THEM FOR EACH SEASON
C       MAXIMUM VALUE FOR NH IS 10
C       MAXIMUM VALUE FOR MAXG IS 10
        IMPLICIT REAL*6(A-H,O-Z)
        REAL*6 NTITLE
        DIMENSION NTITLE(13),FN(21,10,6)
1       READ 100, (NTITLE(I),I=1,13)
2       READ 200, NH,MAXG,NSEAS,NEND
        NF=2*NH+1
        NCARDS=57
        IF(MAXG .LE. 8) NCARDS=42
        DO 3 I=1,6
        DO 3 J=1,NCARDS
        READ 400,NFILE,NH1,NFF,FN(NH1,NFF,I),FN(NH1,NFF+1,I),
     1 FN(NH1,NFF+2,I),FN(NH1,NFF+3,I)
3       CONTINUE
9       PRINT 500
        IPRINT=0
        DO 700 I=1,NF
        MF=MAXG
        IF(I.GE.16) MF=7
        DO 300 J=1,MF
        IPRINT=IPRINT+1
        IF(IPRINT .GT. 48) PRINT 500
        IF(IPRINT .GT. 48) IPRINT=IPRINT-48
        IF(IPRINT .EQ. 1) PRINT 600,(NTITLE(K),K=1,13)
        PRINT 1100,I,J,(FN(I,J,K),K=1,6)
300     CONTINUE
        PRINT 800
700     CONTINUE
        IF(NEND .LT. 10) GO TO 1
C       NEND .GE. 10 WILL HALT PROGRAM
100     FORMAT(13A6)
200     FORMAT(4I10)
400     FORMAT(A2,2I5,4E17.10)
500     FORMAT(1H1)
600     FORMAT(1H1,//13A6,
     1        /3X,1HJ,3X,1HK,6X,4H0000,12X,4H0400,12X,4H0800,12X,
     1 4H1200,12X,4H1600,12X,4H2000,4X,2HUT,1X,5HHOURS)
800     FORMAT(1HA)
1100    FORMAT(2I4,6(2X,1PE14.7))
        END
```

Figure D1 Listing of PRINTUTN, an algorithm for reading and printing the 1 MHz atmospheric noise coefficients

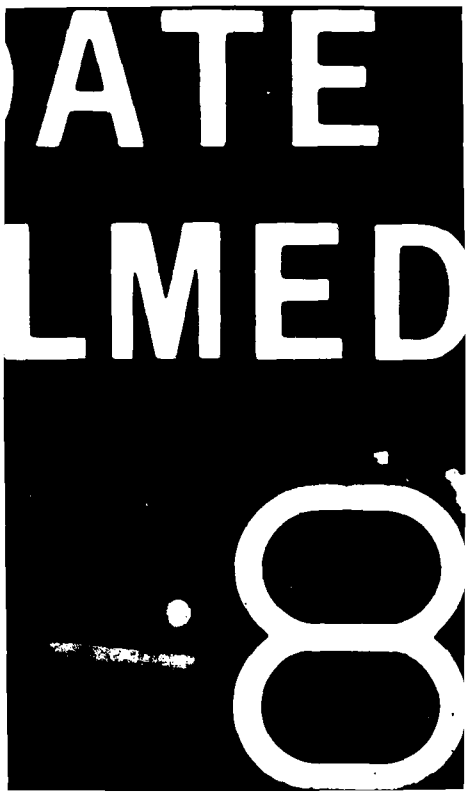
ATE
LMED
8